



UNIVERSITY
OF SOUTHERN
QUEENSLAND
AUSTRALIA

Nuclear ribosomal DNA secondary structures and statistical approach for the phylogeny of *Ampelomyces*

A Thesis submitted by

Rosa Esther Prah

BSc. (Cell Biology)

MSc. (Cell Biology)

MSc. Res. (Biochemistry)

For the award of

Doctor by Philosophy

2022

Abstract

Fungi belonging to the genus *Ampelomyces* are intracellular mycoparasites of the Erysiphales, which cause powdery mildew diseases in economically important crops. As *Ampelomyces* spp. are parasites of other parasites, they are named hyperparasites. Several *Ampelomyces*-based biocontrol agents have been developed but its effectivity against different powdery mildew fungi can vary, causing to still rely on the use of harmful pesticides. Accurate identification of these hyperparasites is essential to discovery newly highly virulent isolates for using in plant protection. In addition, further research is needed in *Ampelomyces* to understand, for example, their underlying mechanisms of virulence.

One of the problems in studying *Ampelomyces* is their unresolved taxonomy, which has been mainly determined by phylogenetic analyses based on the nuclear ribosomal DNA internal transcribed spacer region (nrDNA ITS). The ITS region of the 18S-28S nuclear ribosomal DNA is the preferred fungal barcode and it consists of the ITS spacers 1 (ITS1) and 2 (ITS2), and the 5.8S gene.

Historically, *Ampelomyces* were confused with other closely related pycnidial fungi. Today, many nucleotide sequences are deposited in the GenBank database under the generic name of *Ampelomyces*, but it is unknown if these sequences belong to the type specimen of *Ampelomyces*, *Ampelomyces quisqualis* Ces.. As the hyperparasites asexual structures vary in dimensions and apparently are not linked to a particular mycoparasitic lineage, their identification rely on the use of molecular barcodes. At least four distinct lineages have been identified based on the ITS sequences and actin 1 gene fragments (*actin1*). These DNA markers are insufficient for species delimitation in this genus, and thus, other identifiers are sought to assist in this purpose.

This PhD thesis presents a comprehensive research and analysis conducted to optimise *Ampelomyces* identification. As the early works are showing the ITS spacers and secondary structures (S2s) are important molecular tools in phylogenetic studies. This PhD thesis has conducted an in-depth evaluation of the utility of ITS S2s in *Ampelomyces* phylogeny.

The results of this thesis showed that: 1) putative *Ampelomyces* ITS sequences derived from environmental DNA (eDNA) and deposited in the GenBank do not belong to this genus. Statistical tests revealed that there were significant differences in the sequence lengths of ITS region as well as A/T nucleotide content values between the ‘true’ *Ampelomyces* spp. and those from putative *Ampelomyces*; 2) nrDNA ITS S2s significantly improves likelihood-based estimates of phylogeny; 3) the statistical test, Kruskal-Wallis, supports that the ITS spacers are under functional constraints of their S2s and indicating are not evolving neutrally as usually assumed for the nrDNA gene repeats; 4) variations in the conserved ITS2-proximal stem of two *Ampelomyces* ITS sequences reveals the presence of pseudogenes; 5) the simultaneous alignment of ITS spacers and S2s reflects the *Ampelomyces* phylogeny and reveals strong phylogenetic signal in structure variation across lineages; and 6) DNA repeats of *Ampelomyces* ITS1 sequences were different from those of putative *Ampelomyces*. Altogether, these findings are important for resolving the taxonomic classification of *Ampelomyces* and understanding their evolutionary history.

This computational work has also resolved (1) the previous difficulties in selecting a new DNA barcode with more phylogenetic resolution power than that of the ITS by using nrDNA ITS sequences and S2s based phylogeny and (2) some of the problems associated with selecting the ‘true’ *Ampelomyces* sequences without collecting and sequencing all previous ITS sequences deposited in the GenBank database. These findings will lead to accurately identify fungi in the future, improve DNA sequence data in databases as well as resolve the misidentification of *Ampelomyces* spp. *sensu stricto*.

Keywords: *Ampelomyces*; *Ampelomyces humuli*; biocontrol; environmental DNA; evolution; ITS1 and ITS2 secondary structures; phylogeny; plant protection; powdery mildews; pseudogenes; ribosomal biogenesis.

Certification of Thesis

This thesis is the work of **Rosa Esther Prah** except where otherwise acknowledged, with the majority of the authorship of the papers presented as a Thesis by Publication undertaken by the Student. The work is original and has not previously been submitted for any other award, except where acknowledged.

Rosa Esther Prah

07 Jul. 2022

PhD Candidate

Date

Endorsement

Prof Shahjahan Khan

07 Jul. 2022

Principal Supervisor

Date

Prof Ravinesh C. Deo

07 Jul. 2022

Associate Supervisor

Date

Student and supervisors' signatures of endorsement are held at USQ.

Statement of contributions

The articles produced from this study were a joint contribution of the student, supported by the supervisors. The details of the scientific contribution of each author in journal publications are provided as follows:

- **Article I: Rosa E. Prah**, Shahjahan Khan, and Ravinesh C. Deo. "The role of internal transcribed spacer 2 secondary structures in classifying mycoparasitic *Ampelomyces*". PLoS ONE **16**: e0253772 (2021). [**Impact Factor: 1.35, SNIP; SCImago Journal Rank 0.99 (Q1); it is a journal in multidisciplinary science.**

The overall contributions in this paper are as follows: Rosa E. Prah 70%, Shahjahan Khan 20%, and Ravinesh C. Deo 10%.

Author	Task performed
Rosa Esther Prah (PhD candidate)	Data acquisition and analysis, preparation of tables and figures, writing, and revision of manuscript.
Shahjahan Khan (Principal Supervisor)	Supervised, and provided feedback and comments on manuscript, editing.
Ravinesh C. Deo (Associate Supervisor)	Supervised, and provided feedback and comments on manuscript, editing.

- **Article II: Rosa E. Prah**, Shahjahan Khan, and Ravinesh C. Deo. "*Ampelomyces mycoparasites of powdery mildews: A review*". Submitted to Canadian Journal of Plant Pathology (2021). [**Impact Factor: 1.228, SNIP; SCImago Journal Rank 0.605 (Q1). It is a journal in agricultural and biological sciences.**

The overall contributions in this paper are as follows: Rosa E. Prah1 70%, Shahjahan Khan 20%, and Ravinesh C. Deo 10%.

Author	Task performed
Rosa Esther Prah1 (PhD candidate)	Data acquisition and analysis, preparation of tables and figures, writing, and revision of manuscript.
Shahjahan Khan (Principal Supervisor)	Supervised, and provided feedback and comments on manuscript, editing.
Ravinesh C. Deo (Associate Supervisor)	Supervised, and provided feedback and comments on manuscript, editing.

- **Article III: Rosa E. Prah1, Shahjahan Khan, and Ravinesh C. Deo.** "Secondary Structure Analyses of the Nuclear rRNA Internal Transcribed Spacers of mycoparasites *Ampelomyces*". Paper 3 to be submitted to Organisms Diversity and Evolution (2021) [**Impact Factor: 1.21, SNIP: SCImago Journal Rank 0.94 (Q1). It is a journal in areas, i.e., Ecology, Evolution, Behavior and Systematics.**

The overall contributions in this paper are as follows: Rosa E. Prah1 70%, Shahjahan Khan 20%, and Ravinesh C. Deo 10%.

Author	Task performed
Rosa Esther Prah1 (PhD candidate)	Data acquisition and analysis, preparation of tables and figures, writing, and revision of the manuscript.
Shahjahan Khan (Principal Supervisor)	Supervised, and provided feedback and comments on the manuscript, editing.
Ravinesh C. Deo (Associated Supervisor)	Supervised, and provided feedback and comments on the manuscript, editing.

Acknowledgments

I offer my great appreciation to these researchers and organisations for their wholehearted assistance, scientific guidance, valuable and useful advice, and for humbly sharing their expertise. It is undoubted that without their support, motivation, and encouragement, it would not have been possible for me to complete this research work. In reality, there are no enough words to express my gratitude and sincere appreciation to:

1. *Professor Shahjahan Khan*, my principal supervisor, to whom I am grateful for his untiring advice, support, his encouragement to continue my research, and his professional guidance. I am also grateful for his valuable intellectual engagement, scholarly inspiration, scientific advice and useful comments in the journal articles as well as in the thesis.
2. *Professor Ravinesh C. Deo*, my associate supervisor, for his motivation and guidance, and for patiently guiding me through publishing in high-quality journals. His early response and easy approach helped me to carry out my thesis.
3. *Dr. Douglas Eacersall* for his contribution and comments in the writing of my first paper publication to this doctoral thesis.

University of Southern Queensland through the USQ Postgraduate Research Scholarship for providing me with a full scholarship to pursue my PhD degree in Australia.

The Team of the Graduate Research School at USQ for their prompt assistance and support to accomplish the aims of my research work and thesis.

The Team of ICT at USQ for their ongoing technical support.

I dedicate this doctoral thesis to my lovely husband Torben Prahl for his love and support.

Table of Contents

Abstract.....	ii
Certification of Thesis	iv
Statement of contributions	v
Acknowledgments	vii
Chapter 1.....	1
<i>Introduction</i>	1
1.1 Background of <i>Ampelomyces studies</i>	1
1.2 Taxonomy.....	3
1.3 Phylogeny.....	3
1.4 Mycohost association of <i>Ampelomyces</i> isolates.....	3
1.5 Life Cycle.....	5
1.6 Biocontrol of powdery mildews by <i>Ampelomyces</i>	7
1.7 Data source.....	8
1.8 Research methodology	9
1.9 Statement of the Problem.....	10
1.10 Research Aims and Objectives.....	11
1.11 Scope and Limitations.....	12
1.12 Significance of the study	12
1.13 Organisation of the Thesis.....	13
1.14 Summary	14
Chapter 2.....	17
<i>Literature review</i>	17
2.1. The nuclear ribosomal DNA internal transcribed region	17
2.2. Ribosomal biogenesis.....	17
2.3. Internal transcriber spacer 1 and secondary structures.....	19
2.4. Internal transcriber spacer 2 and secondary structures.....	20

2.5 Utility of the ITS2 secondary structures.....	21
Chapter 3.....	23
<i>Ampelomyces identification by using ITS 2 secondary structures</i>	23
Article I: The role of internal transcribed spacer 2 secondary structures in classifying mycoparasitic <i>Ampelomyces</i>	23
Chapter 4.....	27
<i>The origin of Ampelomyces lineages</i>	27
Article II: The phylogeny of <i>Ampelomyces</i>	27
Chapter 5.....	29
<i>Characterization of the ITS 1 and 2 belonging to Ampelomyces</i>	29
Article III: The ITS 1 and 2 are under functional constraints of their secondary structures	29
Chapter 6.....	30
<i>Discussion, Summary of findings and conclusions</i>	30
6. 1. Discussions.....	30
6.2. Conclusions	36
6.3. Future directions.....	38
References.....	39

TABLE OF FIGURES

TABLE 1.....	1
FIGURE 1.....	6
FIGURE 2.....	25
FIGURE 3.....	37

ACRONYMS AND ABBREVIATIONS

<i>actin1</i> gene	<i>act1</i>
Adenine	A
Apple powdery mildew	APM
Biocontrol agent(s)	BCA(s)
Grapevine powdery mildew	GPM
Cytosine	C
Guanine	G
Compensatory base change(s)	CBC(s)
Environmental DNA	eDNA
Internal transcribed spacer region	ITS
Internal transcribed spacer 1	ITS1
Internal transcribed spacer 2	ITS2
Multiple Alignment using Fast Fourier Transform	MAFFT
The internal transcribed spacer 2 database	ITS2-DB
Thymine	T
nuclear ribosomal DNA	nrDNA
Powdery mildew(s)	PMs
Ribosomal RNA	rRNA
Transitional mutations	Ts
Transversional mutations	Tv
Transitional and transversional mutation ratio	Ts/Tv (<i>R</i>)
Uracil	U

Chapter 1

Introduction

1.1 Background of *Ampelomyces studies*

The Erysiphales are fungal phytopathogens causing powdery mildew (PM) diseases in economically important plants (Table 1) [Glawe 2008], including those with potential medicinal properties [Wiseman et al. 2021] and forest trees (Marmolejo et al. 2018).

Table 1

Main plants affected by powdery mildew diseases.

Plants	Powdery mildew fungi
Common Zinnia (*)	<i>Golovinomyces cichoracearum</i> [Zhu et al. 2020]
Grapevine	<i>Erysiphe necator</i> [Pirrello et al. 2019]
Hazelnut	<i>Erysiphe corylacearum</i> [Mezzalama et al. 2020]
Pumpkin, Zucchini	<i>Podosphaera xanthii</i> [Liang et al. 2020]
Tomato	<i>Oidium neolycopersici</i> [Stevanović et al. 2012]
Wheat	<i>Blumeria graminis</i> f. sp. <i>hordei</i> [Xue et al. 2017]

(*) A highly valuable ornamental plant

There are over 900 species of PM fungi known globally; and are currently classified into 18 genera [Braun and Cook 2012; Marmolejo et al. 2018] by the combined use of characteristics of their asexual structures and/or sexual

structures and nucleotide sequences of the nrDNA ITS and other DNA barcodes [Takamatsu 2004; Takamatsu et al. 2013; Takamatsu et al. 2015a,b; Braun et al. 2018]. Epidemics of PM fungi cause major crop yield losses [Gadoury et al. 2001; Gent et al. 2014], in particular, for cultivars that are susceptible to powder mildews (PMs) [Singh et al. 2016]. In addition, the Erysiphales also pose biosecurity problems for many countries because these pathogens threaten the survival and diversity of native plants. For example, most PMs identified in Australia were simultaneously introduced with their plant hosts during the European colonization. 42 species representing 10 PMs genera were identified in Australia which infected 13 native species of plants [Kiss et al. 2020].

The signs of the PM disease are easily recognizable by the presence of particular circular powdery white spots covering all aerial parts of many plant hosts, such as flowers, fruits, young stems, and leaves [Glawe 2008]. The white spots consist of PM fungi mycelia that include conidia, conidiophores, and hyphae. Chasmothecia, sexual products that contain ascospores, are also noticed spread across the PM mycelia [Glawe 2008; Dean et al. 2012]. During conidial germination of PM fungi, germ tubes are formed, elongated [Glawe 2008; Dean et al. 2012], and used to penetrate plant host cells. Then, haustorium is formed [Glawe 2008; Dean et al. 2012] where the uptake of plant nutrients takes place [Glawe 2008]. During the development of this structure, some fungal effectors are released to suppress plant immunity [Polonio et al. 2021] and PM hyphae continue to spread through all plant cells [Glawe 2008].

The management control of PM epidemics involves the repeated applications of pesticides [Matheron and Porchas 2013] in spite of the well-known health and safety risk concerns [Brauer et al. 2019], and the use of plant resistant varieties [Wei-Li et al. 2019; Riaz et al. 2020]. However, breeding cultivars for genetic resistance against PM fungi cannot be durable as fungal pathogens also evolve and become more virulent. Agrochemicals are highly successful for controlling plant pests, but the potential development of fungicide resistance is a major public health risk [Nicolopoulou-Stamati et al. 2016]. Currently, it is known that some PMs have selected resistance to several fungicides' products worldwide [Colcol and BauDOIn 2016; Cherrad et al. 2018]. Whereas biological control agents are an eco-friendly alternative for plant protection purposes, in particular,

those that are resistant to agrochemicals such as *A. quisqualis* [Sundheim 1982; Gilardi et al. 2008].

1.2 Taxonomy

Fungi belonging to the genus *Ampelomyces* form part of the order Pleosporales (Pleosporomycetidae, Dothideomycetes, Pezizomycotina, Ascomycota) (Zhang et al. 2009). Analyses have placed the type species *A. quisqualis* Ces. within the Phaeosphaeriaceae [de Gruyter et al. 2009; Aveskamp et al. 2010; Wijayawardene et al. 2013; Phookamsak et al. 2014]. The genus *Ampelomyces* is not monospecific but comprises numerous genetically diverse species (Kiss 1997; Liang et al. 2007; Park et al. 2010; Angeli, Maurhofer, et al. 2012). Whether they have a sexual reproductive stage is unknown, although teleomorphs may be present as signs of recombination were detected in some isolates (Kiss et al. 2011; Pintye et al. 2015).

1.3 Phylogeny

Studies using a variety of research methodologies have been conducted to classify *Ampelomyces*. Most investigations utilized phylogenetic analyses based on the ITS region (Szentiványi et al. 2005; Liang et al. 2007; Angeli, Pellegrini, Maurhofer, et al. 2009; Kiss et al. 2011; Nguyen and Lee 2016; Liyanage et al. 2018; Huth et al. 2021). Other investigations used ITS and *act1* (Park et al. 2010; Pintye et al. 2012), with two using a two-locus sequence analysis (ITS and *act1*), whose phylogenies were congruent (Pintye et al. 2012; Németh, Mizuno, et al. 2021),

1.4 Mycohost association of *Ampelomyces* isolates

Some degree of mycohost specificity in *Ampelomyces* hyperparasites was shown via phylogenetic analyses. At least four clades have been recognized in *Ampelomyces* by using the ITS region and *act1* gene fragments (Park et al. 2010).

The phylogenies based on either ITS or *act1* indicated that some isolates grouped in accordance with their original mycohost, suggesting that some degree of adaptation occurred between these strains and their hosts without losing their infection capacity as generalist mycoparasites (Park et al. 2010).

Other studies presented evidence that *Ampelomyces* hyperparasites lack of mycohost specificity by using cross-inoculation tests where *Ampelomyces* isolates can parasitise PMs different from their original hosts [Sztejnberg al. 1989; Szentiványi et al. 2005; Liang et al. 2007; Kiss et al. 2011].

Another example of the association between *Ampelomyces* and their hosts is the genetically different *Ampelomyces* lineage that was separated from its sympatric *Ampelomyces* population by temporal isolation, which was caused by differences in mycohost phenology [Kiss et al. 2011]. In Europe, *Podosphaera leucotricha*, the causal agent of apple PM (APM), overwinters inside apple buds between bud scales as mycelium and chasmothecia [Stalder 1955], and causes epidemics in the spring while non-APM, i.e., *Arthrocladiella mougeotii* on *Lycium halimifolium*, causes infections later in the autumn season [Kiss 1998]. Despite the niches of APM and non-APM overlapping [Szentiványi and Kiss 2003], APM *Ampelomyces* evolved into a genetically different lineage as demonstrated via single-stranded conformation polymorphism analysis of the ITS [Szentiványi et al. 2005] and ITS sequences and microsatellite markers [Kiss et al. 2011]. A subsequent study, using microsatellites, showed that both APM and non-APM strains whose niches overlapped were genetically differentiated and with no signs of gene flow [Pintye et al. 2015]. Further, the European APM *Ampelomyces* from spring with a unique haplotype ITS and those non-APM *Ampelomyces*, extracted from *A. mougeotii*, from autumn were able to infect a determined PM species, i.e., *P. xanthii* on cucumber and *Golovinomyces orontii* on tobacco, with no significant differences in mycoparasitic activities. Further, non-APM *Ampelomyces* can overwinter together with APM *Ampelomyces* in apple buds. These premises suggested that *Ampelomyces* (1) adapted when overwintering with APM and evolved into a different phylogenetic group by temporal isolation as a result of the differences in phenology of their powdery mildew host; and (2) despite of this genetic differentiation, the cross-inoculation tests showed that APM *Ampelomyces* lack of

host specificity [Kiss et al. 2011]. In the lineage containing the European APM *Ampelomyces* [Kiss et al. 2011], there were other strains originally extracted from *Podosphaera pannosa* on rosaceous, including one Chinese *Ampelomyces* strain from *Podosphaera ferruginea* on *Sanguisorba officinalis* [Liang et al. 2007] which contain the same APM *Ampelomyces* haplotype. This finding has not been explained yet.

1.5 Life Cycle

Ampelomyces mycoparasites act by direct invasion of mycelia and degradation of cytoplasmic components of its hosts [Hashioka and Nakai 1980]. At high levels of relative humidity (over 80%) [Romero et al. 2007; Nemeth et al. 2021] and low temperatures (15°C–25°C) [Mhaskar and Rao 1974; Czerniawska 2001; Angeli, Maurhofer, et al. 2012], *Ampelomyces* conidia germinate (Figure 1a), then, germ tubes are formed, extended, and used to penetrate host cell wall. The host cell membranes are hardly altered, and this interaction seems to be biotrophic [Hashioka and Nakai 1980; Sundheim, and Krekling 1982] where nutrients are obtained without killing the host. The growth of *Ampelomyces* hyphae continues intracellularly through all the PM mycelia via mechanical or enzymatic processes [Reviewed in Kiss 2008]. In natural conditions, abiotic factors, i.e., wind and rain, favour the dispersion of PM conidia and chasmothecia together with its mycohost inhabiting in these structures (Reviewed in Kiss *et al.* 2004). In addition, *Ampelomyces* mycoparasites are very efficient in reducing the inoculum of PM for the next epidemic season by parasitizing mycohost chasmothecia (Figure 1b) [Shishkoff and McGrath 2002].

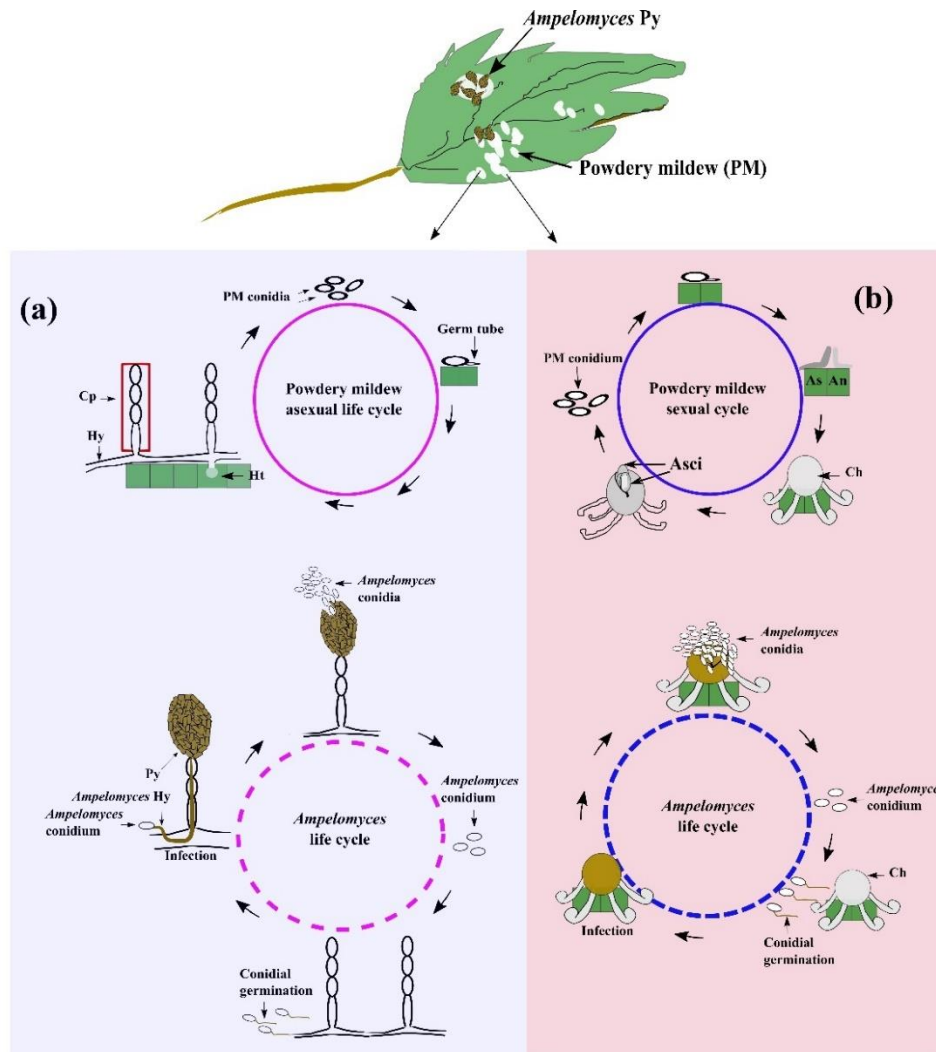


Figure 1

Mycoparasitic interaction of *Ampelomyces* spp. and mycohost. *Ampelomyces* pycnidia developed in powdery mildew-mycelia (white spots). Asexual (a) and sexual structures of the Erysiphales (b). Life cycle of *Ampelomyces* spp. with the asexual (conidia) and sexual morphs (chasmothecia) of their mycohosts is represented with lilac and blue dotted lines, respectively. Abbreviations: Ascogonium (As); Antheridium (An); Chasmothecium (Ch); Conidiophore (Cp); Hypha (Hy); Powdery mildew (PM); Pycnidium (Py). Illustration by Prahl et al. (2022).

Mycoparasitism ends with the intracellular formation and maturation of *Ampelomyces* pycnidia inside PM conidia, conidiophores, chasmothecia, and

hyphae [Reviewed in Kiss 2008; Angeli, Pellegrini, Pertot 2009]. As a result, the cells bearing *Ampelomyces* pycnidia from PM structures are destroyed by direct invasion of *Ampelomyces* (mycoparasitism) and leading to a reduction of the mycohost mycelia. Today, images of this mycoparasitic interaction have been resolved much better by using state-of-the-art digital microscopy [Németh et al. 2021] and fluorescence microscopy [Németh et al. 2019]; and we currently have a better picture of the life cycle of these hyperparasites.

1.6 Biocontrol of powdery mildews by *Ampelomyces*

The potential biocontrol of *Ampelomyces* has been evaluated since 1932 [Yarwood 1932]. In the last 20 years, several studies have been conducted to unveil the molecular mechanisms underlying their virulence patterns to enhance biocontrol potential of *Ampelomyces* strains, although contradictory results have been obtained. Two studies showed that mycoparasitic activity of *Ampelomyces* was reduced when its original mycohost was substituted by different species of PM fungi [Falk, Gadoury, Pearson, et al. 1995] while others did not find significant differences [Kiss et al. 2011, Németh et al. 2021]. As different environmental factors may influence the mycoparasitic activity of *Ampelomyces*, it is not expected that the degree of virulence of strains be the same between greenhouse and field conditions. Consequently, effective plant- disease measures need to be implemented when using *Ampelomyces* as BCAs, i.e., by combining *Ampelomyces* with small doses of fungicides. This is a possible option as some of these hyperparasites are resistant to some agrochemicals [Philipp et al. 1982; Szejnberg et al. 1989; Shishkoff and McGrath 2002].

AQ10[®] was the first *Ampelomyces*-based BCA developed and patented in the USA [Szejnberg et al. 1989]. Another biofungicide based on *Ampelomyces* is Q-fect[®], which was shown to protect cucumber leaves against *P. xanthii* in 92.9% and was more efficient than the commercial AQ10[®] [Lee et al. 2004]. Other biofungicides are PowderyCare[®] [AgriLifeTM. 2021] and CPA-9 from LAINCO, S.A. [Garriga et al. 2014]. CPA-9 can effectively eliminate PM on zucchini [Carbó et al. 2020] and its formulation was recently optimised to protect

it against climatic variations of temperature and relative humidity. This newly formulated product is also compatible with different phytosanitary products, i.e., fungicides and insecticides [Carbó et al. 2021]. There are no published articles about the efficacy of PowderyCare[®] compared to other BCAs.

1.7 Data source

An interesting topic to resolve is the initial confusion of some *Ampelomyces* strains with *Didymella*- or *Phoma*- like fungi. Moreover, some international culture collections, i.e., American Type Culture Collection (ATCC) and the Central Bureau of Fungal Cultures (CBS), have also the misidentified strains deposited under the generic name of *Ampelomyces* [Kiss and Nakasone 1998]. This is a serious problem that needs to be addressed as can jeopardise further studies that rely on database information.

Currently, there are over 800 nucleotide sequences deposited in the GenBank database under the name of *Ampelomyces* that need to be accordingly revised. A large number of fungal specimens were recently validated at the Westerdijk Fungal Biodiversity Institute, Utrecht [Vu et al. 2019]. To avoid duplicate results during the curation of these sequences a computational approach that allows the selection of the ‘true’ *Ampelomyces* nucleotide sequences will be advantageous for the entire scientific community.

According to this, this doctorate thesis used as a dataset all ITS nucleotide sequences deposited in the GenBank under the name of *Ampelomyces*. These ITS sequences were retrieved from the database up to May 2020. The ITS sequences from type specimens of *Ampelomyces*, *Ampelomyces quisqualis* Ces. belong to the ‘true’ *Ampelomyces* or *Ampelomyces* spp. *sensu stricto* as their cell growth rate in culture and morphology of pycnidia are known [Kiss and Vajna 1995; Sullivan and White 2000]. Whereas those *Ampelomyces* sequences derived from PM-free environments, which cultural characteristics or pycnidia morphology are not documented, or from eDNA samples belong to putative *Ampelomyces*. The latter were divided into groups 1 and 2. Group 1 is formed

by ITS sequences derived from PM fungi or host plants while group 2 consists of samples extracted from eDNA. The outgroup consisted of *Didymella* or *Phoma* ITS sequences, which will be used to determine if these putative *Ampelomyces* sequences are closely related to *Phoma* species. Groups 1 and 2 contain the ITS sequences that will be under study to determine if belong to fungi of the genus *Ampelomyces*. Moreover, complete ITS sequences were only considered in this thesis. For the phylogenetic studies, the 18S and 28S nucleotide sequences were eliminated from the analysis.

1.8 Research methodology

The data analyses were based on the use of several bioinformatic and statistical tools available online. For the differences in nucleotide contents and sequence lengths among groups a Kruskal-Wallis's nonparametric test for multiple independent samples was utilised to establish if there were significant differences among groups whose population distributions are unknown. Then, Dunn's post hoc test was conducted on each pair of groups to determine which group was different. This test is available at the web server <https://astatsa.com/KruskalWallisTest/> [Vasavada 2016].

To determine if ITS 1 and 2 sequences are under functional constraints of their S2s two strategies were used from Edger *et al.* (2014) and Zhang *et al.* (2020), respectively. The Kruskal-Wallis' non-parametric test was also used to determine statistically significant differences between minimum free-energy values and number of predicted ITS1 S2s between the 'true' *Ampelomyces* and from nucleotide sequences, which were randomly generated with equal sequence length and C/G content to the *Ampelomyces* ITS1 sequences. The dataset for this analysis were 26 *Ampelomyces* ITS1 sequences representing the four major *Ampelomyces* lineages Whereas 300 sequences were randomly generated by using the online tool at <https://www.molbiotools.com/randomsequencegenerator.php>. If the ITS1 sequences are under functional constraint of their S2s, it is expected that the number

of predicted S2s from nucleotide sequences randomly generated be higher than those of the *Ampelomyces* ITS1.

For the ITS2, ITS2 S2s will be predicted via the ITS2 database (ITS2-DB) [Selig et al. 2008; Merget et al. 2012; Ankenbrand et al. 2015]. Nucleotide contents of adenine (A), and cytosine/guanine (C/G) between loops (unpaired regions) and stems (paired regions) of the *Ampelomyces* ITS2 S2s will be calculated manually by visualising the simultaneous alignment of ITS2 sequences and S2s via the 4SALE software [Seibel et al. 2006]. The 4SALE software was used to visualise the ITS 1 and 2 sequences together with their respective S2s and to, finally, obtain a consensus S2 per *Ampelomyces* lineage. The A nucleotide contents are expected to be higher in unpaired region of the S2s as these mediate interactions with other tertiary molecules and other mechanisms still unclear [8].

The *Ampelomyces* phylogeny was inferred by using a maximum likelihood (ML) approach where the calculated tree topology, branch lengths, and parameters of the DNA model of evolution are the most likely values that represent the data. This method is implemented in the MEGAX v10.1 software [Kumar et al. 2018]. The resulting tree represents the evolutionary history of *Ampelomyces* spp. based on the simultaneous alignment of ITS 1 and 2 sequences and their S2s. It is expected that the clear differences in S2s will be reflected in the phylogram and enhancing the resolution of the barcode gap within and inter -species.

1.9 Statement of the Problem

The taxonomy of *Ampelomyces* mycoparasites remains unresolved. The nrDNA ITS cannot solely distinguish among *Ampelomyces* groups and from other closely related fungi due to their genetic variability among *Ampelomyces* isolates [Kiss and Nakasone 1998; Liang et al. 2007; Park et al. 2010]. This issue can potentially impact future studies in biodiversity and bias research works conducted by researchers without a background in the taxonomy of fungi. There are over 800 sequences deposited only in the GenBank database under the name of *Ampelomyces*, which need to be revised accordingly. The large number of sequences deposited in the database are abysmal and validate them will take a

long time. Further, many sequences derived from type species, *Ampelomyces quisqualis* Ces. are old and have poor quality or have few information about the collection date. To avoid sequencing again, I propose to use a computational work which will allow selecting the ‘true’ *Ampelomyces* ITS nucleotide sequences.

1.10 Research Aims and Objectives

Due to the economic importance of controlling epidemics of PM fungi by using eco-friendly strategies and the urgency in recognizing microbes for further use in agroecological methods and studies of biodiversity, the aim of this research thesis was to find a practical molecular approach to improve the classification of *Ampelomyces* mycoparasites. It was expected that the results of this comprehensive computational work will help the whole scientific community, including those groups working in human health. Some fungi of medical importance have been misidentified with the ‘true’ species of the genus *Ampelomyces*.

Based on the results of this thesis, a workflow can be elaborated to aid in the classification of these hyperparasites. In detail, this study addressed the following three objectives:

1.2.1. **Aim 1:** To perform relevant data acquisition of the ITS nucleotide sequences from the GenBank database deposited as *Ampelomyces* and investigated the suitability of ITS2 S2s to enhance molecular identification of *Ampelomyces*.

1.2.2. **Aim 2:** To undertake a comprehensive review of the *Ampelomyces* phylogeny so that the evolutionary strengths that can originate *Ampelomyces* lineages are discussed, including that identified in aim 1 (the random appearance of pseudogenes with potential functionality).

1.2.3. **Aim 3:** ITS1 S2s will be predicted from the main *Ampelomyces* phylogenetic groups. In addition, it will be determined if ITS 1 and 2 sequences are under evolutionary constraints of their S2s .

1.11 Scope and Limitations

In this doctoral thesis, notable results and valuable new insights are provided in terms of the *Ampelomyces* taxonomy, phylogeny, and evolutionary mechanisms. by using a comparative study among *Ampelomyces* strains based on the ITS1 and ITS2 sequences and their S2s. Nonetheless, this thesis work is limited by the number of complete ITS sequences that are freely available in public databases and the lack of bioinformatic tools to analyse the evolutionary relationship of organisms via RNA models of evolution.

1.12 Significance of the study

The validation and curation of nucleotide sequences from public databases have been a large existing problem [Kappel and Schröder 2020]. Despite several efforts to solve this caveat [Vu et al. 2019; Schäffer et al. 2021], the number of sequences deposited daily in the GenBank is extremely high [Lathe et al. 2008]. Moreover, the verification of some of these sequences has led to obtain redundant data [Chen et al. 2017]. In the case of *Ampelomyces*, these were initially misidentified with other pycnidial fungi whose sequences were deposited in the GenBank as belonging to the genus *Ampelomyces* [Kiss and Nakasone 1998 and Sullivan and White 2000]. This confusion can potentially bias further studies based on database information. Hence, finding an integrate approach that can widely be used to avoid confusing fungi derived from environmental DNA (eDNA) samples will be advantageous for all the scientific community, and in particular, for those researchers with no background in fungal taxonomy. In this thesis, the resulting curated ITS nucleotide sequences belonging to the ‘true’ *Ampelomyces* will be also freely available to the public

for further use. As *Ampelomyces* are of economic importance for their potential biocontrol against PM fungi and probably as natural sources of new compounds for plant protection, their correct identification is important to achieve. The combined analyses of ITS 1 and 2 sequences and their S2s has not been conducted in *Ampelomyces* yet.

1.13 Organisation of the Thesis

The thesis is organized in six chapters as follows:

Chapter 1: The introduction includes the research background, research gaps, aims of the thesis, and significance of the study.

Chapter 2: A literature review of studies has been performed comprised of the ribosomal biogenesis and the role of S2s of the ITS1 and ITS2.

Chapter 3: This chapter performs all relevant data analysis and provides the conclusions of Paper 1, specifically, the data acquisition, ITS2 S2s prediction and characterization, and their use to classify *Ampelomyces* mycoparasites. Paper 1 has been published in *PLoS One* journal.

Chapter 4: In this chapter, it is proposed that some lineages are originated via the random appearance of pseudogenes and are represented by clear S2s suggesting mechanisms of pre-ribosomal processing are differently regulated across *Ampelomyces* groups. Paper 2 is a comprehensive review about *Ampelomyces* mycoparasites. This review is of importance as the last review in this topic was conducted by Manjunatha et al. (2020) and the genomic aspects of *Ampelomyces* were not included as its genome was recently published in 2020. The origins of *Ampelomyces* lineages are also discussed. This paper is currently under revision by the editors of the Canadian The Canadian Journal of Fungi.

Chapter 5: This chapter presents the results of Paper 3, which involves the prediction and analysis of ITS1 S2s of key *Ampelomyces* ITS sequences representing the main lineages of *Ampelomyces*. Further, ITS1 and 2 sequences

were assessed to determine if these are under functional constraints of their S2s. Paper 3 is currently under final preparation.

Chapter 6: In this chapter, we present the discussion, conclusions, future directions, and a proposed flowchart to identify ITS nucleotide sequences belonging to *Ampelomyces* spp. *sensu stricto* from public databases.

1.14 Summary

The identification of fungi that are not possible to maintain in culture and come from eDNA samples is challenging [Wu et al. 2019]. DNA molecular markers can solve the problem but in most cases several barcodes are required for species groups delimitation [Vu et al. 2019]. The universal barcode, the nrDNA ITS region, has been shown to be effective in fungal taxonomy but with some caveats [Kiss 2012; Schoch et al. 2012]. Consequently, other DNA barcodes are sought. In some *Ampelomyces* isolates the genetic distances can reach up to 15% when using the ITS region as a DNA marker [Kiss and Nakasone 1998]. Thus, the barcode gap is poorly resolved and can superpose with those of unknown fungi. To complicate even more this situation, ITS sequences from PM-free environments were unintentionally deposited under the generic name of *Ampelomyces* in the GenBank database. A large validation project was conducted to curate fungal DNA sequences at the Westerdijk Fungal Biodiversity Institute, Utrecht [Vu et al. 2019], but further work is still needed. Moreover, it is a time consuming job due to the large number of sequences deposited per day in the database. As most of the *Ampelomyces* sequences found in the GenBank corresponded to the ITS region and the potential use of S2s of their ITS spacers 1 and 2 have not been investigated yet, this doctorate thesis aimed to predict ITS1 and ITS2 S2s in all ITS sequences included in the GenBank database under the name of *Ampelomyces* and evaluate their utility to improve *Ampelomyces* spp. *sensu stricto* classification.

The results of this thesis document showed that ITS 1 and ITS 2 S2s are valuable molecular tools to enhance the phylogeny of *Ampelomyces* and assist to elucidate

important evolutionary mechanisms occurring in pre-ribosomal processing [Prah et al. 2021]. It is also demonstrated that pseudogenes can randomly appear in the nrDNA ITS region and some are not necessarily unfunctional or ‘dead’, which means these can positively impact pre-ribosomal processing [Coté et al. 2002]. In the present study, putative pseudogenes were identified in the *Ampelomyces* strains originally extracted from *P. xanthii* (GI: DQ490750) (Liang et al. 2007) and from *E. necator* (GI: HM125018) (Falk, Gadoury, Cortesi, et al. 1995). Based on the results of Coté *et al.* [133], mutations affecting the stem length of the ITS2-proximal stem model will reduce the maturation of rRNA. Conversely, the mutation observed in the strain DQ490750 does not affect either the sequence length of the stem or other nearby nucleotides crucial for the assembly of this conserved structure, suggesting that (1) it is not negatively affecting pre-ribosomal processing, or (2) can provide with some flexibility to the structure and acting as regulators of a determine biological function [Pink and Carter 2013; Cheetham et al. 2020]. Recent evidence shows some pseudogenes can produce functional transcripts [Gong et al. 2019] and, thus, create a new phenotype. This needs to be investigated further. In conclusion, these variations indicate that some ITS sequences in *Ampelomyces* are of pseudogenic origin [Prah et al. 2021].

On the other hand, five main ITS2 S2 models were established for the main *Ampelomyces* lineages (Prah et al. 2021). As these S2s reflect the *Ampelomyces* phylogeny, it is proposed to review the taxonomic classification of these hyperparasites. In addition, the ITS1 S2 of *Ampelomyces* from *E. necator* were distinct to those of the rest of *Ampelomyces* strains [Prah et al. 2021]. The contents of cytosine (C) and guanine (G) nucleotides were lower in loops than in the double-stranded regions (stems) of the hyperparasites ITS2 S2s while the adenine (A) content was, surprisingly, higher in stems than in loops. Compared to the A-T pair, which forms two hydrogen bonds, the C-G pair forms three hydrogen bonds, which provides strong stability to the stem (loops) of the ITS2 S2. Furthermore, compensatory base changes (CBCs) occur in one or two nucleotides of base pairs to maintain this stage [Li et al. 2019; Schill et al. 2010]. Adenine nucleotide contents are expected to be higher in unpaired regions than paired regions as these are involved in establishing interactions with tertiary

molecules [Gutell et al. 2000], but, in the case of *Ampelomyces*, the high A contents in paired regions suggest a different role for A nucleotide. For the ITS1 sequences, the number of S2s predicted by minimum free energy approaches was lower than that of the predicted S2s with higher free energy values from nucleotide sequences randomly generated with equal sequence lengths and C/G contents to the *Ampelomyces* ITS1 sequences. Thus, independence of sites across the ITS sequence is not valid. In the case of *Ampelomyces* mycoparasites, RNA models of evolution may describe better their phylogeny as in these models the substitutions occurring in base pairs forming the stems are considered during the phylogenetic reconstruction. Moreover, the analyses of *Ampelomyces* ITS 1 and 2 S2s were also helpful to distinguish the ‘true’ *Ampelomyces* sequences from those derived from PM- free environments, human secretions, and eDNA [Prahl et al. 2021].

The clear differences observed among *Ampelomyces* ITS 1 and ITS 2 S2s belonging to the *Ampelomyces* lineage APM and those extracted from *E. necator*, which causes PM disease in grapes (GPM), indicate that these are powerful tools to differentiate *Ampelomyces* groups. Future studies based on S2s and paired-site RNA models of evolution together with multi-genes phylogenetic analyses will assist to resolve their phylogeny.

Chapter 2

Literature review

2.1. The nuclear ribosomal DNA internal transcribed region

The ITS1, 5.8S and the ITS2, named the internal transcribed spacer (ITS) region, is the preferred DNA barcode in fungal identification and phylogeny [Schoch et al. 2012]. When using a DNA molecular marker, intra-genetic distances are required to be smaller than those from inter-genetic distances among species to obtain an optimum barcode gap [Vu et al. 2019]. Nevertheless, for some fungi the barcode gap can be small and jeopardise species delimitation. In this circumstance another marker is required.

2.2. Ribosomal biogenesis

A ribosome is formed by a complex of proteins and RNA and is responsible for the synthesis of proteins [Lafontaine and Tollervey 2001]. Ribosomes translate the messenger RNA into proteins by catalysing the assembly of amino acids into peptide chains [Opron and Burton 2018]. The model organism used to study the eukaryotic ribosome is the fungus *Saccharomyces cerevisiae* [Venema and Tollervey 1995]; and it is formed by two substructures the 40S small subunit (SSU) and the 60S large subunit (LSU). The SSU consisted of the 18S ribosomal RNA (rRNA) as well as 33 ribosomal proteins (RPs) while the LSU contains the

25S, 5.8S, 5S and 46 RPs [Biedka et al. 2018]. The synthesis of ribosomes starts in the nucleolus where the nrDNA is transcribed by the polymerase I, a DNA-dependent RNA enzyme [Grummt I; Scull and Schneider 2019]; subsequently a series of complex biochemical reactions occur to fold, modify, process, and assemble the pre rRNA [Perry 1976]. Notably, there are at least three nuclear polymerases described in eukaryotes [Scull and Schneider 2019]. Indeed, in eukaryotic mitochondria and chloroplasts, one or more polymerases have been detected that can synthesise rRNA. For instance, a subpopulation of rRNA variants that are tissue specific were identified in *Arabidopsis thaliana* [Sims et al. 2021].

The nrDNA is located in tandem arrays of thousands of copies on chromosomes and consists of the 18S, 5.8S, and 28S genes, which are separated by the ITS 1 and 2 spacers [Biedka et al. 2018]. The nrDNA is transcribed first into the 35S pre-rRNA that contains the 18S, 25S and 5.8S pre-rRNA. These structural parts are flanked by 5' and 3' -external spacers and separated by the ITS1 and ITS2 spacers. ITS 1 and 2 are also transcribed, but later removed by subsequent ribosomal processes depending on their own ITS1 and ITS2 structures.

Deletion of the ITS 1 and 2 spacers starts with the cleavage of the ITS1 A2 or A3 site to obtain two subunits, the 20S and 27SA2. This allows the SSU, and LSU synthesis occurred separately. For the LSU, the 27SA2 is trimmed at the 5' end to produce 27SB_L and 27SB_S. These intermediates are processed in the nucleolus, but the final processing occur in the nucleoplasm. The ITS2 cleavage starts at the C2 site of 27SB_{L/S} by endonuclease Las1 to generate 25.5S and 7S_{L/S} pre-rRNAs. Subsequently, the 25.5S pre-rRNA is phosphorylated at the 5' end by the polynucleotide kinase Grc3 and then trimmed by two nucleases, Rat1 and Rai1, to produce the 25S. The 5' end of 25S rRNA and the 3' end of 5.8S rRNA form a base-paired proximal stem that is conserved across eukaryotes (Reviewed in Zhang *et al.* 2020).

On the other hand, the 7S_{L/S} pre-rRNAs are trimmed two times from 6SS/L to 5.8S_{L/S} by the exosome in the nucleoplasm and then by the NgI2-Rex1-3 complex in the cytoplasm. During these processes several assembly factors,

ribosomal proteins, and nucleases participate orderly [Henras et al. 2008]. Cryo-electron microscopy studies have revealed that (1) the structural arrangement of some of these factors during the 27S/B particle state formed a ‘foot’ structure [142] and (2) the 5.8S and 25S base-paired proximal stem occurs during the co-transcription of the pre-rRNA [Burlacu et al. 2017].

Conversely, the assembly of the 40S ribosomal subunit in yeast occurs (1) in the nucleolus where it is transcribed, modified, and co-transcriptionally cleavage at site A2, and then, followed (2) by another cytoplasmatic cleavage at site D by the endonuclease Nob1 [Lamanna and Karbstein 2009]. The cleavage in D is located at the single-stranded 3’ end of 18S rRNA [Lamanna and Karbstein 2009]. In yeast (*S. cerevisiae*), ITS1 has been shown to bear post-transcriptional pre-rRNA processing sites like D, A2, and A3 that are vital for the production of the mature 17S and 5.8S rRNA genes [van Nues et al. 1994; Allmang et al. 1996].

2.3. Internal transcriber spacer 1 and secondary structures

The internal transcribed spacer 1 (ITS1) is located between 18S and 5.8S rRNA genes in the nrDNA. It has enough variability to be used as a barcode for classification of some organisms at the level of genera or families [Vilnet et al. 2008; Milyutina et al. 2010]. The utility of ITS1 S2s in phylogenetic studies has been less explored [Edger et al. 2014; Ghosh et al. 2017; Giudicelli et al. 2017; Zhang et al. 2017] than to those of the ITS2 S2s. In PUBMED (accessed July 2021) the number of publications related to ITS2 S2s double those of the ITS1 S2s. Conserved motifs (CMs) ITS1 have been identified in several organisms, i.e., flowering plants, angiosperms, Anthocerotophyta, mosses and liverworts. Specifically, CMs at the 5’ end of ITS, located out of the terminal hairpins, and a second motif located nearby the base of the 3’ terminal hairpin in the ITS1 S2s, like that one of the *S. cerevisiae* A3 site [Milyutina and Ignatov 2015].

2.4. Internal transcriber spacer 2 and secondary structures

Despite limitations of the ITS region in phylogenetic analyses [Kiss 2012], it seems the inclusion of S2s of the spacers of the ITS region can be an interesting approach to be used in classifying some organisms [Poczai et al. 2015; Sundaresan et al. 2019]. The ITS2 spacer has a highly conserved structure across eukaryotes with homologous features that are useful for sequence alignments and phylogenetic analysis [Schultz et al. 2005; Wolf et al. 2014]. Moreover, the utility of ITS2 S2s to enhance phylogenetic analysis has been demonstrated across different studies [Khan et al. 2019; Sundaresan et al. 2019]. The stems of the ITS2 are formed by complementary base pairs where the most frequently to occur are the Watson-Crick pairs AU/UA; GC/CG and the intermediates UG/GU (reviewed in [Zhang et al. 2020]). In addition, there are other ten possible base pairs that are established as mismatches. Nucleotide substitutions occurring in stable base pairs in stems can be detrimental to RNA function [Côté and Peculis 2001]; but CBCs, which occur as another nucleotide substitution in the counterpart base of the stem, can return the stability lost [Li et al. 2019]. Thus, this nucleotide dependence occurring in stems regions contradict the independence among sites assumed in routinely phylogenetic studies; and it can lead to wrong evolutionary inferences. This issue was overcome by coding each nucleotide together with its structural states into 12 nucleotide letters (for unpaired, paired left and right regions). Thus, these sequences can be aligned together with its S2s. This strategy has been implemented in the 4SALE open-source software where simultaneous alignments of sequence and structures can be visualized and export to be used for further execution of maximum likelihood (ML) analysis and Bayesian inferences [Seibel et al. 2006]. Despite the utility of ITS2 S2s to enhance accuracy and robustness of phylogenetic analyses compared to the standard use of DNA sequence models, no in many popular programs are implemented RNA-specific models. The Bayesian phylogenetic inference (PHASE), was built for phylogenetic analysis of RNA where it is included the six- seven- and 16- state models, which consider substitutions on both sites of the stem by base pair and in accordance to its CBCs.

Another function of the CBCs in ITS2 S2 is to determine species limited. The concept of species delimitation by CBCs have been investigated in several works [Li et al. 2019; Schill et al. 2010]. Indeed, from a meta study in fungi and plants, 93% of the cases the CBCs in ITS2 successfully identify species [Müller et al. 2007]. For animal lineages, it was possible to identify three new species that were morphologically undistinguished from *Paramacrobiotus richtersi* by using the CBCs in ITS2 [Schill et al. 2010; Sundaresan et al. 2019].

Ampelomyces isolates and the AQ10[®] have different efficacies against different PM species (Legler et al. 2016). To improve in the development of potent biofungicides, several efforts have been performed to elucidate the molecular mechanisms underlying its mycoparasitism as well as its evolutionary relationship with other pycnidial mycoparasites that also infect PM fungi [Sullivan and white 2000]. Today, multi-locus sequences analysis has not been conducted in fungi belonging to the genus *Ampelomyces* which is required to delimitate species. Despite some caveats [Kiss 2012], the nrDNA ITS region is the preferred marker for fungal identification [Schoch et al. 2012]. However, in some *Ampelomyces* lineages ITS sequences divergences are highly variable [Kiss and Nakasone 1998]. Consequently, other identifiers are required for species delimitation , but the design of primers for PCR analysis is difficult to obtain as occur in other fungi [Stielow et al. 2015].

2.5 Utility of the ITS2 secondary structures

The ITS2 is located between the 5.8S gene and the 28S large subunit of the Eukaryotic nrDNA and has been shown to accurately differentiate fungal species in early works when based the phylogenetic analyses on the simultaneous alignment of ITS2 sequences and S2s [Khan et al. 2019; Zhang et al. 2020].

The ITS2 S2 is formed by four helices protruding from a conserved central ring [Joseph et al. 1999]; and it has been found widely across eukaryotes [Schultz et al. 2005]. It typically has four helices, which each is formed by base-paired nucleotides (stems) and unpaired nucleotides (loops). Helices I and IV are most

variable than helices II and III, which are more stable and common to Eukaryotes [Schultz et al. 2005]. These S2s also contain two conserved domains, the U-U mismatch on helix II and the poly adenine nucleotides on the single-stranded ring between helices II and III [Joseph et al. 1999]. These are reported to be present in yeasts and vertebrates [Joseph et al. 1999]. Another interesting characteristic of these S2s is the presence of a conserved motif UGGU at the tip of helix III. This feature has been detected in several organisms including plants [Schultz et al. 2005; Poczai et al. 2015]. The differences in C+G nucleotide contents among stems and loops, the A contents in the single-stranded ring between helices II and III together with the variations in the transition (TS) and transversion (Tv) biases ratio (R) among the sections of the S2s have suggested RNA models of evolution may describe better the evolution of species based on the ITS2 S2s than the common models of DNA evolution based only on nucleotide sequences [Zhang et al. 2020].

Despite the utility of ITS2 S2s in improving phylogenetic analyses, no prior research based on ITS2 S2s has been conducted to study the evolution and diversity of species of the genus *Ampelomyces*, mycoparasites of the Erysiphaceae. This doctoral thesis therefore aims to bridge this knowledge gap in literature by examining the utility of ITS1 and ITS2 secondary structures for *Ampelomyces* classification.

Chapter 3

Ampelomyces identification by using ITS 2 secondary structures

Article I: The role of internal transcribed spacer 2 secondary structures in classifying mycoparasitic *Ampelomyces*

Summary:

The ITS region is the preferred barcode for fungal identification despite some pitfalls [Schoch et al. 2012]. Species of the genus *Ampelomyces* were initially confused with other picnidial fungi of the genera *Didymella*, *Epicoccum* and *Phoma* [Kiss and Nakasone 1998; Sullivan and White 2000]. This was elucidated thanks to phylogenetic analyses based on the ITS region, cultural behaviours, and morphology of pycnidia. This research aimed to establish if ITS nucleotide sequences are still being deposited in the GenBank database under the generic name of *Ampelomyces*. In addition, it was explored if the ITS2 S2s improve the distinction between ITS *sequences* from the ‘true’ *Ampelomyces* and those from *Didymella*- or *Phoma*- like strains.

In this analytical work, it was shown that ITS nucleotide sequences derived from eDNA samples are deposited in the GenBank under the generic name of *Ampelomyces* but do not belong to fungi belonging to the genus *Ampelomyces*. Nucleotide contents and sequence length of the ITS and spacers ITS1 and ITS2 from putative *Ampelomyces* were significantly different to those from type strain of *Ampelomyces*. Furthermore, by analysing the predicted assembly of the proximal stem of the ITS2 region, two pseudogenes were detected for the first time to occur in the nuclear ribosomal RNA of the *Ampelomyces* population, of which one is likely to affect the ribosomal processing (i.e., low levels of transcript are produced) [Côté and Peculis 2001], while the second mutation

probably cannot negatively impact the ribosomal biogenesis or have a biological function.

The phylogeny based on alignment of sequences and structures of the ITS2 improve the barcode gap by two-times between the ‘true’ *Ampelomyces* and putative *Ampelomyces* fungi [Prah et al. 2021]. The phylogenetic tree based on the combined alignment of ITS2 sequences and S2s divides *Ampelomyces* strains in four major clades, of which correspond to four major ITS2 S2 models. The clear differences in motifs contents among *Ampelomyces* ITS2 S2s, which some are found in vertebrates and yeast [Joseph et al. 1999], suggest different mechanisms of ribosomal regulation can occur in *Ampelomyces* lineages [Prah et al. 2021].

A previous published work revealed that some hosts-specificity exists in *Ampelomyces* extracted from APM [Kiss et al. 2011]. The niches of hyperparasites strains infecting APM and non APM overlapped but were genetically different [Kiss et al. 2011]. APM *Ampelomyces* with a unique haplotype was shown to evolve by the evolutionary pressure of the phenology of their mycohost [Kiss et al. 2011], which overwinter in apple buds [Stalder 1955] and cause epidemics in spring, while those non APM cause epidemics in the autumn season [Kiss 1998]. Curiously, in this phylogenetic analysis based on the ITS, the Chinese non-APM *Ampelomyces* originally extracted from *P. ferruginea* (Liang et al. 2007) grouped in the same clade with APM *Ampelomyces*, and this result had not been explained.

The results of this thesis show that these strains grouped in the same clade as share similar ITS2 S2s. In addition, ITS2 S2s reflect the phylogeny of *Ampelomyces*. Clear differences were noticed among these models. Models 4 (APM *Ampelomyces P. leucotricha*) and 5 (non-APM *Ampelomyces* from *P. ferruginea*) contained in clade 2 were grouped based on similarities of their S2s models. As variations in the ITS2-proximal stem model are reliable evidence of the presence of pseudogenes [Harpke and Peterson 2008]. The two variations in the ITS2-proximal stem model were predicted to occur in ITS sequences of two *Ampelomyces* isolates. This finding suggest some *Ampelomyces* lineages can be of pseudogenic origin. In accordance to the work of Côté and Peculis (2001), the

mutations observed in the ITS2-proximal stem of the *Ampelomyces* isolated from *P. xanthii* suggest that the maturation process of the pre-ribosomal RNA is not happening correctly (Reviewed in Prahl et al. 2022). If pseudogenes occur in the nrDNA of *Ampelomyces*, it is also possible that some of them can either have a positive effect on ribosomal synthesis, and then, undergo natural selection (Figure 2), or not effect on ribosomal processing, and then, eliminated by concerted evolution [Elder and Turner 1995; Naidoo et al. 2013; De Luca et al. 2021]. Whether or not pseudogenes are non-functional is currently under debate [Cheetham et al. 2020] as, for example, some pseudogenes were shown to produce functional transcripts (Gong et al. 2019).

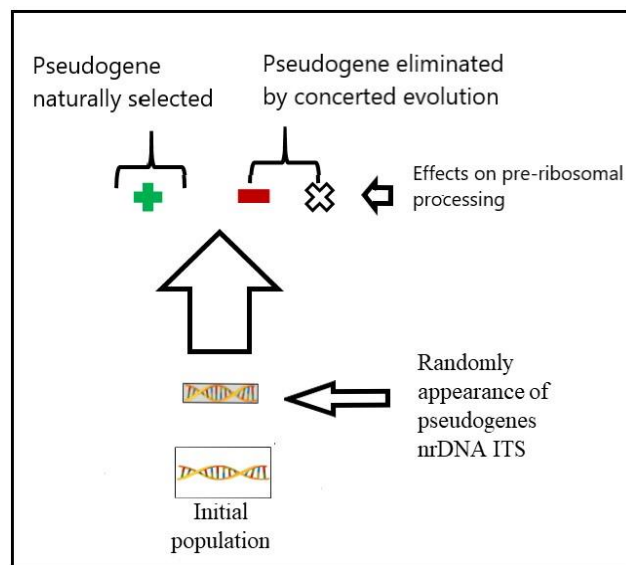


Figure 2

Origin of *Ampelomyces* sister clades. The picture depicts the possible formation of new *Ampelomyces* lineages. Randomly appearance of pseudogenes can occur in the nrDNA ITS region. Some pseudogenes can provide good fit (indicated with a green plus symbol) to the ribosomal processing machinery and be naturally selected. If pseudogenes stop the ribosomal synthesis (red minus symbol) or do not provide any trait (white cross), these are eliminated by concerted evolution and its fate determined by genetic drift. Illustration by Rosa Prahl (2022).

Furthermore, ITS2 S2s models 4, 5, and 6 from *Ampelomyces* extracted from *P. leucotricha*, *P. ferruginea*, and *E. necator*, respectively, share common motifs found in ITS2 S2s of vertebrates and yeast [Joseph et al. 1999]. This finding suggests, for the first time, mechanisms of ribosomal synthesis are shared between *Ampelomyces* mycoparasites and vertebrates.

In conclusion, this study improves the classification of *Ampelomyces* spp. *sensu stricto* from fungi closed related of the genera *Didymella*, *Epiccocum* and *Phoma* based on nucleotide contents of the complete ITS region and the simultaneous alignment of ITS2 sequences and S2s. The findings of this thesis provide significant insights on the evolutionary history of *Ampelomyces* lineages. Moreover, this thesis shows the ‘true’ *Ampelomyces* sequences in public databases can be identified by comparing their ITS sequence length and nucleotide contents together with their S2s. The *Ampelomyces* S2s are functional different as some groups contain previous motifs only found in vertebrates and yeast and related to pre-ribosomal processing. According to this, APM-*Ampelomyces*, non-APM *Ampelomyces* (*P. ferruginea*), and GPM *Ampelomyces* have different mechanisms of pre-ribosomal processing from the rest of the *Ampelomyces* population.

Please see below Paper 1.

RESEARCH ARTICLE

The role of internal transcribed spacer 2 secondary structures in classifying mycoparasitic *Ampelomyces*

Rosa E. Prah^{1*}, Shahjahan Khan², Ravinesh C. Deo³

1 School of Sciences, University of Southern Queensland, Toowoomba, Queensland, Australia, **2** School of Sciences, Centre for Health Research, Centre for Applied Climate Sciences, University of Southern Queensland, Toowoomba, Queensland, Australia, **3** School of Sciences, University of Southern Queensland, Toowoomba, Queensland, Australia

* u1114537@umail.usq.edu.au



OPEN ACCESS

Citation: Prah RE, Khan S, Deo RC (2021) The role of internal transcribed spacer 2 secondary structures in classifying mycoparasitic *Ampelomyces*. PLoS ONE 16(6): e0253772. <https://doi.org/10.1371/journal.pone.0253772>

Editor: Kandasamy Ulaganathan, Osmania University, INDIA

Received: December 13, 2020

Accepted: June 13, 2021

Published: June 30, 2021

Peer Review History: PLOS recognizes the benefits of transparency in the peer review process; therefore, we enable the publication of all of the content of peer review and author responses alongside final, published articles. The editorial history of this article is available here: <https://doi.org/10.1371/journal.pone.0253772>

Copyright: © 2021 Prah et al. This is an open access article distributed under the terms of the [Creative Commons Attribution License](https://creativecommons.org/licenses/by/4.0/), which permits unrestricted use, distribution, and reproduction in any medium, provided the original author and source are credited.

Data Availability Statement: All relevant data are within the manuscript and its [Supporting Information](#) files.

Funding: This research was supported by the financial support of an Australian Postgraduate

Abstract

Many fungi require specific growth conditions before they can be identified. Direct environmental DNA sequencing is advantageous, although for some taxa, specific primers need to be used for successful amplification of molecular markers. The internal transcribed spacer region is the preferred DNA barcode for fungi. However, inter- and intra-specific distances in ITS sequences highly vary among some fungal groups; consequently, it is not a solely reliable tool for species delineation. *Ampelomyces*, mycoparasites of the fungal phytopathogen order *Erysiphales*, can have ITS genetic differences up to 15%; this may lead to misidentification with other closely related unknown fungi. Indeed, *Ampelomyces* were initially misidentified as other pycnidial mycoparasites, but subsequent research showed that they differ in pycnidia morphology and culture characteristics. We investigated whether the ITS2 nucleotide content and secondary structure was different between *Ampelomyces* ITS2 sequences and those unrelated to this genus. To this end, we retrieved all ITS sequences referred to as *Ampelomyces* from the GenBank database. This analysis revealed that fungal ITS environmental DNA sequences are still being deposited in the database under the name *Ampelomyces*, but they do not belong to this genus. We also detected variations in the conserved hybridization model of the ITS2 proximal 5.8S and 28S stem from two *Ampelomyces* strains. Moreover, we suggested for the first time that pseudogenes form in the ITS region of this mycoparasite. A phylogenetic analysis based on ITS2 sequences-structures grouped the environmental sequences of putative *Ampelomyces* into a different clade from the *Ampelomyces*-containing clades. Indeed, when conducting ITS2 analysis, resolution of genetic distances between *Ampelomyces* and those putative *Ampelomyces* improved. Each clade represented a distinct consensus ITS2 S2, which suggested that different pre-ribosomal RNA (pre-rRNA) processes occur across different lineages. This study recommends the use of ITS2 S2s as an important tool to analyse environmental sequencing and unveiling the underlying evolutionary processes.

Award granted to Rosa E. Prah from the Graduate Research School of University of Southern Queensland, Australia.

Competing interests: No authors have competing interests.

Introduction

Ribosomes are RNA-protein complexes that are responsible for translating messenger RNA (mRNA) into protein. The eukaryotic nuclear ribosomal DNA (nrDNA) cistron encodes the rRNAs for the small (18S rRNA) and large (5.8S and 28S rRNA) ribosomal subunits. The nrDNA region also contains two spacers. The 1 internal transcribed spacer, ITS1, is located between the 18S and the 5.8S genes and the 2 internal transcribed spacer, ITS2, resides between the 5.8S and the 28S genes [1,2]. In order to fulfill the demand of protein production for various cellular processes, the nrDNA cistrons are transcribed at a high rate by the enzyme polymerase I [3], which generates pre-rRNA. Subsequently, this pre-rRNA undergoes multiple posttranscriptional processing events as well as ribosome biogenesis, which generates functional rRNAs comprising 5.8S, 18S and 28S units. During processing both spacers are removed [1,2].

rRNA genes are highly similar within and between individuals of the same species. Nevertheless, rRNA sequence variations are sufficiently divergent to differentiate one species from another. Consequently, the ITS1, 5.8S and ITS2, named the internal transcribed spacer (ITS) region, have been widely used for molecular identification and phylogenetic studies [4]. Indeed, the nrDNA ITS region is the preferred barcode in fungi classification [5]. However, the identification of fungal DNA environmental samples is challenging. Several taxonomical and phylogenetic fungal groups require appropriate cultural conditions before identification although many fungi are unculturable [6]. Furthermore, for some fungal groups, specific primers are required for successful amplification of other appropriate molecular markers [5,7]. In accordance with the taxonomy and phylogeny of the fungal group under study, the use of only one molecular marker can result in poor species discrimination resolution [8]. For a barcode gap, the interspecific genetic variability needs to be higher than the intraspecific variability. In fungi, the nrDNA ITS region has been widely used as a DNA barcode [8] as it has enough genetic variability to the species level, but sometimes it does not resolve closely phylogenetic related species and some fungi require extra identifiers for species delimitation within a determined genus or family [9]. For example, if some taxa have low ITS interspecific variability other molecular markers need to be used to precisely report genetic diversity [9]. Conversely, intragenomic variation of the ITS can result in overestimate the intraspecific variability in some fungi [9–12]. Thus, relying in the use of only one molecular marker in some fungi can result in poor species discrimination resolution and other molecular barcodes may be required as the accuracy of the identification can be compromised. Therefore, it is crucial to have an optimum barcode gap.

In addition, the ITS1 and ITS2 are assumed to evolve neutrally. However, it has been probed that they are subjected to secondary structural constraints [13,14], which may have an impact on phylogenetic inferences. For instance, the phylogeny of the species from the genus *Ampelomyces* are primarily based on the ITS region, where some contrasting results have been obtained. Interesting, the utility of *Ampelomyces* ITS2 secondary structures (S2s) to study its phylogeny has not been investigated even when several works have demonstrated ITS2 S2s can provide with important features to improve phylogenetic analyses [13,15].

Ampelomyces spp. are mycoparasites of the Erysiphaceae fungi [16], which are devastating plant pathogens [17,18] that are responsible for powdery mildew (PM) diseases that afflict important agricultural and ornamental crops worldwide [19]. Despite environmental and health risks [20], agrochemicals are mainly used to control and prevent these PM infections [21]. The potential use of *Ampelomyces* strains as biocontrol agents against PM fungi have been tested in both field [22–24] and laboratory environments [25,26]. Two different strains [25,27] have been commercialized as biofungicides with some degree of effectiveness [22]. In

order to advance the development of potent pest control products based on *Ampelomyces* strains, it is important to fully characterize their intra- and inter-population genetic diversity over space and time. Some studies suggest that the *Ampelomyces* mycoparasites are complex organisms that lack host specificity [28,29]. Nevertheless, temporal isolation can lead to genetic variability within populations [23]. *Ampelomyces* strains that infect apple powdery mildew (APM, caused by *Podosphaera leucotricha*) were found to be cryptic species of non-apple powdery mildew (non-APM) that resulted from an effective allopatric process. Furthermore, recombination events between APM and non-APM *Ampelomyces* were also detected, although their sexual reproductive stage was not observed [23].

Undoubtedly, population genetic studies in *Ampelomyces* are difficult to carry out. For example, some nucleotide sequences deposited in public databases under the name of *Ampelomyces* are not related to the mycoparasites by comparing their phylogeny and growth rates in culture [30,31]. In addition, most phylogenetic studies have been based on the ITS region [28–30,32–34] and other molecular markers may be required for species identification due to the high genetic divergence of ITS sequences from some *Ampelomyces* lineages that can reach up to 15% [24,30]. Nevertheless, the successful design of primers for other markers are difficult to obtain, which often occurs for other fungi. In order to resolve these issues and contribute to knowledge and future research in this area, we have investigated whether ITS2 S2s contain specific features that may be incorporated into phylogenetic analysis and provide with novel important information regarding evolutive processes occurring in *Ampelomyces*. Indeed, the utility of the ITS2 S2 to study the phylogeny of several organisms have been demonstrated [15,35] but it has not been investigated in *Ampelomyces*.

This study also has investigated whether the nucleotide sequences of the ITS region from fungi sampled in PM-free environments are still being deposited in the GenBank database as species of the genus *Ampelomyces*. Here, we also evaluated the potential use of the ITS2 S2 as an additional identifier of *Ampelomyces* against the related fungus *Didymella glomerata* (previously known as *Phoma glomerata*) [36] and other putative *Ampelomyces* fungi isolated from non-PM hosts [37–40]. This analysis included all of the nucleotide sequences comprising the ITS region from *Ampelomyces* spp. *sensu stricto* deposited in GenBank until the May 2020 period.

Lastly, we propose that the predicted S2 of ITS2 from *Ampelomyces* spp. obtained from the ITS2 Database (ITS2-DB) web server [41–45] can be utilized as a new guideline for future molecular identification of ITS sequences extracted from environmental DNA samples.

Materials and methods

Sequence acquisition from the GenBank database

The nucleotide sequences of the nrDNA ITS region of all species identified with the name of *Ampelomyces* were searched in the GenBank database using the query: *Ampelomyces* (in plain text). Partial sequences of the ITS region were not included in this analysis. In Table 1 in [S1 File](#) shows the details of all the 376 nucleotide sequences used in this study, which were derived from 376 *Ampelomyces* spp. *sensu stricto*. The former sequences were compared to the following sequences: (1) 10 sequences derived from putative *Ampelomyces* species (Groups 1 and 2), (2) four sequences belonging to *Didymella* species and (3) one sequence from *Phoma* species formed the outgroup taxa ([Tables 2–4 in S1 File](#)).

Group 1 contains two sequences of fungi identified as *Ampelomyces humuli*, which was derived from plant tissues of *Picea abies* decayed root [46] and from *Zea mays* [40]. Group 1 also contains three sequences from fungi known to form a different phylogenetic group from the ‘true’ species of the genus *Ampelomyces* [30,31] and are referred to as *A. humuli* (GenBank

sequence identifier (GI) AF035779), *Ampelomyces quercinus* (GI: AF035778) and *Ampelomyces* sp. (GI: U82452). *Ampelomyces quercinus* is currently known as *Nothophoma quercina* [36], **Table 2 in S1 File**.

Group 2 has five nucleotide sequences belonging to three fungi identified as *A. humuli* isolated from human nasal mucus [39] and soil [37], as well as two fungi identified as *Ampelomyces* spp. derived from creosote-treated cross-tie waste [38] and air samples [47], **Table 3 in S1 File**. Finally, the outgroup is formed by ITS sequences belonging to four *Didymella* species [31,48–50] and one *Phoma* species [51], **Table 4 in S1 File**.

These groups were established in order to differentiate ITS sequences extracted from PMs that were unrelated to the genus *Ampelomyces* by cultural growth and phylogeny [30,31] from those sequences extracted from plant material and PM; and no plant material and human mucus, which were defined as groups 1 and 2, respectively.

Selection and extraction of complete nrDNA ITS sequences from *Ampelomyces* spp. *sensu stricto*

Complete nucleotide sequences of ITS regions belonging to the *Ampelomyces* mycoparasites were selected as ‘true’ if their original references indicated that isolates or strains were derived from PM environments and if their cultural growth characteristics were also indicated. Any other relevant information such as photographs of fruiting bodies (pycnidia) and the type of phylogenetic analysis were considered important for the preliminary selection of key sequences.

We did not include partial sequences of ITS regions even when these were extracted from *Ampelomyces* species infecting PM fungi that had a phylogenetic analysis that correctly identified the mycoparasites from the outgroup taxa. This approach was required to correctly model their ITS2 S2s and to visualize the hybridization model of its proximal stem. All complete ITS sequences were retrieved directly from GenBank in the FASTA format. Redundant or partial sequences that were deposited by different authors that corresponded to the same type of culture were not selected even if they belonged to the genus *Ampelomyces*. We confirmed that these sequences belonged to the *Ampelomyces* mycoparasites by manually checking their original references.

Comparison of ITS sequence length and nucleotide content between species of the genus *Ampelomyces* and to those *Ampelomyces* identified from PM-free environments

In this report, a total of 376 ITS sequences that correspond to the ‘true’ *Ampelomyces* species (**Table 1 in S1 File**) were compared to those from fungal species identified with the generic name of *Ampelomyces* and comprised by (1) putative *Ampelomyces* groups 1 and 2 and (2) outgroup taxa, (**Tables 2–4 in S1 File, respectively**).

Sequence statistics of the nrDNA ITS region and its individual components (ITS1, 5.8S and ITS2)

Statistics of the nucleotide pair bases (G/C) and (A/T) expressed as total percentages from the ITS region and its components (ITS1, 5.8S and ITS2) were calculated for all groups using the Sequence Manipulation Suite at https://www.bioinformatics.org/sms2/dna_stats.html [52]. In order to determine the statistical significance of the sequence lengths and nucleotide contents of the ITS regions among fungal groups, the Kruskal-Wallis rank sum test for multiple independent samples was performed with the web server <https://astatsa.com/KruskalWallisTest/> [53]. In brief, the differences among groups were evaluated by the Dunn post-hoc pairwise multiple comparison test after confirming that at least one group was different using the

Kruskal-Wallis test. Values were statistically significant with a $p < 0.05$. The Dunn p -values were calculated without p -value adjustment.

Partial 18S and 28S sequences that flank the ITS region were deleted before the analysis. Nevertheless, some DNA environmental sequences do not contain the common sequence motifs at the borders of the ITS region (partial 18S and 28S sequences) despite being deposited as complete ITS region sequences; and it is difficult to delimitate them. Thus, the total nucleotide length of the complete ITS region for each fungus was normalized to the maximum length (697 base pairs) expected from ITS region sequences belonging to ascomycetes fungi that were amplified using the primers ITS1f and ITS4 as previously reported [54]; and statistical significance was determined by the Kruskal-Wallis rank sum test as described above.

Insertion-deletion polymorphic analysis of the ITS1 among *Ampelomyces* groups and between unrelated groups

We investigate the distribution of insertion-deletion polymorphisms in ITS1 sequences that could cause sequence length variations. Multiple sequence alignment (MSA) of *Ampelomyces* ITS sequences extracted from each genus of PM were aligned independently, while those from putative *Ampelomyces* Groups 1 and 2 together with the outgroup were conducted with the 'multiple alignment using fast Fourier transform' (MAFFT) web service tool available at <https://mafft.cbrc.jp/alignment/server/> [55–57]. The following parameters were used: (1) a scoring matrix 200 PAM/k = 2 and (2) a gap opening penalty of 1.53. The plots and alignments were executed with a threshold score of 39 ($E = 8.4e-11$). The sequences were aligned using the program MAFFTWS v7 and through the iterative refinement method L-INS-i (accuracy oriented) that includes local pairwise alignment. Resulting multiple alignments were saved in the FASTA format. All ITS1 sequences were extracted from the ITS alignment with MEGA-X V10.1.8 software [58]. Nucleotide polymorphism analysis was conducted with the DnaSP 6.0 software [59,60].

ITS2 structure prediction

To evaluate the utility of ITS2 S2s, the ITS2 sequences from each *Ampelomyces* spp. *sensu stricto* and those from the putative *Ampelomyces* groups were extracted from the alignment between the 5.8S and 28S gene proximal stem motifs using the new version of the web interface Internal Transcribed Spacer 2 Ribosomal RNA Database, ITS2-DB, at <http://its2.bioapps.biozentrum.uni-wuerzburg.de/> [41]. The complementary hybridization of both regions was observed using the ITS2-DB together with its 'Annotate' tool, which functions based on the hidden Markov models (HMMs), [61]. In order to predict the folding of the ITS2 S2, we used an expected value for detection of significant hits below 0.001 ($E\text{-value} < 0.001$) and HMMs for fungal organisms with a minimum size of 150 nucleotides. Visualization of the ITS2 S2 was conducted using the program PseudoViewer v3.0 at <http://pseudoviewer.inha.ac.kr/> [62]. We selected only those S2s that were obtained by direct folding and preferred over other modelled S2s.

We also obtained minimum free energy structures of the ITS2 using the RNAfold online tool, which were visualized using a force directed graph layout (forna) [63] via the web application from ViennaRNA Web Services [64].

Multiple ITS2 sequence-structure alignment and phylogenetic tree of *Ampelomyces* strains

To determine *Ampelomyces* lineages based on its ITS2 S2s, a simultaneous multiple sequence alignment of ITS2 S2s was firstly estimated. We used the online tool LocARNA v4.8.3 at

<http://rna.informatik.uni-freiburg.de> [65] for multiple alignment of RNA molecules. The input data were extracted from the ITS2-DB and comprised 25 ITS2 sequences and structures, which were obtained from the following sources: (1) 21 *Ampelomyces* spp., (2) two putative *Ampelomyces* Group 1 extracted from *Golovinomyces cichoracearum* (GI: U82452) and *P. abies* decayed root (GI: DQ093657), (3) one Putative *Ampelomyces* Group 2 extracted from creosote-treated crosstie waste (GI:GQ241274) and (4) one outgroup member from *Phoma herbarum* (GI: JF810528), (Table 5 in S1 File). The selected parameters consisted of a global alignment in LocARNA-P (probabilistic) mode where the complete input ITS2 sequences were aligned. For the alignment scoring, the default values were used. Thus, the values for structure weight, insertion-deletion (indel) opening score and indel score were 200, -800 and -50, respectively. The match score for the alignment of two identical sequences was 50, while the mismatch score for the alignment of two different sequences was 0. The RIBOSUM matrix was used to score sequence match/mismatch. The parameters of RNA folding energy were used with a temperature of 37°C. The energy parameter settings were described by the Turner model 2004 [66].

The resulting multiple ITS2 sequence-structure alignment was analysed by the molecular evolutionary genetics analysis (MEGA)-X v10.1.8 software in order to calculate a maximum likelihood tree based on the Kimura two-parameter DNA model of evolution [67]. This analysis was conducted with a gamma distribution for the evolutionary rate among sites. The branches of the inferred unrooted tree were assayed using the bootstrap analysis with 1 000 replicates. The phylogram of 21 *Ampelomyces* sequence structure pairs was visualized using FigTree v1.4.4 software [68].

A second phylogenetic tree based on ITS sequences was built to compare the distribution of *Ampelomyces* clades and not related fungi with those obtained using ITS2 S2s, but the dataset consisted of 21 ITS from *Ampelomyces* spp. *sensu stricto* extracted from seven powdery mildew genera and four from the following sources: (1) two putative *Ampelomyces* Group 1 extracted from *Golovinomyces cichoracearum* (GI: U82452) and *P. abies* decayed root (GI: DQ093657), (2) one Putative *Ampelomyces* Group 2 extracted from creosote-treated crosstie waste (GI: GQ241274) and (3) one outgroup member from *Phoma herbarum* (GI: JF810528), (Table 5.1 in S1 File) were utilized as the input dataset to conduct a MSA via the MAFFT web server at <https://mafft.cbrc.jp/alignment/server/> [57] under the previous conditions. Next, phylogenetic analysis was performed with MEGA-X software [58] using the maximum likelihood method and the Tamura-Nei model [69] with gamma distribution among the sites. The branches of the inferred unrooted tree were assayed using bootstrap analysis with 1 000 replicates. The phylogram was visualized using FigTree v1.4.4 software [68].

For a comprehensible analysis, a second phylogenetic tree was constructed as described above, but the input data consisted of 26 ITS2 S2s from *Ampelomyces* spp. *sensu stricto* extracted from seven powdery mildew genera and four from the following sources: (1) Group 1, putative *Ampelomyces* extracted from *P. abies* (GI: DQ093657); (2) Group 2 that consisted of creosote-treated crosstie waste (GI: GQ241274) and (3) two of the outgroup members, *D. glomerata* (GI: MH864401) from soil and *Malus sylvestris* (GI: JF810528), (Table 5.2 in S1 File).

Evolutionary distance estimation among *Ampelomyces* lineages and putative *Ampelomyces*

The resolution power of the phylogeny based on the ITS2 S2s to distinguish the 'true' *Ampelomyces* from putative *Ampelomyces* was evaluated by comparing the genetic divergences obtained among groups based on the simultaneous ITS2 sequences and structures alignment,

and on the MSA of complete ITS sequences. The input data was the 25 ITS2 sequences consisted of 21 from *Ampelomyces* spp., three from putative *Ampelomyces* and one from the out-group taxa as described in the previous section, **Table 5 and 5.1 in S1 File**.

The mean sequence divergence values among the major clades were estimated using MEGA-X software with the log-determinant (log-det) method and the Tamura-Kumar model [70]. The rate variation among sites was modelled using a gamma distribution (with the shape parameter = 5) and standard errors of the estimate distances were calculated with MEGA-X software using the bootstrap method.

Prediction of consensus ITS2 S2s from *Ampelomyces*

For comparative purposes of sequence-structure motifs among fungal groups, the resulting simultaneous alignment of ITS2 sequences and structures obtained via the ITS2-DB was used as input into the 4SALE v1.7.1 software [71,72] to obtain consensus ITS2 S2s from the following sources: (1) five from *Ampelomyces* spp. extracted from *Arthrocladiella mougeotii*; (2) four from *P. leucotricha*; (3) one from *Podosphaera ferruginea*; (4) four from *Erysiphe necator*; (5) one from *Uncinula necator*; (6) four from *Podosphaera fusca* (GI: DQ490745, DQ490747, DQ490754 and DQ490757); (7) one from *Podosphaera xanthii* (GI: DQ490759) and (8) four from putative *Ampelomyces* (GI: DQ093657, GQ241274, JF810528 and U82452).

Results

The first aim of this study was to verify the authenticity of the nucleotide sequences of the ITS regions that were deposited in GenBank under the name *Ampelomyces*. Until May 2020, 808 sequences were retrieved and 19% were derived from environmental sampling of fungi or plant tissues. Amongst all nucleotide sequences belonging to *Ampelomyces* spp. *sensu stricto*, 68% corresponded to the ITS region (complete and partial sequences), 27% were from the *actin1* gene, 2.97% corresponded to nucleotide sequences from the small subunit ribosomal (18S) and the large subunit ribosomal (28S) genes (complete and partial sequences) and 0.98% corresponded to those from microsatellites and the sequence of the complete genome of *Ampelomyces quisqualis* strain MHLAC05119 [8], (**Table 1 in S1 File**). Since most of the sequences corresponded to the nrDNA ITS region, we focused our analysis on complete sequences of this molecular marker that reduced the dataset to 376 sequences.

Ampelomyces spp. ITS nucleotide content and sequence length do not resemble those extracted from environmental DNA and human mucus samples

From the dataset of *Ampelomyces* spp. *sensu stricto* extracted from seven genera of PM fungi (*Arthrocladiella*, *Erysiphe*, *Golovinomyces*, *Neoerysiphe*, *Oidium* sp. subgenus *Pseudoidium*, *Phyllactinia* and *Podosphaera*), we found that the sequence lengths of the complete ITS regions (492–502 bp) and their constituents, the ITS1 (182–193 bp), and ITS2 (149–155 bp) varied across the whole population, **Table 2 in S1 File**.

In contrast, the sequence length from the 5.8S ribosomal gene (157 bp) remained constant. The A/T and G/C content for both spacers and the 5.8S ribosomal gene were above and below 50%, respectively. The lowest G/C content value (39.25%) was observed for the ITS1 (**Table 1**), **Table 3 in S1 File**.

In order to verify if the complete fungal ITS sequences from environmental DNA are related to those from *Ampelomyces* lineages, we have investigated whether they can be differentiated by comparing nucleotide content and sequence length of their complete nrDNA ITS

Table 1. Characterization of the ITS region and their constituents ITS1, 5.8S and ITS2 from *Ampelomyces* spp.

	ITS	ITS1	5.8S	ITS2
Sequence length (bp)	492–502	182–193	157	149–155
Average length (S.E.M.)	498 (0.004)	188 (0.005)	157 (0.00)	152 (0.002)
A/T content (%) range	54.05–58.92	54.59–60.75	53.5–57.32	50.00–58.82
G/C content (%) range	41.08–45.95	39.25–46.5	42.68–46.5	41.18–50.00

n = 376 *Ampelomyces* ITS sequences. Abbreviations: Base pair (bp); Standard error of the mean (S.E.M.).

<https://doi.org/10.1371/journal.pone.0253772.t001>

regions. In addition, we used five ITS sequences retrieved from species of the *Didymella* and *Phoma* genera, as a reference outgroup. These species are commonly used as outgroup taxa in phylogenetic studies of the *Ampelomyces* mycoparasites [23,33]. Thus, we compared the sequence length and nucleotide content of the ITS sequences from *Ampelomyces* spp. *sensu stricto* to ITS sequences belonging to two groups of putative *Ampelomyces*. Group 1 contains sequences from *Ampelomyces heraclei*, *A. humuli*, and *Ampelomyces* sp. that were previously shown to be unrelated to the genus *Ampelomyces* [30,31]. It also contains two other sequences of fungi classified as *A. humuli*, which were isolated from plant material (*P. abies* and *Zea mays*) (Table 4 in S1 File).

On the other hand, Group 2 contains sequences extracted from human and environmental DNA samples, which were classified under the generic name of *Ampelomyces* (Table 5 in S1 File). We found that the average ITS sequence length for Groups 1 (453.6 bp ± 0.92) and 2 (453 bp ± 1.84), Table 2, differed significantly (*p*-values: < 0.001) by 50 bp when compared to those extracted from the entire *Ampelomyces* population (498 bp ± 0.004). Indeed, the average sequence lengths of the putative *Ampelomyces* ITSs were similar to those extracted from species of the *Didymella* and *Phoma* genera (452 bp ± 0.0), (Table 6 in S1 File).

Several fungal environmental DNA ITS samples from GenBank do not contain nucleotide sequence information at the borders flanking the complete ITS region. Thus, all of the sequence lengths were normalized to the maximum sequence length that can be obtained for fungal species ascomycetes using the primers ITS1f and ITS4 as previously described [54]. After normalizing the sequence lengths, we observed the same differences in length variation of ITS sequences among all fungal groups (S2 File, Table 7 and 7.1 in S1 File) as described above. In addition, the normalized sequence length of the complete ITS region from the *Ampelomyces* lineages is significantly (*p*-values: < 0.001) higher than those from the putative *Ampelomyces* (Fig 1), S2 File, Table 7.1 in S1 File.

On the other hand, the normalized sequence lengths of the 5.8S gene and the ITS2 were similar across all the fungal groups. Conversely, the normalized sequence lengths of the ITS1

Table 2. Variations in ITS region sequence length can distinguish between *Ampelomyces* spp. and misidentified fungi.

	ITS1 (bp)	5.8S (bp)	ITS2 (bp)	ITS (bp)
<i>Ampelomyces</i> spp. <i>sensu stricto</i>	182–193	157	149–155	492–502
Putative <i>Ampelomyces</i> , Group 1	139–143	156–157	156–157	452–457
Putative <i>Ampelomyces</i> , Group 2	140–142	157	148–157	446–456
Outgroup taxa	139	157	156	452

The sequence lengths of the ITS region from *Ampelomyces* spp. (n = 376) were significantly higher than those from putative *Ampelomyces* Groups 1 and 2 (n = 5 each) as well as the outgroup (n = 5) with a Kruskal-Wallis chi-squared statistic value of 53.27 and *p*-values of 1.598204e-11. No differences in the sequence lengths of the ITS regions were observed between the misidentified fungi and the outgroup taxa with *p*-values of 1.0 and 3 degrees of freedom.

<https://doi.org/10.1371/journal.pone.0253772.t002>

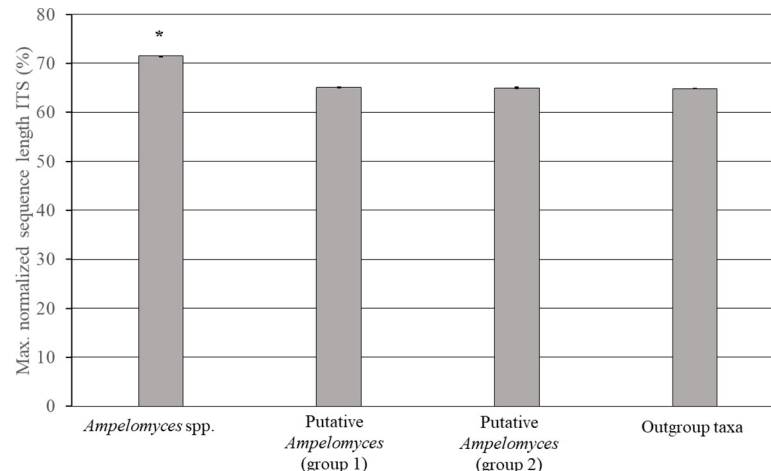


Fig 1. Normalized nrDNA ITS sequence lengths from environmental fungi are similar to those from the outgroup. The graph shows the normalized sequence length (%) of the ITS region from *Ampelomyces* strains ($n = 376$), putative *Ampelomyces* Groups 1 ($n = 5$) and 2 ($n = 5$) as well as the outgroup ($n = 5$). The normalized ITS sequence length of the *Ampelomyces* strains was significantly higher than those from putative *Ampelomyces* Groups 1 and 2 as well as from fungi belonging to the outgroup taxa, with a Kruskal-Wallis chi-squared statistic value of 53.27, a p -value of $1.59e-11$ and 3 degrees of freedom. The error bars indicate the S.E.M. and the * indicates the statistical significance at the 5% confidence level.

<https://doi.org/10.1371/journal.pone.0253772.g001>

from *Ampelomyces* spp. were significantly (p -values: < 0.001) higher than those from Groups 1 and 2 as well as the outgroup taxa (Table 3).

In addition, the A/T content of the ITS sequences from *Ampelomyces* spp. (Fig 2A) were significantly (p -values: < 0.001) higher than those from putative *Ampelomyces* Groups 1 and 2 as well as the outgroup taxa based on the Kruskal-Wallis test and Dunn's post-hoc test for multiple comparisons. Conversely, the C/G content (Fig 2B) around the median of the ITS sequences from *Ampelomyces* spp. were significantly (p -values: < 0.001) lower than those from putative *Ampelomyces* groups and the outgroup taxa based on the Kruskal-Wallis test and Dunn's post-hoc test for multiple comparisons.

Even though this study was not focused on identifying the ITS sequences from PM-free environments, we have found that the A/T and C/G median values of fungal Group 1 overlapped the median value from the outgroup. This indicated that the putative *Ampelomyces* from Group 1 are likely related to the outgroup taxa. We also observed that the nucleotide content values from fungal Group 2 were more varied, but not statistically different from fungal Group 1 (p -value: 0.98 and significance at 5%) and the outgroup taxa (p -value: 0.95 and

Table 3. The maximum normalized sequence lengths of the 5.8S gene and ITS2 spacer were conserved among all fungal groups.

	ITS1 (%)	5.8S (%)	ITS2 (%)
<i>Ampelomyces</i> spp. <i>sensu stricto</i> , $n = 376$	27.01 (0.00)	22.52 ($4.9.e-6$)	21.85 (0.00)
Putative <i>Ampelomyces</i> , Group 1, $n = 5$	20.14 (0.04)	22.46 (0.14)	22.46 (0.01)
Putative <i>Ampelomyces</i> , Group 2, $n = 5$	20.25 (0.02)	22.52 (0.00)	22.20 (0.09)
Outgroup taxa, $n = 5$	19.94 (0.00)	22.52 (0.00)	22.38 (0.00)

Only the normalized ITS1 sequence length from *Ampelomyces* spp. *sensu stricto* was significantly different to those from the other groups, with a Kruskal-Wallis chi-squared statistic value of 46.26 and a p -value of $4.972997e-10$ with 3 degrees of freedom. The S.E.M. is indicated in parenthesis.

<https://doi.org/10.1371/journal.pone.0253772.t003>

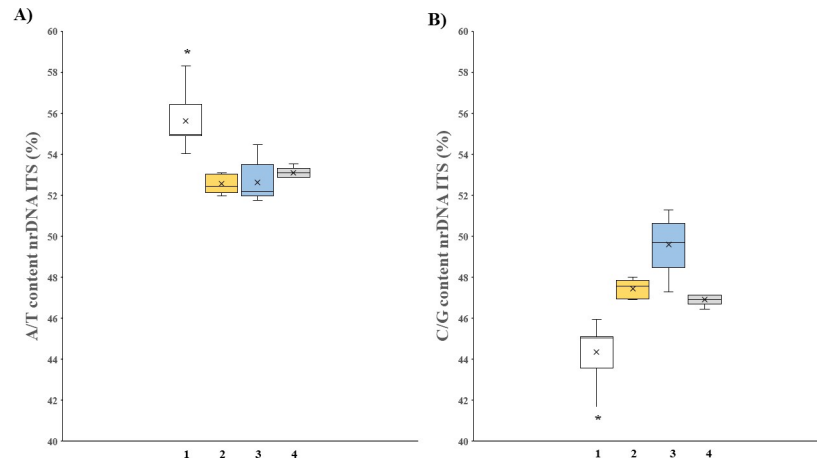


Fig 2. Differences in ITS nucleotide contents help in distinguishing putative *Ampelomyces* from the ‘true’ *Ampelomyces*. (A) The A/T and (B) C/G content values around the median for ITS sequences from *Ampelomyces* spp. (1; n = 376), putative *Ampelomyces* Groups 1 (2; n = 5) and 2 (3; n = 5) as well as the outgroup (4; n = 5). For each box plot, the central line as well as the top and bottom of each box represent the median, the third and first quartile, respectively. The whiskers indicate the maximum and minimum values, while circles above each box plot represent the outliers of each dataset. The statistical significance of the results was assessed using the Kruskal-Wallis test with Dunn’s post-hoc test for multiple comparisons (p -values < 0.05) with 3 degrees of freedom. The differences were statistically significant at the 5% confidence level.

<https://doi.org/10.1371/journal.pone.0253772.g002>

significance at 5%). In summary, no statistically significant differences in the A/T and C/G content were found between putative *Ampelomyces* and the outgroup taxa.

Analysis of deletion/insertion polymorphisms in *Ampelomyces* ITS1 sequences and unrelated sequences

We found that the total number of indels ($I = 8$) between groups of *Ampelomyces* isolated from the same PM genera varied as assessed with DnaSP software [59,60]. Visualization of the MSA comprised of 376 ITS1 sequences, revealed that *Ampelomyces* ITS1 sequences extracted from PM of the genera *Erysiphe*, *Golovinomyces* and *Podosphaera* have indels that are evenly distributed along the sequence. In contrast, the ITS1s from *Ampelomyces* extracted from *Podosphaera fusca* in Korea, contained indels, which are more distributed at the beginning of the ITS1 sequence (first 100 nucleotides), while the same *Ampelomyces* sampled in China harboured indels at the end of the sequence. Conversely, *Ampelomyces* extracted from the genera *Arthrocladiella*, *Oidium* and the subgenus *Pseudoidium* had indels at the beginning and at the end of the sequence, while *Ampelomyces* derived from *Phyllactinia* contained indels localized at the end of the sequence. We also compared the number of indels ($I = 8$) for all *Ampelomyces* ITS1 sequences with those from putative *Ampelomyces* Groups 1 and 2 as well as the outgroup taxa ($I = 6$) where the ITS1 sequences for all outgroup samples contained indels at various positions across the sequence.

Variations in the hybridization model of a proximal stem containing the 5.8S and 28S motifs were found in two *Ampelomyces* strains

We further characterized the ITS sequences by modelling the hybridization of a proximal stem containing the 5.8S and 28S motifs that delimitate the S2 of the ITS2 (Table 8 in S1 File). Among the 376 ITS sequences from the ‘true’ *Ampelomyces* spp., 257 were not amenable for modelling with the ITS2-DB web server because these sequences contained a short 28S motif. Nevertheless, 120 ITS2 sequences were modelled and 118 exhibited the typical hybridization of

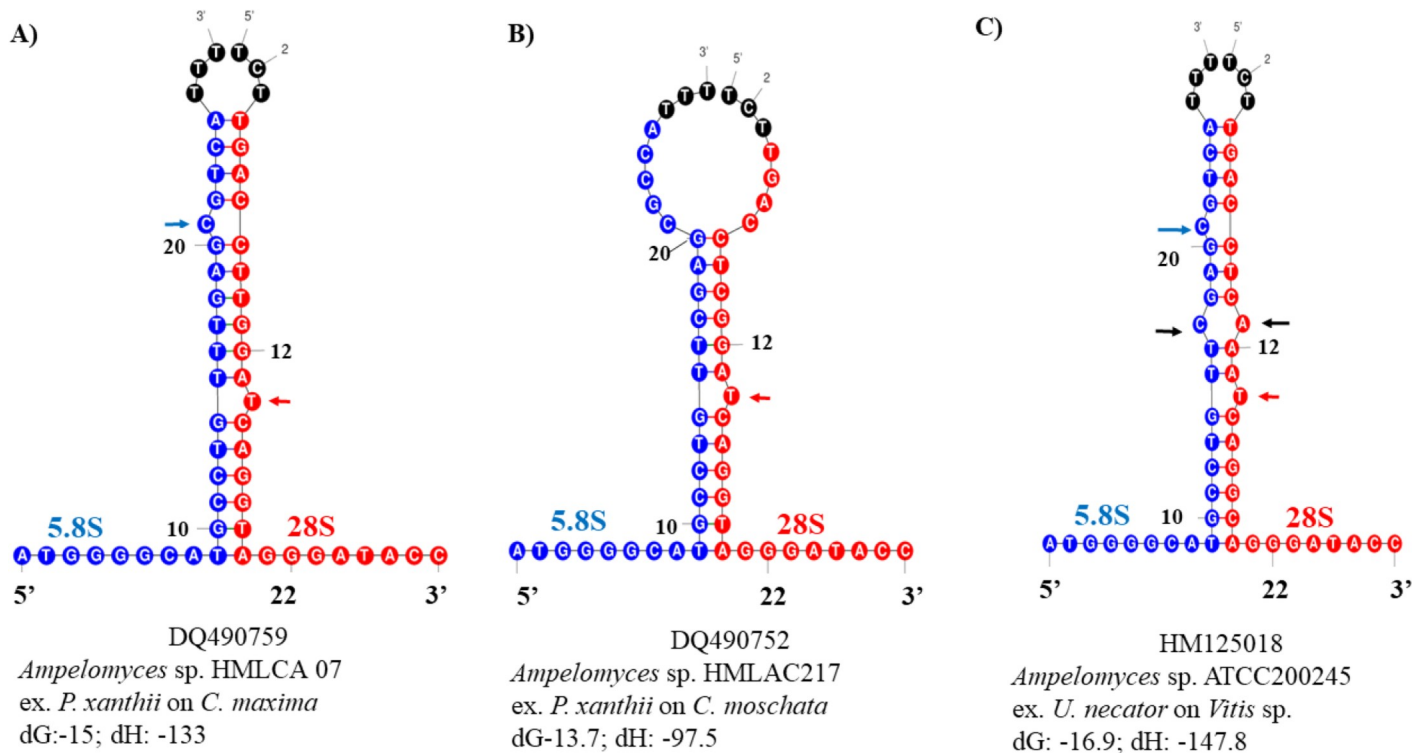


Fig 3. Two variations in the hybridization model of the proximal stem region were found in *Ampelomyces*. (A) The typical 5.8S and 28S hybridization model was obtained from an ITS2 sequence extracted from *Ampelomyces* conidia infecting *P. xanthii*. (B) A variation in the 5.8S and 28S hybridization model detected in *Ampelomyces* sp. infecting *P. xanthii*. (C) Another variation in the 5.8S and 28S hybridization model obtained from *Ampelomyces* sp. infecting *E. necator* (Section *Uncinula*) chasmothecia. The blue nucleotides denote the 5.8S strand, the red nucleotides indicate the 28S strand and the black nucleotides comprise the flanking regions of the ITS2 spacer. The formation of an internal loop is indicated by the two black arrows. The typical free nucleotides found in the 5.8S and 28S strands are indicated with blue and red arrows, respectively. The GenBank accession number is shown below each structure. The Gibbs free energy (dG) and enthalpy (dH) values are shown after the taxon name.

<https://doi.org/10.1371/journal.pone.0253772.g003>

the proximal stem containing 5.8S and 28S motifs with a Gibbs free energy (dG) of -19 and enthalpy (dH) of -147.1 for the ensemble (Table 8 in S1 File). This S2 is formed by an imperfect stem that harbors one free nucleotide on the 5.8S strand and one free nucleotide on the 28S strand. Interestingly, variations in the dG and dH were detected from three other sequences. For example, DQ490759 had a dG and dH of -15 and -133, respectively, but the assembly of the typical proximal stem was not modified (Fig 3A).

Conversely, the DQ490752 and HM125018 sequences exhibited variations in the model along with thermodynamic changes in energies -13.7 and -16.9, respectively. DQ490752 (Fig 3B) corresponded to *Ampelomyces* sp. isolated from the conidia of *P. xanthii* infecting *Cucurbita*. The typical single free nucleotide in the 5.8S motif is absent and it is directly substituted with unaligned nucleotides from both strands that terminate in three free nucleotides. Another variation of the model was identified in the *Ampelomyces* ITS sequence extracted from the chasmothecia of *Erysiphe necator* (Section *Uncinula*) on grapevine bark (Fig 3C). In this model variant, the typical single free nucleotide from the 5.8S motif is absent and it is directly substituted with unaligned nucleotides from both strands that terminate in three free nucleotides. In addition, the dG and dH values for the ensemble of the typical hybridization model of the proximal stem from 118 *Ampelomyces* ITS2 sequences was -19 and -147.1, respectively. Even though we modelled a small sample of predicted hybridized stems, it appeared that stems with dGs less than -13.7 destabilized this secondary structure while values energy between -15 and -19 confer to the structure with some flexibility.

One common ITS2 S2 was found across *Ampelomyces* spp. extracted from seven PM genera

From the dataset comprised of 120 ITS2 sequences, only 87 were directly folded and modelled (Table 8 in S1 File). We obtained seven different models. All contained a core structure with four helices (I–IV) and helix III was the longest (Fig 4A). All helices III contained a motif that varied across the *Ampelomyces* lineages (Fig 4A and 4B).

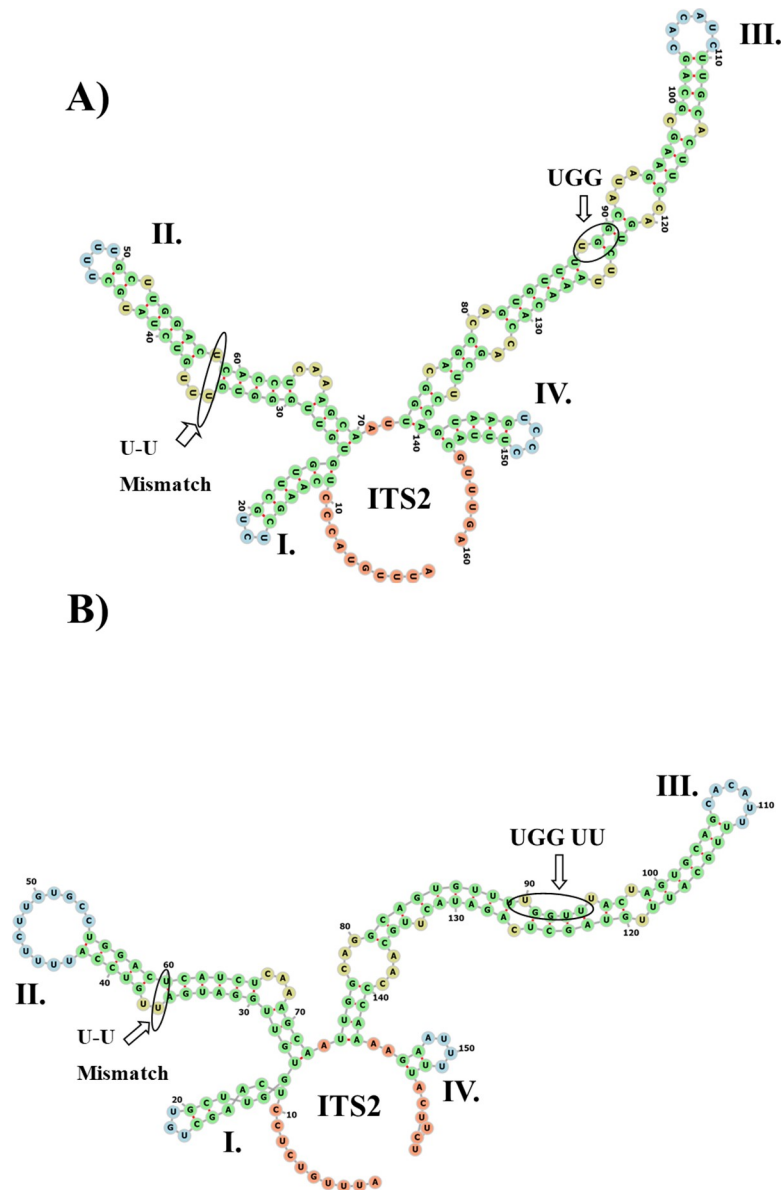


Fig 4. Common features of the ITS2 S2 from *Ampelomyces*. (A) The ITS2 S2 from *Ampelomyces* extracted from seven PM genera. The ITS2 contained a core structure with four helices (I–IV), a U-U mismatch on helix II and a large helix III containing a UGG motif. (B) This ITS2 S2 was found in *Ampelomyces* sampled in China (GI: DQ490752). The UGGU and UU motifs were located in helix III. The minimum free energy structures were calculated with RNAfold and visualized using a force directed graph layout with the Vienna RNA Web Services [64]. The helices are indicated with Roman numerals (I–IV). The U-U mismatch on helix II and the UGG, UGGU and UU motifs are indicated with arrows.

<https://doi.org/10.1371/journal.pone.0253772.g004>

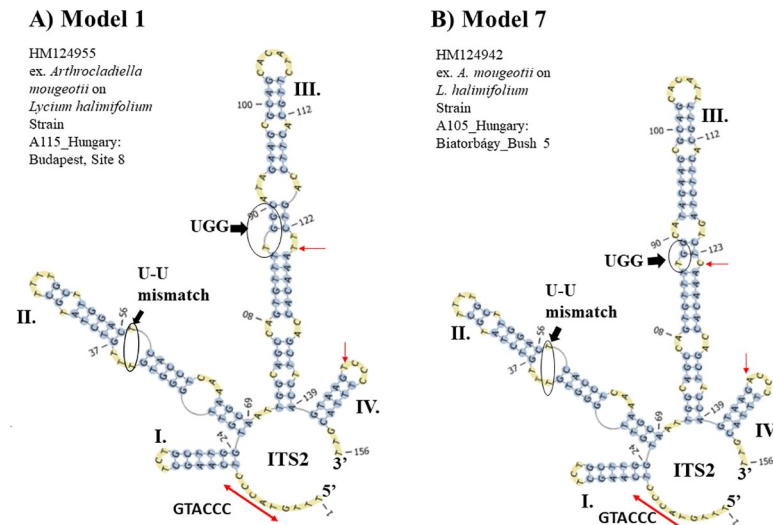


Fig 5. The most common ITS2 S2 (Model 1) found in the *Ampelomyces* population. (A) The ITS2 S2 Model 1 derived from *Ampelomyces* extracted from seven PM genera. (B) The ITS2 S2 Model 7 derived from *Ampelomyces* extracted from *A. mougeotii*. Compared to Model 1, Model 7 contains several nucleotide substitutions. Specifically, nucleotides cytosine and uracil in helices III and IV, respectively of Model 1 are present as uracil and thymine in the helices III and IV, respectively of Model 7; (red arrows indicate nucleotide substitutions). The helices are indicated by Roman numerals (I–IV). The following shared ITS2 features are shown in black arrows and circles: (1) a U–U mismatch on helix II and (2) the UGG motif on helix III. A single-stranded ring between helices I and IV is indicated with red left right arrows. It comprises the sequence GTACCC or *UACCC when T is substituted with U. The structures were directly folded and modelled using the ITS2-DB.

<https://doi.org/10.1371/journal.pone.0253772.g005>

The most common S2 (Model 1) found in the *Ampelomyces* population is represented by a four-fingered model with a single-stranded ring rich in pyrimidines situated between helices I and IV. Model 1 also contains the conserved sequence, GTACCC (Fig 5A). In addition, between helices II and III there is another single-stranded ring of two nucleotides (A and T). Helix III comprises the largest helix with five internal loops that terminates in a single-stranded loop of six unpaired nucleotides.

Variations of Model 1, referred to as 1–2 and 1–3, were observed in two *Ampelomyces* sequences extracted from *A. mougeotii* (Slides 1–3 in S2 File). The variations included a deletion of a pyrimidine in an internal loop of helix II and pyrimidine additions in the single-stranded rings between helices II and III as well as III and IV (slide 3 in S2 File). Model 1 was found in those *Ampelomyces* spp. infecting several PM species representing seven genera, specifically from *A. mougeotii* on *Lycium hamilifolium*, *Erysiphealni*, *Erysipheberberidis*, *Erysipheconvolvuli*, *Erysiphecruciferarum*, *Erysipheeuonymi*, *Erysipheheraclei*, *Erysiphepolygona*, *Erysiphesordida*, *Erysiphe* sp., *Erysiphetrifolii*, *Golovinomycescichoracearum* on *Aster salignus* and on *Lactuca* sp., *Golovinomycesorontii*, *Neoerysiphegaleopsidis*, *Oidium* sp., *Phyllactiniafraxini*, and *Podosphaera pannosa* (slides 4–13 in S2 File).

A major variation of Model 1 referred to as Model 7 was found from an ITS2 S2 from *Ampelomyces* sp. extracted from *A. mougeotii* infecting *L. hamilifolium* and sampled in Biatorbágy, Hungary (Fig 5B, slide 14 in S2 File). Model 7 contained transition and transversion mutations on helices III and IV, respectively. The common features of Models 1 and 7 are the presence of the U–U mismatch on helix II and the UGG motif on helix III.

The second most common S2, Model 2, (Fig 6A) contains a distinctive helix II that has two bulges ending in a large single-stranded loop of 12 unpaired nucleotides (slide 14 in S2 File). Between helices II and III there is a single ring with one nucleotide (A). In addition, helix III

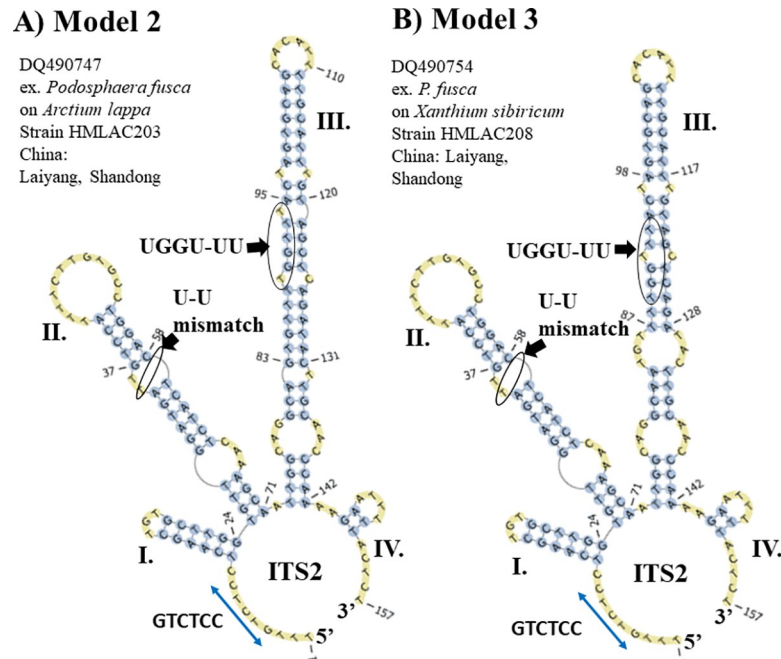


Fig 6. The second most common ITS2 S2 (Model 2) found in the *Ampelomyces* population. (A) The ITS2 S2 Model 2 derived from mycoparasites extracted from the three PM genera *Arthrocladiella*, *Golovinomyces* and *Podosphaera*. (B) The ITS2 S2 Model 3 was only found in one ITS2 sequence (GenBank accession number DQ490754) from *Ampelomyces* sp. extracted from *P. fusca*. The helices are indicated by Roman numerals (I–IV). Single-stranded rings (between helices I and IV) for Models 2 and 3 with the sequence GTGTCC are indicated with blue left right arrows. The following shared ITS2 features are indicated by black arrows and circles: (1) a U-U mismatch on helix II and (2) the UGGU and UU motifs on helix III. The structures were directly folded and modelled with the ITS2-DB.

<https://doi.org/10.1371/journal.pone.0253772.g006>

has three internal loops, and two bulges with one unpaired nucleotide on each strand. A single-stranded ring with two nucleotides (A-A) is located between helices III and IV. In addition, Model 2 contains a single-stranded ring between helices I and IV that contains the highly conserved sequence, GTCTCC.

A Model 2 variant, referred to as Model 3, contains a major variation (Fig 6B) in helix III, which comprises four internal bulges. Model 3 is derived from an *Ampelomyces* ITS2 sequence (GI: DQ490754) extracted from *Podosphaera fusca* infecting *Xanthium sibiricum*, which was sampled in China. Model 2 was found in *Ampelomyces* ITS2 sequences isolated from the three PM genera, *Arthrocladiella*, *Golovinomyces* and *Podosphaera* (slides 14–19 in S2 File).

In addition, models 2 and 3 contain the U-U mismatch in helix II and the UGGU and UU motifs in helix III (Fig 6A and 6B).

On the other hand, the three ITS2 S2 Models 4–6 (Fig 7A–7C) were only found in *Ampelomyces* ITS2 sequences isolated from *P. leucotricha*, *Podosphaera ferruginea* and *E. necator* (section *Uncinula*), respectively (slides 20–22 in S2 File). Models 4–6 contain an internal loop in helix I and a single-stranded ring between helices II and III that is rich in purines (Fig 7A–7C). Between Models 4 and 5 (Fig 7A and 7B, respectively), major variations were observed in the internal loops and bulges of helix III. Model 6 was only found in *Ampelomyces* extracted from *E. necator*. The helix IV in Model 6 contains a stack of three paired nucleotides and terminates in a single-stranded loop of three unpaired Cs (Fig 7C). Unlike Models 1–3 and 7, Models 4–6 contain a single-stranded ring between helices II and III that is rich in As and a large helix III with a UGGU motif.

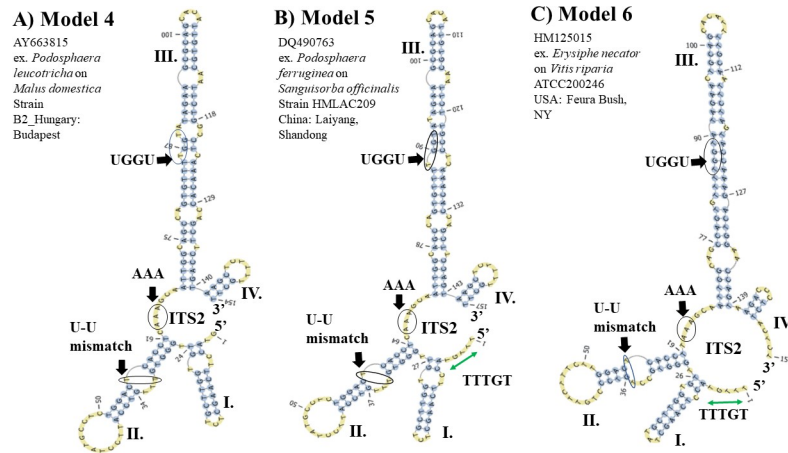


Fig 7. Predicted ITS2 S2 found in the *Ampelomyces* population isolated from two PM genera, *Podospaera* and *Erysiphe*. (A) The ITS2 S2 Model 4 predicted from *Ampelomyces* spp. strains extracted from *P. leucotricha* on *Malus domestica*. (B) The ITS2 S2 Model 5 from *P. ferruginea* on *Sanguisorba officinalis*. (C) The ITS2 S2 Model 6 from *E. necator* infecting *Vitis* sp. *M. domestica* and *S. officinalis* are plants from the family Rosaceae, whereas *Vitis* sp. is a plant from the family Vitaceae. The U-U mismatch motifs, a single-stranded ring rich in adenine nucleotides between helices II and III and a large helix III with a UGGU motif are indicated with black arrows and circles. The structures were directly folded and modelled with the ITS2-DB. The helices are indicated with Roman numerals (I–IV). The single-stranded ring between helices I and IV is indicated with green left right arrows. However, the one from Model 4 is not complete and the green arrow is not shown.

<https://doi.org/10.1371/journal.pone.0253772.g007>

Conversely, most of the ITS2 sequences from *Ampelomyces* strains extracted from the PM *Erysiphe* genus had an ITS2 S2 represented by Model 1, except for those mycoparasitic strains extracted from *E. necator*, which comprise the distinctive ITS2 S2 Model 6 (Fig 7C). Minor changes in Model 6 were observed for *Ampelomyces* strains extracted from *E. necator*. These changes included transition mutations (C ↔ T) in the internal loop and hairpin of helix II and in the single-stranded ring between helices II and III (slides 23–26 in S2 File).

Characterization of the ITS2 S2 improved environmental sequencing analysis

The predicted S2 of the putative *Ampelomyces* spp. from Groups 1 and 2 had the same four-fingered model, but the largest helix (helix III) contains between three and four internal loops and four or six bulges (Fig 8A–8E). In addition, all these S2s only contain the U-U mismatch motif on helix II. Unlike the ITS2 S2 from *Ampelomyces* spp. *sensu stricto*, S2 models from putative *Ampelomyces* contain a single-stranded ring between helices I and IV with the sequence, TCCATG. No variations in the hybridization model of the proximal stem were observed in fungal Group 1, Table 4.1 in S1 File. The ITS2 sequences from the putative *Ampelomyces* Group 1 isolated from plant material or from PM fungi were correctly annotated using both the ITS2-DB and homology modelling (Table 4.2 in S1 File).

The sequences from *A. humuli* (AF035779) and *A. quercinus* (AF035778) (Fig 8A) were homology modelled with the S2 of *D. glomerata* [GenInfo Identifier (GI) model: 332002412] and exhibited 99.4% similarity. Another sequence from an endophytic fungi referred to as *A. humuli* DQ093657 (Fig 8B) was homology modelled based on the GI model 226933708 of the ITS2 from *Didymella pomorum* formerly known as *Peyronella pomorum* [36]. This analysis revealed 98.8% identity between ITS2 sequences of *A. humuli* and *D. pomorum*. In addition, the homology modelling of *A. humuli* (KU204751), Fig 8C, based on the GI model 296840485 of the ITS2 from *Epicoccum* sp. ASR-245 revealed a 98.8% identity.

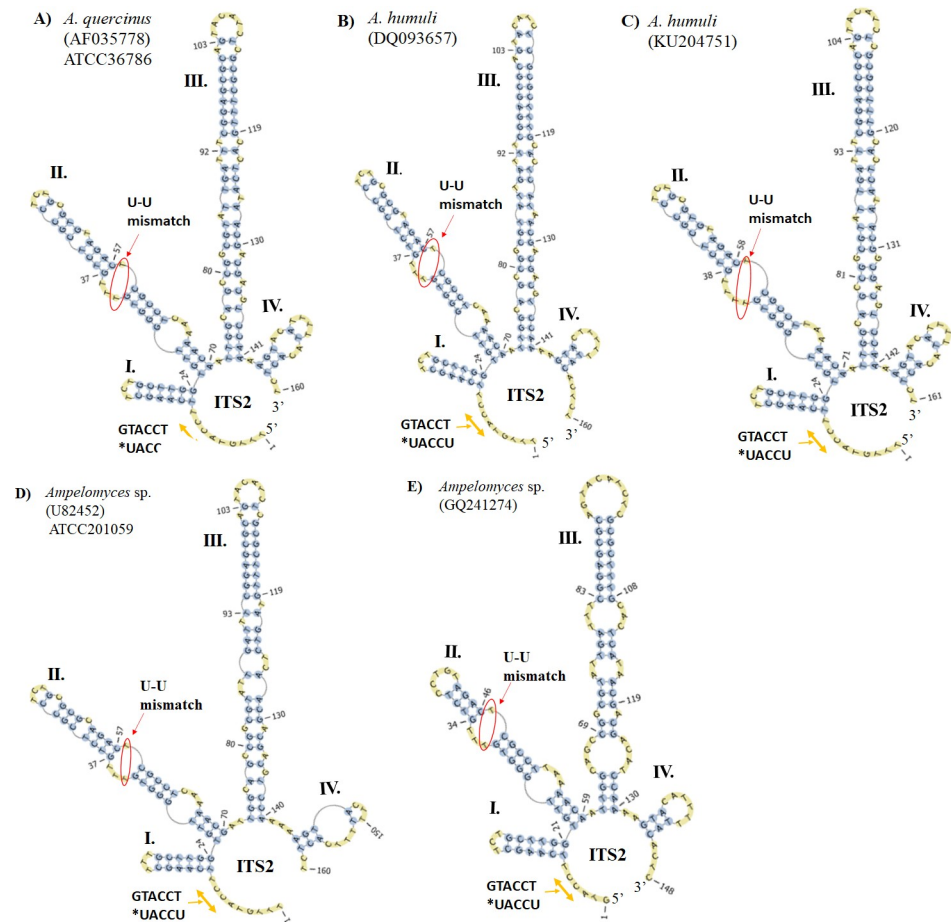


Fig 8. Predicted putative *Ampelomyces* ITS2 S2s were modelled to those from *Didymella*, *Epicoccum* and *Phoma*. (A) The ITS2 S2 from *A. quercinus* was homology modelled based on the ITS2 S2 from *D. pomorum* (FJ839851). (B) The ITS2 S2 from *A. humuli* were modelled according to the ITS2 S2 from *Epicoccum* sp. (GU973791) and (C) from the ITS2 S2 from *D. glomerata* (FJ839851). (D) The ITS2 S2 from putative *Ampelomyces* sp. (Group 1) was homology modelled based on the structure of *P. labilis* (GU237868). (E) The ITS2 S2 from putative *Ampelomyces* sp. (Group 2) extracted from crosstie waste was directly folded and modelled. The helices are indicated with Roman numerals (I–IV). The single-stranded ring between helices I and IV is indicated by orange left right arrows. The U-U mismatch on helix II is indicated with red arrows and circles. The S2s were obtained with the ITS2-DB.

<https://doi.org/10.1371/journal.pone.0253772.g008>

The last ITS2 sequences from Group 1 belonged to an *Ampelomyces* strain (U82452) extracted from *G. cichoracearum* infecting *Cucurbita pepo* (Fig 8D). This sequence was modelled with the structure of *Phoma labilis* (GI model: 294346519) and exhibited 98.8% identity. These results indicated that the Group 1 fungi are not related to the *Ampelomyces* lineages, but are related to the genera *Didymella*, *Epicoccum* and *Phoma*.

For Group 2 fungi (Table 5.1 in S1 File), only three ITS2 sequences were amenable for predicting the hybridization model of the proximal stem. These sequences are from putative *A. humuli* (AF455498, AF455518 and KT363070) and no variations in the hybridization model of their proximal 5.8S and 28S stem were detected. In addition, their S2s were not amenable to direct folding and instead a Basic Local Alignment Search Tool (BLAST) was conducted to search for their homologous sequences and S2s. This analysis demonstrated that fungi identified as *A. humuli* (AF455518 and AF455498) from human nasal mucus were amenable for modelling of their S2 based on the structure of the fungus *Cumuliphoma omnivirens*. In contrast, the S2 from *A. humuli* (KT363070) derived from soil could be predicted using a model of

the ITS2 S2 from the species *D. glomerata* with 99.4% of identity (Table 5.2 in S1 File). Two other ITS2 sequences (GQ241274 and LN80895) from putative *Ampelomyces* spp., which were extracted from environmental DNA samples (treated crosstie waste and air, respectively), were not amenable to verification of the hybridization of the proximal 5.8S and 28S stem due to the short length of the 28S strand. Nevertheless, the S2 from the fungus named *Ampelomyces* sp. (GQ241274) and isolated from creosote-treated crosstie waste could be folded directly (Fig 8E). It has a distinct S2; helix III has only four internal loops and a large hairpin formed by 10 unpaired nucleotides.

On the other hand, in order to predict the ITS2 S2 of the fungus identified as *A. humuli* from air samples, we conducted a BLAST search. This ITS2 S2 could only be partially modelled using the ITS2 S2 from species of the *Phoma* genus as a template with 32.5% of coverage. In addition, the ITS2 S2 of Group 2 were homology modelled using the ITS2 S2 models from the two fungal genera, *Cumuliphoma* and *Phoma*. These results support the hypothesis that these fungi are not related to the genus *Ampelomyces*. In summary, the ITS2 S2 from putative *Ampelomyces* sp. were homology modelled or directly folded and exhibited lower negative energy values between -25.8 and -35.9 than those from *Ampelomyces* spp. *sensu stricto*, which were obtained by direct folding and exhibited energy values between -47.3 and -36.8. This was another difference found between the ITS2 S2s of both fungal groups. The ITS2 S2 of fungi from the outgroup taxa were modelled using the structures from species of the *Didymella* and *Phoma* genera. This suggested that these sequences belonged to fungi from the genera *Didymella* and *Phoma* (Table 6.1 and 6.2 in S1 File).

The ITS2 sequence-structure from PM-free environments did not cluster with those from *Ampelomyces* lineages

We aligned a sample of 21 directly predicted ITS2 S2s from *Ampelomyces* spp. *sensu stricto* together with those extracted from plant tissues and creosote-treated crosstie waste. The ITS2 sequence U82452, included in this analysis, was originally identified as belonging to *Ampelomyces* and was isolated from *G. cichoracearum*. Even though this mycoparasite co-infects the same PM host, this sequence was identified in early studies as belonging to fungi of the genus *Phoma*.

The evolutionary relationship of these fungi was estimated using the maximum likelihood method. The highest log likelihood of the ITS2 S2-based tree was -866.33 (Fig 9A) and the *Ampelomyces* population was grouped into three main clades. The first clade 1a contains all *Ampelomyces* sequences extracted from PM of the genus *Podosphaera* and it is represented by the ITS2 S2 Model 2 as well as its variations. Clade 1b contains *Ampelomyces* sequences extracted from *E. necator* on grapes and it is represented by the ITS2 S2 Model 6 and its variations. All clade 1b samples were collected in the USA. A very well-supported and independent clade 2 was formed by *Ampelomyces* sequences extracted from *P. leucotricha* from several parts of Europe and from *P. ferruginea* sampled in China. This clade 2 is represented by the ITS2 S2 Models 4 and 5. Clade 3 consists of *Ampelomyces* sequences that were isolated from *A. mougeotii* in different locales in Hungary and it is represented by the ITS2 S2 Models 1 and its variations as well as Model 7. Conversely, similar to the ITS2 S2 sequence from *P. herbarum* (GI JF810528), fungi strains isolated from *G. cichoracearum*, *P. abies* decayed root and creosote-treated crosstie waste were not grouped into clades 1–3. This result is in agreement with our previous findings, which confirm that these environmental DNA sequences are not related to the *Ampelomyces* genus.

We also compared the previous tree (Fig 9A) with the one based on the complete ITS region (Fig 9B). We found similar results. However, clade 2a emerged as a sister clade of clade

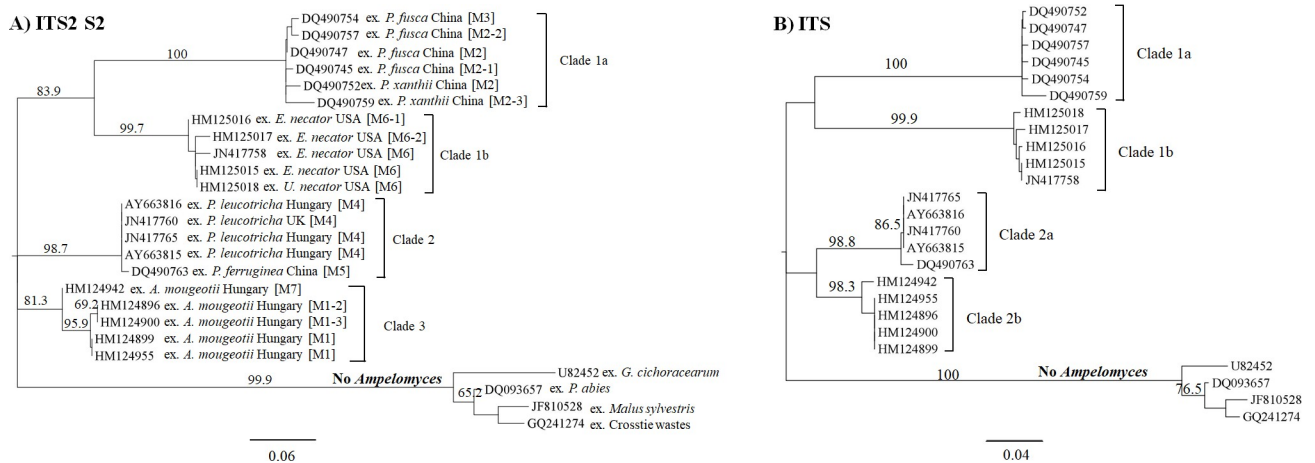


Fig 9. Phylogram based on ITS2 S2s enhance the discrimination between fungal DNA environmental samples and the ‘true’ *Ampelomyces*. (A) The phylogram with the highest log likelihood (-866.33) was based on the ITS2 S2s and inferred via the maximum likelihood (ML) method and the Kimura two-parameter model. An evolutionary rate among sites was modelled with a discrete gamma distribution (+G) parameter = 0.99. (B) The phylogenetic tree with the highest log likelihood (-2040.24) was based on the ITS region and estimated with the maximum likelihood method and the Tamura-Nei model with a discrete gamma distribution (+G) parameter = 0.48. The ML bootstrap values >60% are indicated over the branches and are expressed as percentages. The scale bar represents the nucleotide substitutions per site. The tree was edited with FigTree v1.4.4 software. The GenBank accession numbers are indicated before the taxa names. Abbreviations: ITS2 S2 variations of main Models 1 (M1, M1-2 and M1-3); Models 2 (M2, M2-1, M2-2 and M2-3); Model 3 (M3); Model 4 (M4); Model 5 (M5); Models 6 (M6-1 and M6-2); and Model 7 (M7).

<https://doi.org/10.1371/journal.pone.0253772.g009>

2b. Among the outgroup taxa samples, the ITS region resolved better than the ITS2 S2. Part of this could be due to the small number of samples used in the ITS2 S2 analysis. Even though clades 1a and 3 were represented by *Ampelomyces* extracted from PMs of the genera *Podosphaera* and *Arthrocladiella*, respectively, it does not indicate that these S2s are mycohost-associated. Indeed, in the clade of *Podosphaera*, other Model 2 sequences from *Ampelomyces* extracted from other PMs such as *Arthrocladiella* and *Golovinomyces* were grouped together (Fig 10). Nevertheless, no additional S2 Models (2 nor 3) were found in those samples from Europe. Instead, they were only found in China. Conversely, the ITS2 S2 Model 1 was grouped with others from *Ampelomyces* extracted from seven PM genera.

In order to support our hypothesis that the ITS2 S2 analysis can improve the differentiation between the ‘true’ *Ampelomyces* and unrelated fungi, we determined the genetic divergence distances among groups between the phylogenies. These distance calculations were based on the simultaneous alignment of the ITS2 S2 (Table 4) and the complete ITS region (Table 5). For the ITS2 S2 analysis, the maximum distance observed between clades 1a and 3 was 0.298 ± 0.056 standard error (S.E.) while those between the outgroup taxa and clade 3 was 0.403 ± 0.073 (S.E.), (Table 5).

In contrast, by using the ITS-like DNA barcode, we found that the maximum distance between closed related *Ampelomyces* clades 1a and 2b was 0.186 ± 0.021 (S.E.), while the minimum distance between the outgroup and an *Ampelomyces* clade (clade 2a) was 0.195 ± 0.021 (S.E.), (Table 5). These findings suggested that the ITS could not distinguish *Ampelomyces* from other closely related fungal genera, while the ITS2 S2 exhibited greater discrimination between the outgroup taxa and the closely related *Ampelomyces* clade 3.

Other differences were observed when comparing all consensus ITS2 S2s belonging to each clade (Fig 11A–11D). All *Ampelomyces* consensus structures contain the U-U unpaired motif in helix II. In helix III, the UGG and UU motifs in Models 2 and 3 (Fig 11A), the UGGU motif in Models 6 (Fig 11B), 4 and 5 (Fig 11C) and the UGG motif in Models 1 and 7 (Fig 11D) formed the clades 1a, 1b, 2 and 3, respectively. The AAA motif between helices II and III was

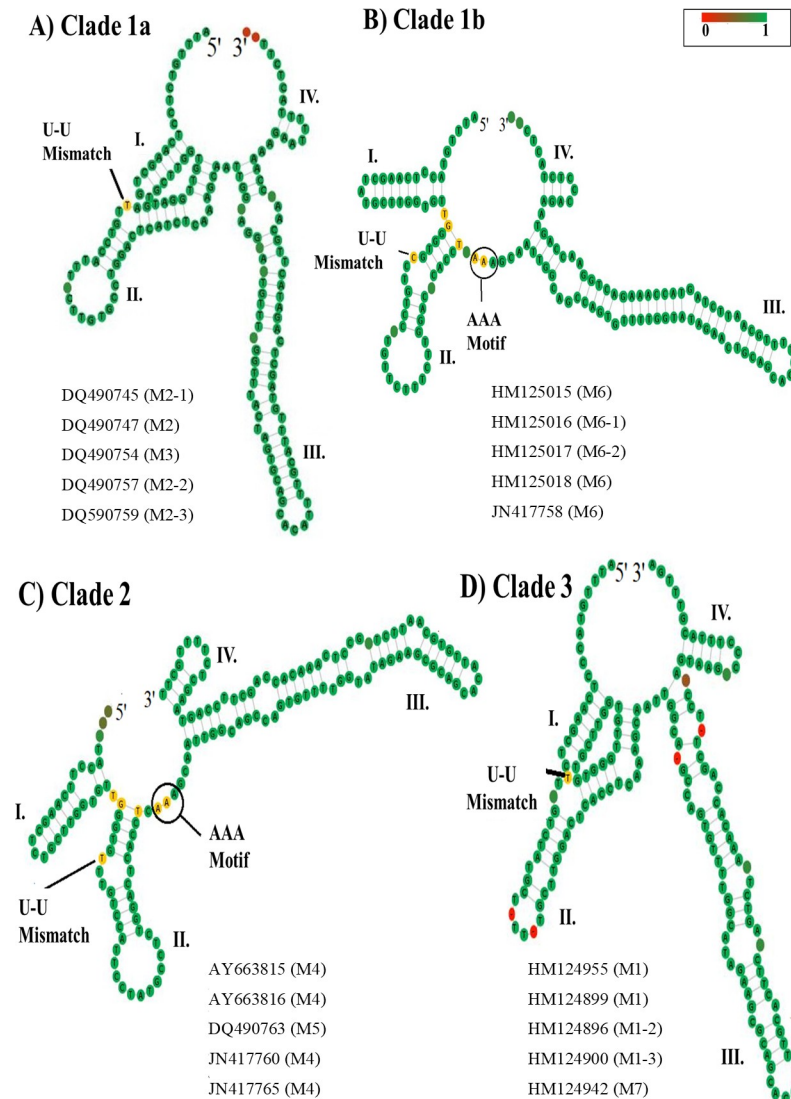


Fig 10. Phylogram based on 26 *Ampelomyces* ITS2 S2s shows that the S2s are not associated with PM hosts. The phylogram with the highest log likelihood (-829.62) is shown based on the Kimura two-parameter DNA model and an evolutionary rate among sites modelled with a discrete gamma distribution (+G) parameter = 0.90. The ML bootstrap values >60% are indicated over the branches and are expressed as percentages. The scale bar represents the nucleotide substitutions per site. The tree was edited with FigTree v1.4.4 software. The GenBank accession numbers are indicated before the taxa names. Abbreviations: ITS2 S2 variations of main Models 1 (M1, and M1-3); Models 2 (M2, M2-1 and M2-3); Model 3 (M3); Model 4 (M4); Model 5 (M5); Models 6 (M6-1 and M6-2); and Model 7 (M7).

<https://doi.org/10.1371/journal.pone.0253772.g010>

only present in *Ampelomyces* extracted from *E. necator* in clade 1b (Fig 11B) and in *Ampelomyces* extracted from *P. leucotricha* and *P. ferruginea* in clade 2 (Fig 11C).

Conversely, the consensus structure from the outgroup taxa do not contain the AAA motif between helices II and III but it does harbor the unpaired U-U motif in helix II (Fig 12A). When the predicted consensus ITS2 S2 from the outgroup was built based on the alignment of the four ITS2 sequences and structures including the gaps (Fig 12B), the consensus S2 was highly modified, indicating that these sequences belong to diverse fungi.

After this comprehensive analysis, the selected nucleotide sequences belonging to *Ampelomyces* spp. *sensu stricto* were included in the S3 File.

Table 4. Estimates of evolutionary divergence over sequence pairs between fungal groups when analysing the ITS2 sequences and structures.

ITS2	1	2	3	4	5
1. Clade 1a		0.045	0.050	0.056	0.090
2. Clade 1b	0.238		0.049	0.042	0.079
3. Clade 2	0.275	0.235		0.033	0.080
4. Clade 3	0.298	0.204	0.137		0.073
5. Outgroup taxa	0.533	0.477	0.444	0.403	

The simultaneous ITS2 S2 alignment was used to calculate the genetic distances among groups via the log-det (Tamura-Kumar) method using MEGA-X V10.1.8 software. The values represent the number of base substitutions per site obtained by averaging over all sequence pairs between groups. The standard error estimates are shown in blue.

<https://doi.org/10.1371/journal.pone.0253772.t004>

Discussion

Improving the accuracy in identifying the ITS sequences derived from environmental DNA sampling of fungi is expected to benefit future fungal genetic population studies including those for *Ampelomyces*. In addition, it may also provide insight into the mechanisms of parasitism, which may improve the use of biocontrol agents against PMs. Previous researches have shown that fungi identified as *A. humuli* or *A. quercinus* were not related to the mycoparasites *Ampelomyces* based on their culture characteristics and phylogeny [30,31]. Indeed, this research shows ITS sequences from plant tissues, environmental DNA samples and human mucus do not belong to species of the genus *Ampelomyces*. This classification is based on their ITS sequence length and nucleotide content, their ITS2 S2 together with simultaneous ITS2 sequence-structure alignment and its corresponding maximum likelihood tree.

On the other hand, S2 analysis has provided insight into the regulatory mechanisms of mycoparasite pre-rRNA S2. Based on the phylogenetic tree of ITS2 sequences and structures, we propose that a basic ribosomal regulatory mechanism exists across the entire mycoparasite population since the S2 Model 1 was observed in strains extracted from seven PM genera. Moreover, major differences in S2 were found in the internal loops of hairpins that are essential for alternative splicing during pre-rRNA processing [74]. Indeed, mutations occurring adjacent to these areas are known to stop the rRNA maturation process [75]. Interestingly, only ITS2 S2 Models 4–6 from *Ampelomyces* strains isolated from *P. leucotricha*, *P. ferruginea* and *E. necator*, respectively, share conserved motifs i.e., poly adenine nucleotides in the single-stranded ring between helices II and III, that were previously reported in yeasts and vertebrates [73]. This suggests that in some *Ampelomyces* mycoparasites, post-transcriptional processes for ribosomal biogenesis may be similar across higher organisms, such as fish and mammals [73]. Conversely, ITS2 S2 models 1–3 and 7 that do not have this conserved motif may have different regulatory mechanisms.

Table 5. Estimates of evolutionary divergence over sequence pairs between fungal groups when analysing the ITS region.

ITS	1	2	3	4	5
1. Clade 1a		0.0197	0.0189	0.0206	0.0265
2. Clade 1b	0.1659		0.0125	0.0203	0.0247
3. Clade 2a	0.1561	0.0798		0.0183	0.0213
4. Clade 2b	0.1861	0.1717	0.1532		0.0263
5. Outgroup taxa	0.2733	0.2287	0.1948	0.2548	

The values represent the number of base substitutions per site obtained by averaging over all sequence pairs between groups. The distances were determined via the log-det (Tamura-Kumar) method using MEGA-X V10.1.8 software. The standard error estimates are shown in blue.

<https://doi.org/10.1371/journal.pone.0253772.t005>

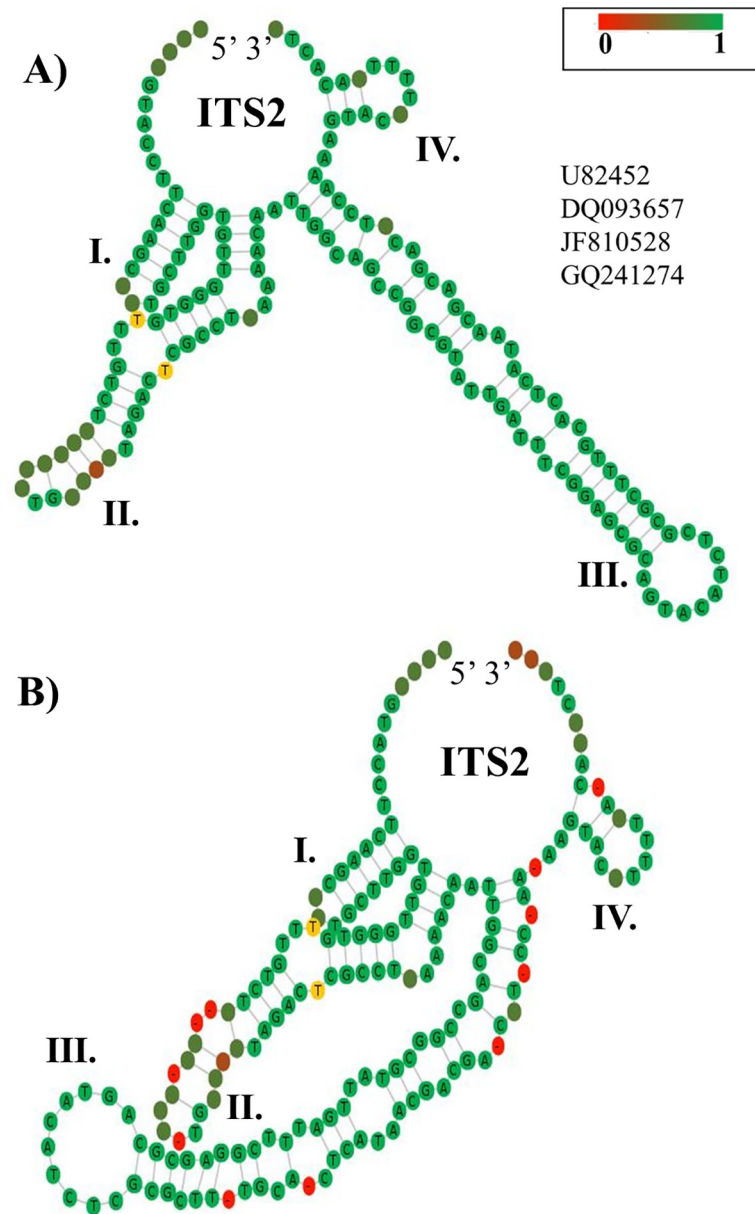


Fig 11. Four major consensus ITS2 S2s from *Ampelomyces* are represented in three main clades. (A) Consensus ITS2 S2 of Models 2 and 3, which are grouped in clade 1a. (B) Consensus ITS2 S2 belonging to clade 1b are represented by Model 6. (C) Consensus ITS2 S2 of Models 4 and 5 that belong to clade 2. (D) Consensus ITS2 S2 of Models 1 and 7 that belong to clade 3. All consensus ITS2 S2s have gaps and were obtained with the 4SALE v1.7.1 software. Yellow nucleotides indicate conserved motifs (U-U mismatch and AAA motifs) known to be found in yeasts and vertebrates [73]. UGG, UGGU and GGUU motifs on helix III are indicated with black circles. The bar on the upper right side indicates the level of nucleotide conservation, with the most conserved nucleotides in green. The gaps are depicted in red. The GenBank IDs used to build each consensus are indicated below each S2.

<https://doi.org/10.1371/journal.pone.0253772.g011>

Early studies demonstrated that when using ITS sequences and microsatellites as DNA barcodes, the only haplotype found in *Ampelomyces* extracted from *P. leucotricha* on apples (APM *Ampelomyces*), which caused epidemics in the spring, may be the result of its PM host phenology [23]. However, there was an exception to this finding; APM *Ampelomyces* grouped with non-APM *Ampelomyces* (isolated from *P. ferruginea* and *P. pannosa*). Moreover, isolation

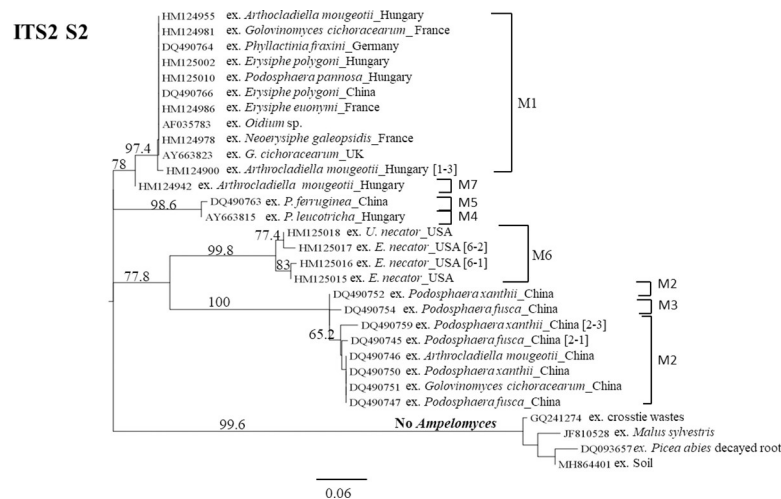


Fig 12. Highly diverse consensus ITS2 S2s from the outgroup taxa. (A) The consensus ITS2 S2 was elaborated without gaps. The GenBank ID numbers of four ITS2 sequences used to predict the ITS2 S2 are indicated. (B) The consensus ITS2 S2 build with gaps. The consensus ITS2 S2s were obtained using the 4SALE v1.7.1 software. The helices are indicated by Roman numerals (I–IV). Nucleotides in yellow indicate the U-U mismatch motifs in helix II. The bar on the upper right side indicates the nucleotide conservation across the four ITS2 sequences used to obtain the consensus structure. Gaps in the structure are indicated in red.

<https://doi.org/10.1371/journal.pone.0253772.g012>

date of one of the strains was unknown, thus the impact of mycohost phenology on the evolution of the only *Ampelomyces* ITS haplotype remains unclear. In our phylogenetic study based on ITS2 sequence and structure, we obtained clustering patterns similar to those reported previously, but in our case each clade indicated that *Ampelomyces* can be grouped into four major S2s. This also explains why non-APM *Ampelomyces* clustered with APM *Ampelomyces*. These different structures also imply that different mechanisms of ribosomal regulation may occur.

These results beg the question: how did these different ITS2 S2s originate? In a previous study, it was proposed that the four major ITS2 S2s found in the ITS sequences of the hyperparasitic fungus *Sphaeropsis visci* may be due to sexual recombination, although no teleomorphs were found [35]. Microsatellite analysis of APM *Ampelomyces* [23] showed that they undergo frequent asexual reproduction and regular recombination, and an *Ampelomyces* sexual reproductive state was not observed. Interestingly, unequal crossing over occurs during mitosis in other fungi such as *Saccharomyces cerevisiae* [76] and *Ceratocystis manginecans* [77]; we cannot discount its occurrence in *Ampelomyces*, whose sexual reproductive stages were not detected in the early studies. It is also possible that the ITS2 S2 found in APM *Ampelomyces* in Europe is the result of a recombination process with other non-APM *Ampelomyces*. However, this S2 was also observed in *Ampelomyces* extracted from other PMs, such as *P. ferruginea* and was found in other locales, such as China. Another explanation is derived from a previous report [78], which demonstrated that specific regions of the rRNA cistron in humans and several primates maintain polymorphic sites by natural selection. Since the ITS2 C/G content and minimum free energy values of ITS2 structure formation were not significantly different to those from the rest of the population (data not shown), we hypothesize that the variations observed in the proximal 5.8S and 28S stem indicate an early stage of pseudogene formation in two *Ampelomyces* ITS sequences extracted from *U. necator* and *P. xanthii*. The polymorphisms observed in the proximal 5.8S and 28S stem and the ITS2 can be either homogenized across the cistrons by unequal crossing over [76] or gene conversion through concerted evolution, and their fate determined by genetic drift. Nevertheless, the modifications observed in the proximal 5.8S and 28S stem may affect positively or negatively ITS2

processing. For example, the first variation of the hybridization model, an ITS2 derived from an *Ampelomyces* strain extracted from *P. xanthii* contains a short proximal 5.8S and 28S stem. This short stem may affect the enzymatic machinery that processes the ITS2 because the length of the stem is important for processing [75]. Consequently, the mutations observed in both strands 5.8S and 28S may be eliminated by genetic drift through concerted evolution [77,79]. On the other hand, the second variation of the hybridization model, an ITS2 derived from an *Ampelomyces* isolated from *U. necator*, may have a more relaxed structure that is still functional. The function of the secondary molecules resulting from the processing of the ITS2 remains to be elucidated. In addition, it remains to be determined whether these secondary molecules provide a specific trait to the fungus. Indeed, it has recently been shown that ribosomes containing rRNA variants have altered gene expression and physiology [80]. If the ITS sequence becomes a ghost pseudogene that favours the synthesis of proteins via ribosomal regulation, then it may be naturally selected by inhabiting a new environment under different biotic or abiotic pressures. Based on this, we think that the random appearance of a ghost pseudogene may lead to the formation of new individuals that form sister clades. For instance, in the phylogram of ITS2 S2s, clade 2 will be divided into two sister clades where each is formed by APM *Ampelomyces* and non-APM *Ampelomyces* ITS2 S2s. This evolutionary process may be initiated by the random appearance of a ghost pseudogene in ITS sequences of APM *Ampelomyces* that was selected by phenology of its powdery mildew host. Nevertheless, no additional samples were available from *Ampelomyces* isolated from *P. ferruginea* in China; and this needs to be addressed in the future.

On the other hand, the interspecific genetic distances between the 'true' *Ampelomyces* -containing clades and the whole outgroup taxa were higher than the intraspecific genetic divergences among the 'true' *Ampelomyces* clades calculated by using either the ITS2 S2s alignment or the ITS alignment. However, the barcode gap was notably enhanced by using the ITS2 S2s. This demonstrates that ITS2 S2s are an important tool to enhance the identification of *Ampelomyces* mycoparasites from DNA environmental samples.

Further research is required in this area together with sampling across different crops, countries and seasons. Partial sequences of the ITS region deposited in GenBank and belonging to *Ampelomyces* spp. are valuable, but we can obtain more information when whole sequences are used. We propose that future studies publish complete *Ampelomyces* ITS sequences and sample the same host at least two times.

In summary, we found that ITS sequences from fungi derived from PM-free environments are still being deposited in the GenBank database under the generic name of *Ampelomyces*. We also showed that these sequences are not related to the genus *Ampelomyces* based on their ITS sequence length, nucleotide composition and the simultaneous alignment of their ITS2 sequences and structures. Finally, we detected for the first time that pseudogene formation could occur in the nrDNA ITS region of *Ampelomyces* mycoparasites. Our study suggested that complete ITS2 sequences are crucial for understanding the phylogeny of these understudied *Ampelomyces* mycoparasites.

Conclusions

In this study, we demonstrated the utility of ITS2 S2 analysis to unveil underlying evolutionary processes in the *Ampelomyces* mycoparasites. Furthermore, the predicted S2s represent a valuable source of information that enhanced the analysis of environmental sequencing and advanced our knowledge in the field of fungal genetic population biodiversity. We highly recommend using the ITS2-DB for this purpose. On the other hand, the controversy surrounding whether the ITS region alone is suitable to discriminate between closely related species may be

ameliorated by analysing S2 together with phylogenetic studies based on simultaneous sequence-structure alignment of the ITS2s. Our results support the utility of this strategy as well as the view that the ITS region is an excellent primary fungal barcode marker, and we are beginning to uncover its real potential.

Supporting information

S1 File. DNA ITS and ITS2 secondary structures sequence analyses.

(ZIP)

S2 File. ITS2 secondary structures from *Ampelomyces* spp. *sensu stricto* and putative *Ampelomyces* spp.

(ZIP)

S3 File. Datasets.

(TXT)

Acknowledgments

We thank Dr. Douglas Eacersall from USQ and the reviewers for their valuable suggestions.

Author Contributions

Conceptualization: Rosa E. Prahl.

Data curation: Rosa E. Prahl.

Formal analysis: Rosa E. Prahl, Shahjahan Khan, Ravinesh C. Deo.

Supervision: Shahjahan Khan, Ravinesh C. Deo.

Writing – original draft: Rosa E. Prahl.

Writing – review & editing: Shahjahan Khan, Ravinesh C. Deo.

References

1. Peña C, Hurt E, Panse V. Eukaryotic ribosome assembly, transport and quality control. *Nat Struct Mol Biol.* 2017; 24:689–699. <https://doi.org/10.1038/nsmb.3454> PMID: 28880863
2. Perry R. Processing of RNA. *Annu Rev Biochem.* 1976; 45:605–629. <https://doi.org/10.1146/annurev.bi.45.070176.003133> PMID: 786158
3. Grummt I. Life on a planet of its own: regulation of RNA polymerase I transcription in the nucleolus. *Genes Dev.* 2003; 17:1691–1702. <https://doi.org/10.1101/gad.1098503R> PMID: 12865296
4. Eberhardt U. Methods for DNA barcoding of fungi. *Methods Mol Biol.* 2012; 858:183–205. https://doi.org/10.1007/978-1-61779-591-6_9 PMID: 22684957
5. Schoch C, Seifert K, Huhndorf S, Robert V, Spouge J, Levesque C, et al. Nuclear ribosomal internal transcribed spacer (ITS) region as a universal DNA barcode marker for fungi. *PNAS USA.* 2012; 109:6241–6246. <https://doi.org/10.1073/pnas.1117018109> PMID: 22454494
6. Wu B, Hussain M, Zhang W, Stadler M, Liu X, Xiang M. Current insights into fungal species diversity and perspective on naming the environmental DNA sequences of fungi. *Mycology.* 2019; 10:127–140. <https://doi.org/10.1080/21501203.2019.1614106> PMID: 31448147
7. Asemaninejad A, Weerasuriya N, Gloor G, Lindo Z, Thorn R. New primers for discovering fungal diversity using nuclear large ribosomal DNA. *PLoS One.* 2016; 11:e0159043. <https://doi.org/10.1371/journal.pone.0159043> PMID: 27391306
8. Haridas S, Albert R, Binder M, Bloem J, LaButti K, Salamov A, et al. 101 Dothideomycetes genomes: a test case for predicting lifestyles and emergence of pathogens. *Stud Mycol.* 2020; 96:141–153. <https://doi.org/10.1016/j.simyco.2020.01.003> PMID: 32206138

9. Lücking R, Aime M, Robbertse B, Miller A, Ariyawansa H, Aoki T, et al. Unambiguous identification of fungi: where do we stand and how accurate and precise is fungal DNA barcoding? *IMA Fungus*. 2020; 11:14. <https://doi.org/10.1186/s43008-020-00033-z> PMID: 32714773
10. O'Donnell K, Cigelnik E. Two divergent intragenomic rDNA ITS2 types within a monophyletic lineage of the fungus *Fusarium* are nonorthologous. *Mol Phylogenet Evol*. 1997; 7:103–116. <https://doi.org/10.1006/mpev.1996.0376> PMID: 9007025
11. Lindner D, Banik M. Intragenomic variation in the ITS rDNA region obscures phylogenetic relationships and inflates estimates of operational taxonomic units in genus *Laetiporus*. *Mycologia*. 2011; 103:731–740. <https://doi.org/10.3852/10-331> PMID: 21289107
12. Kovács G, Balázs T, Calonge F, Martín M. The diversity of *Terfezia* desert truffles: new species and a highly variable species complex with intrasporocarpic nrDNA ITS heterogeneity. *Mycologia*. 2011; 103:841–853. <https://doi.org/10.3852/10-312> PMID: 21289106
13. Zhang W, Tian W, Gao Z, Wang G, Zhao H. Phylogenetic utility of rRNA ITS2 sequence-structure under functional constraint *Int J Mol Sci* 2020; 21:6395. <https://doi.org/10.3390/ijms21176395> PMID: 32899108
14. Paredes-Esquivel C, Townson H. Functional constraints and evolutionary dynamics of the repeats in the rDNA internal transcribed spacer 2 of members of the *Anopheles barbirostris* group. *Parasit Vectors*. 2014; 7:106. <https://doi.org/10.1186/1756-3305-7-106> PMID: 24646478
15. Giudicelli G, Mäder G, Silva-Arias G, Zamberlan P, Bonatto S, Freitas L. Secondary structure of nrDNA Internal Transcribed Spacers as a useful tool to align highly divergent species in phylogenetic studies. *Genet Mol Biol*. 2017; 40:191–199. <https://doi.org/10.1590/1678-4685-GMB-2016-0042> PMID: 28199443
16. Manjunatha L, Singh S, Ravikumara B, Narasa Reddy G, Senthilkumar M. *Ampelomyces*. In: Beneficial microbes in agro-ecology. Amaresan NSenthil Kumar M, Annapurna K, Kumar Kand Sankaranarayanan A, (eds). 44: Academy Press; 2020. pp. 833–860.
17. Braun U, Cook R, Shin H. The taxonomy of the powdery mildew fungi. In: The powdery mildews: a comprehensive treatise. Bélanger RR Bushnell WR, Dik AJ, Carver TLW, (eds). St. Paul, MN, U.S.A. American Phytopathological Society; 2002. pp. 13–55.
18. Braun U, Takamatsu S. Phylogeny of *Erysiphe*, *Microsphaera*, *Uncinula* (*Erysipheae*) and *Cystotheca*, *Podospheera*, *Sphaerotheca* (*Cystothecaceae*) inferred from rDNA ITS sequences some taxonomic consequences. *Schlechtendalia*. 2000; 4:1–33.
19. Li J, Liu X, Yang X, Li Y, Wang C, He D. Proteomic analysis of the impacts of powdery mildew on wheat grain. *Food Chem*. 2018; 261:30–35. <https://doi.org/10.1016/j.foodchem.2018.04.024> PMID: 29739597
20. Nougadère A, Sirot V, Cravedi J, Vasseur P, Feidt C, Fussell R, et al. Dietary exposure to pesticide residues and associated health risks in infants and young children—results of the French infant total diet study. *Environ Int*. 2020; 137:105529. <https://doi.org/10.1016/j.envint.2020.105529> PMID: 32045778
21. Valdés-Gómez H, Araya-Alman M, Pañitruir-De la Fuente C, Verdugo-Vásquez N, Lolás M, Acevedo-Opazo C, et al. Evaluation of a decision support strategy for the control of powdery mildew, *Erysiphe necator* (Schw.) Burr., in grapevine in the central region of Chile. *Pest Manag Sci*. 2017; 73:1813–1821. <https://doi.org/10.1002/ps.4541> PMID: 28156050
22. Legler S, Pintye A, Caffi T, Gulyas S, Bohar G, Rossi V, et al. Sporulation rate in culture and mycoparasitic activity, but not mycohost specificity, are the key factors for selecting *Ampelomyces* strains for bio-control of grapevine of powdery mildew (*Erysiphe necator*). *Eur J Plant Pathol* 2016; 144:723–736.
23. Kiss L, Pintye A, Kovács G, Jankovics T, Fontaine M, Harvey N, et al. Temporal isolation explains host-related genetic differentiation in a group of widespread mycoparasitic fungi. *Mol Ecol*. 2011; 20:1492–1507. <https://doi.org/10.1111/j.1365-294X.2011.05007.x> PMID: 21261766
24. Tollenaere C, Pernechele B, Mäkinen H, Parratt S, Németh M, Kovács G, et al. A hyperparasite affects the population dynamics of a wild plant pathogen. *Mol Ecol*. 2014; 23:5877–5887. <https://doi.org/10.1111/mec.12908> PMID: 25204419
25. Lee S-Y, Kim Y-K, Kim H-G. Biological control of cucumber powdery mildew using a hyperparasite, *Ampelomyces quisqualis* 94013. *Res Plant Dis*. 2007; 13:197–203.
26. Angeli D, Maurhofer M, Gessler C, Pertot I. Existence of different physiological forms within genetically diverse strains of *Ampelomyces quisqualis*. *Phytoparasitica* 2012; 40:37–51.
27. Lee S-Y, Lee S-B, Kim C-H. Biological control of powdery mildew by Q-fect WP (*Ampelomyces quisqualis* 94013) in various crops. *IOBC/wprs Bulletin* 2004; 27:329–331.
28. Liang C, Yang J, Kovács G, Szentiványi O, Li B, Xu X, et al. Genetic diversity of *Ampelomyces* mycoparasites isolated from different powdery mildew species in China inferred from analyses of rDNA ITS sequences. *Fungal Divers*. 2007; 24:225–240.

29. Pintye A, Bereczky Z, Kovács G, Nagy L, Xu X, Legler S, et al. No indication of strict host associations in a widespread mycoparasite: grapevine powdery mildew (*Erysiphe necator*) is attacked by phylogenetically distant *Ampelomyces* strains in the field. *Phytopathology*. 2012; 102:707–716. <https://doi.org/10.1094/PHYTO-10-11-0270> PMID: 22512466
30. Kiss L, Nakasone KK. Ribosomal DNA internal transcribed spacer sequences do not support the species status of *Ampelomyces quisqualis*, a hyperparasite of powdery mildew fungi. *Curr Genet*. 1998; 33:362–367. <https://doi.org/10.1007/s002940050348> PMID: 9618587
31. Sullivan R, White JJ. *Phoma glomerata* as mycoparasite of powdery mildew. *Appl Environ Microbiol*. 2000; 6:425–427. <https://doi.org/10.1128/AEM.66.1.425-427.2000> PMID: 10618259
32. Liyanage K, Khan S, Brooks S, Mortimer P, Karunarathna S, Xu J, et al. Morpho-molecular characterization of two *Ampelomyces* spp. (Pleosporales) strains mycoparasites of powdery mildew of *Hevea brasiliensis*. *Front Microbiol*. 2018; 9:12. <https://doi.org/10.3389/fmicb.2018.00012> PMID: 29403464
33. Park M, Choi Y, Hong S, Shin H. Genetic variability and mycohost association of *Ampelomyces quisqualis* inferred from phylogenetic analyses of ITS rDNA and *actin* gene sequences. *Fungal Biol*. 2010; 114:235–247. <https://doi.org/10.1016/j.funbio.2010.01.003> PMID: 20943134
34. Szentiványi O, Kiss L, Russell J, Kovács G, Varga K, Jankovics T, et al. *Ampelomyces* mycoparasites from apple powdery mildew identified as a distinct group based on single-stranded conformation polymorphism analysis of the rDNA ITS region. *Mycol Res*. 2005; 109:429–438. <https://doi.org/10.1017/s0953756204001820> PMID: 15912930
35. Poczai P, Varga I, Hyvönen J. Internal transcribed spacer (ITS) evolution in populations of the hyperparasitic European mistletoe pathogen fungus, *Sphaeropsis visci* (*Botryosphaeriaceae*): The utility of ITS2 secondary structures. *Gene*. 2015; 558:54–64. <https://doi.org/10.1016/j.gene.2014.12.042> PMID: 25536165
36. Chen Q, Jiang J, Zhang G, Cai L, Crous P. Resolving the *Phoma* enigma. *Stud Mycol*. 2015; 82:137–217. <https://doi.org/10.1016/j.simyco.2015.10.003> PMID: 26955202
37. Aburto A, Torres C, Camps R, Besoain X. Complete nucleotide sequence of the ITS region from *Ampelomyces humuli* isolate UT20 from soil [Internet]. Pontificia Universidad Católica de Valparaíso. 2015 [cited 02 Aug. 2015]. Available from: <https://www.ncbi.nlm.nih.gov/nuccore/KT363070.1>.
38. Kim M, Lee H, Choi Y, Kim G, Huh N, Lee S, et al. Diversity of fungi in creosote-treated crosstie wastes and their resistance to polycyclic aromatic hydrocarbons. *Antonie Van Leeuwenhoek*. 2010; 97:377–387. <https://doi.org/10.1007/s10482-010-9416-6> PMID: 20127413
39. Buzina W, Braun H, Freudenschuss K, Lackner A, Habermann W, Stammberger H. Fungal biodiversity—as found in nasal mucus. *Med Mycol*. 2003; 41:149–161. <https://doi.org/10.1080/mmy.41.2.149.161> PMID: 12964848
40. Mashiane RA, Adeleke RA, Bezuidenhout CC. Diversity of endophytes associated with Bt and non-Bt maize [Internet]. The National Center for Biotechnology (NCBI)—GenBank. 2015 [cited 24 Mar 2020]. Available from: <https://www.ncbi.nlm.nih.gov/nuccore/KU204751.1>.
41. Ankenbrand MJ, Keller A, Wolf M, Schultz J, Förster F. ITS2 database V: twice as much. *Mol Biol Evol*. 2015; 32:3030–3032. <https://doi.org/10.1093/molbev/msv174> PMID: 26248563
42. Koetschan C, Förster F, Keller A, Schleicher T, Ruderisch B, Schwarz R, et al. The ITS2 database III—sequences and structures for phylogeny. *Nucleic Acids Res*. 2010; 38:D275–D279. <https://doi.org/10.1093/nar/gkp966> PMID: 19920122
43. Koetschan C, Hackl T, Müller T, Wolf M, Förster F, Schultz J. ITS2 database IV: interactive taxon sampling for internal transcribed spacer 2 based phylogenies. *Mol Phylogenet Evol*. 2012; 63:585–588. <https://doi.org/10.1016/j.ympev.2012.01.026> PMID: 22366368
44. Merget B, Koetschan C, Hackl T, Förster F, Dandekar T, Müller T, et al. The ITS2 database. *J Vis Exp*. 2012; 61:3806. <https://doi.org/10.3791/3806> PMID: 22433429
45. Selig C, Wolf M, Müller T, Dandekar T, Schultz J. The ITS2 Database II: homology modelling RNA structure for molecular systematics. *Nucleic Acids Res*. 2008; 36:D377–D380. <https://doi.org/10.1093/nar/gkm827> PMID: 17933769
46. Menkis A, Vasiliauskas R, Taylor A, Stenlid J, Finlay R. Afforestation of abandoned farmland with conifer seedlings inoculated with three ectomycorrhizal fungi—impact on plant performance and ectomycorrhizal community. *Mycorrhiza*. 2007; 17:337–348. <https://doi.org/10.1007/s00572-007-0110-0> PMID: 17277941
47. Dominguez-Monino I. Evaluación y control de comunidades microbianas en cuevas turísticas [Thesis]. Universidad de Sevilla: CSIC—Instituto de Recursos Naturales y Agrobiología de Sevilla (IRNAS) Universidad de Sevilla; 2014.
48. Vu D, Groenewald M, de Vries M, Gehrman T, Stielow B, Eberhardt U, et al. Large-scale generation and analysis of filamentous fungal DNA barcodes boosts coverage for kingdom fungi and reveals

- thresholds for fungal species and higher taxon delimitation. *Stud Mycol.* 2019; 92:135–154. <https://doi.org/10.1016/j.simyco.2018.05.001> PMID: 29955203
49. Aveskamp M, Verkley G, de Gruyter J, Murace M, Perelló A, Woudenberg J, et al. DNA phylogeny reveals polyphyly of *Phoma* section *Peyronellaea* and multiple taxonomic novelties. *Mycologia.* 2009; 101:363–382. <https://doi.org/10.3852/08-199> PMID: 19537209
 50. Yang C, Yao Y, Zhang Z, Xue L. First report of leaf blight of *Poa pratensis* caused by *Peyronellaea glomerata* in China. *Plant Dis.* 2016; 100:862. <https://doi.org/10.1094/PDIS-08-15-0954-PDN>
 51. Woudenberg J, De Gruyter J, Crous P, Zwiers L. Analysis of the mating-type loci of co-occurring and phylogenetically related species of *Ascochyta* and *Phoma*. *Mol Plant Pathol.* 2012; 13:350–362. <https://doi.org/10.1111/j.1364-3703.2011.00751.x> PMID: 22014305
 52. Stothard P. The sequence manipulation suite: JavaScript programs for analyzing and formatting protein and DNA sequences. *Biotechniques.* 2000; 28:1102–1104. <https://doi.org/10.2144/00286ir01> PMID: 10868275
 53. Vasavada N. Kruskal-Wallis rank sum (omnibus) test calculator: with follow-up post-hoc multiple comparison calculator by the methods of Conover, Dunn and Nemenyi 2016 [cited 2020]. Available from: <https://astatsa.com/KruskalWallisTest/>.
 54. Manter D, Vivanco J. Use of the ITS primers, ITS1F and ITS4, to characterize fungal abundance and diversity in mixed-template samples by qPCR and length heterogeneity analysis. *J Microbiol Methods.* 2007; 71:7–14. <https://doi.org/10.1016/j.mimet.2007.06.016> PMID: 17683818
 55. Katoh K, Kuma K, Miyata T, Toh H. Improvement in the accuracy of multiple sequence alignment program MAFFT. *Genome Inform.* 2005; 16:22–33. PMID: 16362903
 56. Katoh K, Misawa K, Kuma K, Miyata T. MAFFT: a novel method for rapid multiple sequence alignment based on fast Fourier transform. *Nucleic Acids Res.* 2002; 30:3059–3066. <https://doi.org/10.1093/nar/gkf436> PMID: 12136088
 57. Katoh K, Rozewicki J, Yamada K. MAFFT online service: multiple sequence alignment, interactive sequence choice and visualization. *Brief Bioinform.* 2019; 20:1160–1166. <https://doi.org/10.1093/bib/bbx108> PMID: 28968734
 58. Kumar S, Stecher G, Li M, Knyaz C, Tamura K. MEGA X: molecular evolutionary genetics analysis across computing platforms. *Mol Biol Evol.* 2018; 35:1547–1549. <https://doi.org/10.1093/molbev/msy096> PMID: 29722887
 59. Librado P, Rozas J. DnaSP v5: a software for comprehensive analysis of DNA polymorphism data. *Bioinformatics.* 2009; 25:1451–1452. <https://doi.org/10.1093/bioinformatics/btp187> PMID: 19346325
 60. Rozas J. DNA sequence polymorphism analysis using DnaSP. *Methods Mol Biol* 2009; 537:337–350. https://doi.org/10.1007/978-1-59745-251-9_17 PMID: 19378153
 61. Keller A, Schleicher T, Schultz J, Müller T, Dandekar T, Wolf M. 5.8S-28S rRNA interaction and HMM-based ITS2 annotation. *Gene.* 2009; 430:50–57. <https://doi.org/10.1016/j.gene.2008.10.012> PMID: 19026726
 62. Byun Y, Han K. PseudoViewer3: generating planar drawings of large-scale RNA structures with pseudoknots. *Bioinformatics.* 2009; 25:1435–1437. <https://doi.org/10.1093/bioinformatics/btp252> PMID: 19369500
 63. Kerpedjiev P, Hammer S, Hofacker I. Forna (force-directed RNA): simple and effective online RNA secondary structure diagrams. *Bioinformatics.* 2015; 31:3377–3379. <https://doi.org/10.1093/bioinformatics/btv372> PMID: 26099263
 64. Gruber A, Lorenz R, Bernhart S, Neuböck R, Hofacker I. The Vienna RNA Websuite. *Nucleic Acids Res.* 2008; 36:W70–W74. <https://doi.org/10.1093/nar/gkn188> PMID: 18424795
 65. Will S, Joshi T, Hofacker I, Stadler P, Backofen R. LocARNA-P: accurate boundary prediction and improved detection of structural RNAs. *RNA.* 2012; 18:900–914. <https://doi.org/10.1261/rna.029041.111> PMID: 22450757
 66. Mathews D, Disney M, Childs J, Schroeder S, Zuker M, Turner D. Incorporating chemical modification constraints into a dynamic programming algorithm for prediction of RNA secondary structure. *PNAS USA.* 2004; 101:7287–7292. <https://doi.org/10.1073/pnas.0401799101> PMID: 15123812
 67. Kimura M. A simple method for estimating evolutionary rates of base substitutions through comparative studies of nucleotide sequences. *J Mol Evol.* 1980; 16:111–120. <https://doi.org/10.1007/BF01731581> PMID: 7463489
 68. Rambaut A. FigTree. Computer program distributed by the author, website: <http://treebioedacuk/software/figtree/>. 2009.
 69. Tamura K, Nei M. Estimation of the number of nucleotide substitutions in the control region of mitochondrial DNA in humans and chimpanzees. *Mol Biol Evol.* 1993; 10:512–526. <https://doi.org/10.1093/oxfordjournals.molbev.a040023> PMID: 8336541

70. Tamura K, Kumar S. Evolutionary distance estimation under heterogeneous substitution pattern among lineages. *Mol Biol Evol.* 2002; 19:1727–1736. <https://doi.org/10.1093/oxfordjournals.molbev.a003995> PMID: 12270899
71. Seibel P, Müller T, Dandekar T, Schultz J, Wolf M. 4SALE—A tool for synchronous RNA sequence and secondary structure alignment and editing. *BMC Bioinformatics.* 2006; 7:498. <https://doi.org/10.1186/1471-2105-7-498> PMID: 17101042
72. Seibel P, Müller T, Dandekar T, Wolf M. Synchronous visual analysis and editing of RNA sequence and secondary structure alignments using 4SALE. *BMC Res Notes.* 2008; 1:91. <https://doi.org/10.1186/1756-0500-1-91> PMID: 18854023
73. Joseph N, Krauskopf E, Vera M, Michot B. Ribosomal internal transcribed spacer 2 (ITS2) exhibits a common core of secondary structure in vertebrates and yeast. *Nucleic Acids Res.* 1999; 27:4533–4540. <https://doi.org/10.1093/nar/27.23.4533> PMID: 10556307
74. Svoboda P, Di Cara A. Hairpin RNA: a secondary structure of primary importance. *Cell Mol Life Sci.* 2006; 63:901–908. <https://doi.org/10.1007/s00018-005-5558-5> PMID: 16568238
75. Côté C, Peculis B. Role of the ITS2-proximal stem and evidence for indirect recognition of processing sites in pre-rRNA processing in yeast. *Nucleic Acids Res.* 2001; 29:2106–2116. <https://doi.org/10.1093/nar/29.10.2106> PMID: 11353080
76. Szostak J, Wu R. Unequal crossing over in the ribosomal DNA of *Saccharomyces cerevisiae*. *Nature.* 1980; 284:426–430. <https://doi.org/10.1038/284426a0> PMID: 6987539
77. Naidoo K, Steenkamp E, Coetzee M, Wingfield M, Wingfield B. Concerted evolution in the ribosomal RNA cistron. *PLoS One.* 2013; 8:e59355. <https://doi.org/10.1371/journal.pone.0059355> PMID: 23555022
78. Arnheim N, Krystal M, Schmickel R, Wilson G, Ryder O, Zimmer E. Molecular evidence for genetic exchanges among ribosomal genes on nonhomologous chromosomes in man and apes. *PNAS USA.* 1980; 77:7323–7327. <https://doi.org/10.1073/pnas.77.12.7323> PMID: 6261251
79. Elder J, Turner B. Concerted evolution of repetitive DNA sequences in eukaryotes. *Q Rev Biol.* 1995; 70:297–320. <https://doi.org/10.1086/419073> PMID: 7568673
80. Parks M, Kurylo C, Batchelder J, Vincent C, Blanchard S. Implications of sequence variation on the evolution of rRNA. *Chromosome Res.* 2019; 27:89–93. <https://doi.org/10.1007/s10577-018-09602-w> PMID: 30719681

Chapter 4

The origin of Ampelomyces lineages

Article II: The phylogeny of *Ampelomyces*

Summary:

A comprehensive review about the phylogeny of *Ampelomyces* was written, including the results of chapter 3 from this thesis. In the review it was proposed to include ITS2 S2s in phylogenetic analyses of *Ampelomyces* as these can enhance the resolution of the barcode gap within- and inter-species. Moreover, the differences observed in S2s across lineages of the hyperparasites, suggests (1) a common mechanism of pre-ribosomal processing occurs in the *Ampelomyces* population, (2) APM *Ampelomyces*, *Ampelomyces* extracted from *P. ferruginea*, and GPM *Ampelomyces* share similar mechanisms of ribosomal regulation with vertebrates and yeast, (3) as these S2s seem to be functionally distinct across lineages together with the agreement of phylogenies based on a two-locus analysis conducted in an early study, the *Ampelomyces* taxonomy is proposed to be revisited. The analysis of ITS2 sequences and S2s also shows pseudogenes can randomly appear in the *Ampelomyces* nrDNA ITS repeats as variations in the conserved ITS2-proximal stem are a reliable indication of the presence of pseudogenes [Harpke and Peterson 2008] with few exceptions [Keller et al. 2009]. In the lineage containing hyperparasites strains from *E. necator* and originally sampled in the USA (Falk, Gadoury, Pearson, et al. 1995), the strain (HM125018) is from pseudogenic origin [Prahl et al. 2021]. The mutation in the ITS2 proximal stem can significantly reduce the length of the stem suggesting low levels of transcripts are produced. In the study of Angeli, Maurhofer, Gesler, et al. (2012), this strain was among those GPM *Ampelomyces* clustering as very slow growing. The second mutation contained in the ITS2-proximal stem was observed in the strain isolated from *P. xanthii* (DQ490750)

[Liang et al. 2007]. This mutation seems to have no impact in the pre-ribosomal processing of the subunit 28S.

The clade formed by AMP *Ampelomyces* can be originated due to the phenology of their mycohost, APM, [Kiss et al. 2011] while other clades can evolve by the random appearance of pseudogenes where a few can be functional and undergo natural selection [Prahl et al. 2021]. This hypothesis needs to be confirmed by further biochemical and physiological studies.

Please see below Paper 2. Paper 2 is currently under review by editors of the *Journal of Fungi*.

1 ***Ampelomyces* mycoparasites of powdery mildews: A review**

2

3 Rosa E. Prahl¹, Shahjahan Khan², and Ravinesh C. Deo³

4

5 ¹*School of Sciences, University of Southern Queensland, Toowoomba, Queensland 4350,*

6 *Australia*

7 ²*School of Sciences, University of Southern Queensland, Centre for Health Research and Centre*

8 *for Applied Climate Sciences, Toowoomba, Queensland 4350, Australia*

9 ³*School of Sciences, University of Southern Queensland, Springfield Lakes, Queensland 4300,*

10 *Australia*

11

12 Correspondence to: Rosa Prahl. Email: u1114537@uemail.usq.edu.au

13 ORCID: <https://orcid.org/0000-0003-1243-9881>

14

15

16

17

18

19 Manuscript for consideration as a Review in *Canadian Journal of Plant Pathology*

20 13 June 2022

21

22 *Ampelomyces* mycoparasites of powdery mildews: A review

23

24 **Abstract:** This review paper highlights the significant research conducted on the fungi belonging
25 to the genus *Ampelomyces*. They are among the first mycoparasites used to control
26 phytopathogenic powdery mildew fungi and can efficiently eliminate mycelial growth and reduce
27 the overwintering inoculum of their mycohosts. In addition, these mycoparasites are resistant to
28 some fungicides and insecticides, i.e., Sulphur and Abamectin, respectively, an attractive feature
29 for their selection as biocontrol agents. In *Ampelomyces*, transcriptome analyses revealed that
30 expression of the genes that encode proteins putatively associated with virulence and plant
31 immune answers enhanced during host recognition. Apart from that, the existence of proteins
32 linked to antibiotic resistance was predicted in *Ampelomyces* via whole-genome analysis.
33 Proteomic studies are needed to confirm whether the putative proteins function in virulence and
34 can therefore be used for biocontrol purposes or as bacterial antibiotic-resistant proteins, and
35 which of these may trigger plant immune responses to facilitate plant protection. Phylogenies
36 based on ITS and actin sequences have grouped *Ampelomyces* into different lineages; and the
37 ITS2 spacer, one constituent of the ITS region, together with their secondary structures (S2s),
38 showed that these lineages are represented by different S2s; also, pseudogenes occur in the ITS of
39 two isolates, and S2s in *Ampelomyces* are different from those in *Phoma*-like fungi.
40 Comprehensive characterization of most *Ampelomyces* isolates is lacking, and future multi-locus
41 analysis will assist in delimiting species. We encourage the continuation of these studies to
42 benefit crop protection research.

43

44 **Keywords:** *Ampelomyces*; biocontrol agents; ITS; ITS2 secondary structures; phylogeny; plant
45 protection

46

47

48 **Introduction**

49 The genus *Ampelomyces* consists of intracellular mycoparasites of Erysiphales (Haridas et al.
50 2020), which include species of fungi responsible for causing powdery mildew (PM) diseases on
51 economically important crops and naturally occurring plants (Glawe 2008). Because
52 *Ampelomyces* are parasites of other parasites, they are considered as hyperparasites. The study of
53 these mycoparasites as potential biocontrol agents (BCAs) of PM fungi is of economic interest
54 for developing integrated disease management (IDM) strategies. Several *Ampelomyces*-based
55 biofungicides are available in the market, such as, AQ10[®] that is used against PM attacking
56 mainly fruit (Lewis et al. 2016). As other economically important plants are affected by different
57 PM species, and the efficacy of AQ10[®] against different PM fungi can vary (Dik et al. 1998;
58 McGrath and Shishkoff 1999; Legler et al. 2016), further studies in these mycoparasites are
59 needed to understand, for example, the underlying mechanisms of virulence and, subsequently,
60 discovery new strategies to enhance the biocontrol potential of *Ampelomyces* isolates for plant
61 protection purposes.

62 Previous reviews on *Ampelomyces* were focused on its biocontrol potential (Paulitz and
63 Bélanger 2001; Kiss 2003), interactions *Ampelomyces* and PM fungi (Kiss 2008), its use in
64 agriculture as a beneficial microorganism for plant health (Berg 2009), and risk assessments of
65 the commercial fungicide AQ10[®] (European Food Safety Authority [EFSA] et al. 2017). A
66 recent book chapter covers taxonomy, life cycle, diversity, mycoparasitism, and commercial
67 applications of *Ampelomyces* (Manjunatha et al. 2020), although the genomic aspects of
68 *Ampelomyces* were not addressed as the *Ampelomyces* genome was recently sequenced (Haridas
69 et al. 2020). In this sense, this review aims to present key findings on the latest research

70 conducted in *Ampelomyces* hyperparasites, including genomic studies, to promote further
71 research in these mycoparasites.

72 In this review paper the original fungal names from previously published works were
73 updated via the MycoBank database at <https://www.mycobank.org/>.

74

75 **Survey methodology**

76 For this review paper the following databases were used: PubMed, Google Scholar, EBSCO,
77 ScienceDirect, Wiley, and SciELO. English, German, and Spanish peer-reviewed journals were
78 included from the earliest available record to January 2022. The following keywords were used
79 in our literature search: “*Ampelomyces*” AND “mycoparasitism”; “*Ampelomyces*” AND
80 “biocontrol”; “*Ampelomyces*” AND “biology”; “*Ampelomyces*” AND “epidemiology”;
81 “*Ampelomyces*” AND “genome”; “*Ampelomyces*” AND “phylogeny”; “*Ampelomyces*” AND
82 “plant protection”.

83

84 **Taxonomy**

85 Mycoparasites belonging to the genus *Ampelomyces* form part of the largest Dothidiomycetes
86 order named Pleosporales (Pleosporomycetidae, Dothideomycetes, Pezizomycotina,
87 Ascomycota) (Zhang et al. 2009). analyses have placed the type species of *Ampelomyces*, *A.*
88 *quisqualis* Ces. within the Phaeosphaeriaceae (de Gruyter et al. 2009; Aveskamp et al. 2010;
89 Wijayawardene et al. 2013; Phookamsak et al. 2014). Moreover, this genus is not monospecific
90 but comprises numerous genetically diverse species (Kiss 1997; Liang et al. 2007; Park et al.
91 2010; Angeli, Maurhofer, et al. 2012). The anamorph stage of *Ampelomyces* has been observed in
92 nature, but whether they have a sexual reproductive stage is unknown. However, signs of

93 recombination were detected in some isolates (Kiss et al. 2011; Pintye et al. 2015), suggesting
94 that teleomorphs may be present.

95

96 **The early identification of *Ampelomyces* mycoparasites**

97 Historically, *Ampelomyces* were classified into several species based on the size and forms of
98 their pycnidia, asexual fruiting bodies, and combined with the names of their original mycohosts,
99 which has led to taxonomic inaccuracies (Kiss and Nakasone 1998; White and Sullivan 2000;
100 Prah et al. 2021). Still today, their taxonomic classification remains unresolved. Further, the
101 identification of *Ampelomyces* has been problematic since its discovery. A pycnidium developing
102 inside the cell of a conidiophore from *Erysiphe necator*, which causes grape powdery mildew,
103 was described for the first time by Cesati, who denominated it *Ampelomyces* (Ampelus: vine;
104 myces: fungus) *quisqualis* Ces. (Cesati 1852). Conidiophores are asexual structures responsible
105 for conidial formation (Glawe 2008). In parallel, the identification of the *Ampelomyces*
106 pycnidium-PM conidiophore structure was initially confused by some authors who considered
107 both pycnidium and conidiophore as unique species and different names were used to describe
108 them, such as *Cicinobolus florentinus* Ehrenb. (Ehrenberg 1853) and *Byssocystis* Riess. (Riess
109 1852). In addition, other names were introduced based on the originally discovered host plant
110 and mycohost, morphology of conidia, and cultural characteristics. For instance, a pycnidial
111 fungus found on PM infecting *Quercus* sp. was initially identified as *Ampelomyces quercinus*
112 (Rudakov 1979), and 17 new name combinations were introduced by Rudakov (1979), such as,
113 *Ampelomyces artemisiae*, *Ampelomyces humuli*, and *Ampelomyces uncinulate*. However, a
114 subsequent work found that these strains and others named *Ampelomyces* spp. do not belong to
115 the genus *Ampelomyces* in terms of their growth rate *in vitro* (Kiss and Vagna 1995) and genetic

116 patterns (Kiss 1997). The latter was shown via the analysis of the restriction fragment length
117 polymorphism (RFLP). Based on the growth rate *in vitro* these putative *Ampelomyces*, named
118 type I, grew more quickly (3–4 mm radial growth/day) than others *Ampelomyces*, named type II,
119 (0.1–1 mm radial growth/day) when these isolates were grown in culture consisting of Czapek-
120 Dox agar and supplemented with 2% malt extract (MCzA) at 23°C (Kiss and Vajna 1995). The
121 fast-growing strains were also closely related to the *Epicoccum* species but not to those of type
122 species *Ampelomyces quisqualis* Ces., as was shown from the phylogenetic analysis based on the
123 nuclear ribosomal DNA internal transcribed spacer (nrDNA ITS) region (Kiss and Nakasone
124 1998), which consists of two ITS spacers, 1 and 2, that are separated by the 5.8S gene. Further,
125 those slow-growing strains were also genetically diverse, and, thus, it showed that the genus
126 *Ampelomyces* consists of several genetically different species and cannot be represented by a
127 single species name, *Ampelomyces quisqualis* (Kiss and Nakasone 1998).

128 The binomial name *A. quisqualis* is still in use, but it represents a problematic species
129 complex (Kiss and Nakasone 1998). Several other studies showed the genetic diversity among
130 *Ampelomyces* isolates (Liang et al. 2007; Park et al. 2010; Angeli, Maurhofer, et al. 2012).
131 Currently, many *Ampelomyces* species are described, and although they are still included in the
132 MycoBank database, most of these names are not currently in use.

133 *Ampelomyces* were also confused with *Phoma* species (Ascomycota - Pleosporales);
134 however, hyperparasitic *Ampelomyces* were shown to form intracellular pycnidia while the
135 species *Phoma glomerata* (and later re-named *Didymella glomerata*) formed sessile pycnidia
136 (Sullivan and White 2000). Subsequently, *A. quercinus* was re-classified as *Phoma fungicola* and
137 placed in the family Didymellaceae based on a phylogenetic tree using 28S nrDNA (Large
138 Subunit - LSU), 18S nrDNA (Small Subunit - SSU), ITS, β -tubulin (TUB) gene fragments, and

139 morphological characters of pycnidia and cultural characteristics (Aveskamp et al. 2010). Later,
140 the taxonomy of the *Phoma* genus was revisited and enhanced, and *P. fungicola* was assigned as
141 belonging to the new genus *Nothophoma*, and thus, re-named *Nothophoma quercina* via a multi-
142 locus sequence analyses (MLSA) using LSU, ITS, RNA polymerase II second largest subunit
143 (*rpb2*) fragment genes, and partial gene regions of β -tubulin (*tub2*) (Chen et al. 2015). In terms
144 of pathogenicity, some *Phoma*-related fungi are plant pathogens, including *N. quercina*, but not
145 *D. glomerata*, which is a mycoparasite of PM (Sullivan and White 2000). To our knowledge,
146 conventional MLSA have not been conducted in *Ampelomyces* spp. and, consequently, species
147 belonging to the genus *Ampelomyces* have not been delimited yet.

148

149 **Phylogeny**

150 As the phylogeny of *Ampelomyces* is still unresolved, studies using a variety of research
151 methodologies have been conducted to classify them properly. Several studies have used the
152 preferred barcode for fungal species identification, the nrDNA ITS region (Szentiványi et al.
153 2005; Liang et al. 2007; Angeli, Pellegrini, Maurhofer, et al. 2009; Kiss et al. 2011; Nguyen and
154 Lee 2016; Liyanage et al. 2018; Huth et al. 2021). Other studies tried to resolve the phylogeny
155 using ITS and actin gene 1 (*act1*) fragments (Park et al. 2010; Pintye et al. 2012), with two using
156 a two-locus sequence analysis (ITS and *act1*), whose phylogenies were congruent (Pintye et al.
157 2012; Németh, Mizuno, et al. 2021), and one using a simultaneous alignment of ITS2 sequences
158 and their secondary structures (S2) where the *Ampelomyces* clades are represented by distinct
159 ITS2 S2s (Prahl et al. 2021).

160 In terms of species delimitation, morphological differences in asexual or sexual structures
161 can assist in identifying species boundaries (Lücking et al. 2020). In regard to asexual structures,

162 the morphological shape and size characteristics of pycnidia and conidia are relatively simple
163 and conserved across *Ampelomyces* isolates and do not provide enough distinction to delimitate
164 species (Clare 1964; Liang et al. 2007; Nguyen and Lee 2016; Banupriya et al. 2019; Németh,
165 Mizuno, et al. 2021).

166

167 **Detailed morphological study of *Ampelomyces* mycoparasites**

168 In a recent study, 26 *Ampelomyces* strains were extracted from six different PM species in Japan,
169 of which eight strains represented four distinct haplotypes and extracted from four different PM
170 species were selected to determine in detail their morphological characteristics when grown *in*
171 *vitro* and during mycoparasitism by using a high resolution digital microscope (Németh, Mizuno,
172 et al. 2021).

173 The selected isolates had the following features: Firstly, when the isolates were
174 maintained *in vitro* in CMCzA media at 25°C, spores were unicellular, hyaline, ovoid to
175 doliiform in shape, and dimensions 5.7–9.2 µm length x 2.6–5.0 µm width. Secondly, in the
176 same culture conditions, the isolates had *in vitro* radial growth rates between 0.5 and 1.0
177 mm/day, which were similar to those from other known type species *A. quisqualis* Ces. (Kiss and
178 Nakasone 1998). Thirdly, when *Pseudoidium neolycopersici*, PM extracted originally from
179 tomato plant in Japan (Nonomura et al. 2014), was parasitised by each of the selected
180 *Ampelomyces* strains, *Ampelomyces* pycnidia were found mostly developing within the basal
181 cells of *Ps. neolycopersici* conidiophores. The mature pycnidia developed within the PM
182 conidiophores were similar in length (40.2–84.2 µm) and width (22.6–48.1 µm), but the sizes of
183 pycnidia and the number of spores produced in a single pycnidium varied among isolates.

184 Finally, immature *Ampelomyces* pycnidia developed in the tomato PM mycelia were pale yellow
185 colour and smaller than mature pycnidia, which were black coloured and ovoid in shape.

186

187 **Mycohost association of *Ampelomyces* isolates**

188 Some degree of mycohost specificity in *Ampelomyces* hyperparasites was shown via
189 phylogenetic analyses. At least four clades have been recognized in *Ampelomyces* by using the
190 ITS region and *act1* gene fragments (Park et al. 2010). Based on the ITS region, Clade 1
191 consisted of isolates extracted mainly from *Podosphaera* spp. (section *Sphaerotheca*) and few
192 from other genera of the Erysiphaceae, i.e., five Korean strains from mycohosts of the genera
193 *Erysiphe*, *Golovinomyces*, and *Oidium* (subgen. *Pseudoidium*); Clade 2 contained isolates from
194 phylogenetically distinct PM genera, such as Korean isolates from *Arthrocladiella*, *Erysiphe*
195 (section *Erysiphe*), *Golovinomyces*, and *Phyllactinia*, and a Chinese strain derived from the
196 genus *Podosphaera* (section *Sphaerotheca*); Clade 3 grouped one Korean, one Chinese, and
197 eight European strains from PMs whose plant hosts were derived from the family Rosaceae; and
198 Clade 4 consisted of *Ampelomyces* isolates extracted from *Erysiphe* (sections *Microsphaera* and
199 *Uncinula*) (Park et al. 2010). Similarly, the phylogeny based on the *act1* grouped the
200 *Ampelomyces* isolates into four clades, but clade 2 was more variable (Park et al. 2010). The
201 phylogenies based on either ITS or *act1* indicated that some isolates grouped in accordance with
202 their original mycohost suggesting that some degree of adaptation occurred between these strains
203 and their mycohosts without losing their infection ability as generalist mycoparasites (Park et al.
204 2010).

205 In a posterior investigation, a phylogenetic analysis based on ITS sequences of 15
206 *Ampelomyces* isolates representing the four major phylogenetic groups reported by Park et al.

207 (2010), including other isolates from PM species from different geographical regions, formed
208 five distinct genetic groups that can be associated with the mycohost of origin, growth rate
209 pattern *in vitro* (slow and very slow growing), and morphological characteristics, i.e., colony
210 color (Angeli, Maurhofer, et al. 2012). For example, on six different artificial media, including
211 Czapek agar, at 25°C, *Ampelomyces* strains extracted from *Podosphaera xanthii* on cucumber
212 and *E. necator* on grapes were distinguished as slow-growing (0.70–0.82 mm/day) and forming
213 dark-brown colonies, and very slow-growing cultures (0.34–0.63 mm/day) with light green
214 colonies, respectively.

215 Other investigations presented evidence that *Ampelomyces* hyperparasites lack of
216 mycohost specificity by using cross-inoculation tests where *Ampelomyces* isolates from different
217 PMs can parasitise other PMs either *in vitro* (Sztejnberget al. 1989; Szentiványi et al. 2005;
218 Liang et al. 2007) or in field experiments (Kiss et al. 2011). A recent study, after using
219 inoculation tests with the eight selected Japanese strains and five different PM species,
220 demonstrated that the Japanese isolates had the capacity to parasitise and degenerate mycohost
221 hyphae regardless of the original host. This finding was shown using the spray method where
222 *Ampelomyces* conidia of each strain were inoculated on the distinct PM-infected leaves (Németh,
223 Mizuno, et al. 2021).

224 Conversely, inoculum tests conducted in greenhouses by Falk, Gadoury, Pearson, et al.
225 (1995) showed that three *Ampelomyces* isolates developed a larger number of pycnidia in their
226 original mycohost, *E. necator*, than in two different PM fungi, *Podosphaera fuliginea* and
227 *Podosphaera macularis*.

228 Another example of the association between *Ampelomyces* and PMs is the genetically
229 different *Ampelomyces* lineage that was separated from its sympatric *Ampelomyces*

230 mycoparasites by temporal isolation, which was caused by differences in mycohost phenology
231 (Kiss et al.2011). In Europe, *Podosphaera leucotricha*, the causal agent of apple PM (APM),
232 overwinters inside apple buds between bud scales as mycelium and chasmothecia (Stalder 1955),
233 and causes epidemics in the spring while non-APM, i.e., *Arthrocladiella mougeotii* on *Lycium*
234 *halimiifolium*, causes infections later in the autumn season (Kiss 1998). Despite the niches of
235 APM and non-APM overlapping (Szentiványi and Kiss 2003), APM *Ampelomyces* evolved into
236 a genetically different group as demonstrated via single-stranded conformation polymorphism
237 analysis of the ITS (Szentiványi et al. 2005) and ITS sequences and microsatellite markers (Kiss
238 et al. 2011). A subsequent study, using microsatellites, showed that both APM and non-APM
239 strains were genetically differentiated and with no signs of gene flow (Pintye et al. 2015).
240 Further, the European APM *Ampelomyces* from spring with a unique haplotype ITS and those
241 non-APM *Ampelomyces*, extracted from *A. mougeotii*, from autumn can infect a determined PM
242 species, i.e., *P. xanthii* on cucumber and *Golovinomyces orontii* on tobacco, with no significant
243 differences in mycoparasitic activities, and non-APM *Ampelomyces* can overwinter together with
244 APM *Ampelomyces* in apple buds. These premises suggest *Ampelomyces* (1) adapted when
245 overwintering with APM and evolved into a different phylogenetic group by temporal isolation
246 as a result of the phenology of their powdery mildew hosts; and (2) despite of this genetic
247 differentiation, the cross-inoculation tests showed that APM *Ampelomyces* lack of host
248 specificity (Kiss et al. 2011).

249 In the lineage containing the European APM *Ampelomyces* (Kiss et al. 2011), there were
250 other strains originally extracted from *Podosphaera pannosa* on rosaceous, including one
251 Chinese *Ampelomyces* strain from *Podosphaera ferruginea* on *Sanguisorba officinalis* (Liang et
252 al. 2007) which contain the same APM *Ampelomyces* haplotype. A recent computational work

253 showed that the APM *Ampelomyces* grouped with that of the Chinese strain, as these share
254 similar S2s (Prahl et al. 2021).

255

256 **Differentiating *Ampelomyces* ITS sequences from those of false *Ampelomyces***

257 The initial confusion of *Ampelomyces* with other pycnidial mycoparasites of PMs has not been
258 resolved as there are nucleotide sequences deposited in the GenBank database under the name of
259 *Ampelomyces*, though do not actually belong to this genus (Prahl et al. 2021). The ITS barcode
260 gap in *Ampelomyces* mycoparasites are highly variable (Kiss and Nakasone 1998) that can
261 overlap with others close and unknown fungi, but when combining ITS2 sequences and their
262 S2s, the barcode gap among *Ampelomyces* groups and *Phoma*-like fungi increases (Prahl et al.
263 2021). Thus, this molecular approach showed to be more appropriate for discrimination of the
264 ‘true’ *Ampelomyces* sequences from those *Phoma*-like fungi from PM-free environments or
265 environmental DNA samples (Prahl et al. 2021).

266

267 **Utility of ITS2 sequences and secondary structures in studying *Ampelomyces***

268 New insights about pre-ribosomal RNA processing in *Ampelomyces* mycoparasites were
269 unveiled when using ITS2 sequences and S2s. For example, It was found that mechanisms of
270 pre-rRNA processing may be different across *Ampelomyces* lineages (Prahl et al. 2021) where
271 some of their S2s share motifs found in vertebrates and yeast (Joseph et al. 1999). In addition,
272 pseudogenes can be present in *Ampelomyces* nrDNA ITS as variations in the ITS2-proximal stem
273 model were detected in two isolates (Prahl et al. 2021) named G273 and HMLAC227, which
274 were originally extracted from *E. necator* (Falk, Gadoury, Pearson, et al. 1995) and *P. xanthii*
275 (Liang et al. 2007), respectively. Mutations in the ITS2-proximal stem model are reliable

276 evidence of the presence of pseudogenes (Harpke and Peterson 2008). This finding suggests that
277 some *Ampelomyces* groups are of pseudogenic origin. Further, the presence of pseudogenes can
278 mislead the phylogenetic analysis by generating a new clade or originate a new lineage. The
279 latter situation is possible to occur if some pseudogenes produce functional transcripts, which
280 can undergo natural selection and probably originate a new *Ampelomyces* lineage. The concept
281 of pseudogenes as un-functional genes is currently under debate, and it needs to be revised
282 (Cheetham et al. 2020).

283

284 **Phenotypic variations within *Ampelomyces* isolates**

285 Phenotypic variations within *Ampelomyces* strains have been reported in several works (Falk,
286 Gadoury, Pearson, et al. 1995; Németh, Mizuno, et al. 2021). Németh, Mizuno, et al. (2021)
287 showed that four Japanese *Ampelomyces* isolates derived from the same host sample had
288 significant differences in hyphal lengths, germinal grow rates, and number of spores produced by
289 a single pycnidium. Falk, Gadoury, Pearson, et al. (1995) also found that the strain G273,
290 compared to another congeneric strain, G5, and also extracted from *E. necator* on *Vitis* sp. and
291 from the same geographical region, had different mycoparasitic phenotypes in two out of 19
292 different *E. necator* isolates.

293 We hypothesize that the phenotypic variations in the strain G273 originated due to the
294 natural disturbance of ribosomal biogenesis as a shorter stem than that of the ITS2-proximal stem
295 model was predicted to occur in this strain (Prahl et al. 2021) which suggests ITS2 pre-ribosomal
296 processing can be negatively affected (Côté and Peculis 2001). This hypothesis is based on a
297 recent study which showed that when the process of ribosome assembly is altered, cells from
298 *Saccharomyces cerevisiae* suffer a precipitated crumble of protein folding, which independently

309 affects cell growth, and if it is re-established, then cell fitness is restored (Tye et al. 2019). The
300 latter can explain why cellular growth of G273 significantly improved when its original growth
301 medium based on malt-extract agar was supplemented with an extract of wheat bran (Falk,
302 Gadoury, Pearson, et al. 1995). In this context, the random appearance of pseudogenes, some of
303 which can impact a biological function, can undergo natural selection and lead to the formation
304 of sister clades (Prahl et al. 2021). There is some debate over whether pseudogenes are indeed
305 nonfunctional (Chen et al. 2020); furthermore, recent evidence has highlighted that a review of
306 pseudogenes is needed as some have been shown to produce functional transcripts (Gong et al.
307 2019) or appear to possess some functionality (Pink and Carter 2013; Groen et al. 2014; Gong et
308 al. 2019; Cheetham et al. 2020).

309 To select potential *Ampelomyces* isolates for development of BCAs, it is important to
310 understand the causes of these phenotypic variations. Further studies are needed in this topic to
311 determine if the variations observed in the ITS2-proximal stem model of strains G273 and
312 HMLAC227 have an impact on pre-ribosomal processing.

313

314 **The *Ampelomyces* genome**

315 In a recent genomic study, the *Ampelomyces* genome of a strain from Australia was sequenced. It
316 is 40.38 Mb in size and contains CG-regions spread along large and short segments of A/T rich
317 areas (Huth et al. 2021). In an earlier investigation, a gene family was predicted to exist in the
318 *Ampelomyces* genome, which encodes a group of bacterial antibiotic resistance proteins
319 (Haridas et al. 2020). The function of this family gene in mycoparasitism in *Ampelomyces*
320 remains to be determined as these genes have also been identified in other fungi with different
321 lifestyles (Haridas et al. 2020). In another genomic study, genes encoding methionine sulfoxide

322 reductase enzymes were identified in most fungi across the fungal kingdom, including in *A.*
323 *quisqualis* (Hage et al. 2021). These enzymes provide protection against oxidative stress but their
324 role in hyperparasitism remains to be unveiled also.

325

326 **Functional genetics in *Ampelomyces***

327 In terms of the analysis of gene functions, the *Ampelomyces*-PM association remains largely
328 unexplored. Two research works have investigated the expression levels of *Ampelomyces* genes
329 during mycoparasitism. In one of those studies, the transcript of the exoglucanase A (*exgA*)
330 gene, encoding a putative exoglucanase (exo- β -1,3-glucanase), increased along the *Ampelomyces*
331 mycelium, within *Podosphaera fusca* mycelium, and in the late stages of hyperparasitism
332 (Rotem et al. 1999). Glucanases are enzymes capable of hydrolyzing glycosidic bonds in glucans
333 that form part of the fungal cell wall. In the second study, a genome-wide transcriptional analysis
334 conducted on *A. quisqualis* strain AQ10 from the commercial AQ10[®], in the presence of its
335 mycohost, *P. xanthii*, was utilized to determine its whole set of mRNAs and their relative
336 abundance (Siozios et al. 2015). The study revealed the reprogramming of 1536 putative genes,
337 which overexpressed after host recognition. During conidial germination, the most active genes
338 were associated with transcriptional and translational processes, and after the elongation of germ
339 tubes, the most active genes were involved in proteasome degradation pathways. From that
340 study, it was determined that approximately 50% of the hyperparasite transcripts were not related
341 to those of any known protein sequences and, consequently, their functions were undetermined
342 (Siozios et al. 2015). Deciphering the *Ampelomyces* proteome will aid in protein identification
343 and the discovery of ‘hit’ molecules of interest for industrial applications, i.e., antibiotics.

344 A recent investigation showed that the nitrate reductase (*euknr*) gene is not involved in
345 parasitism as the deletion of the gene did not affect the mycoparasitic activity of *Ampelomyces* on
346 two distinct PM hosts (Németh, Li, et al. 2021). The gene function can be associated with other
347 biological functions, i.e., fungal nitrate assimilation from agroecosystems (Gorfer et al. 2011) as
348 *Ampelomyces* can survive on PM-free soil (Németh et al. 2019), but this role remains to be
349 elucidated.

350

351 **Life cycle**

352 *Ampelomyces*, among other pycnidial fungi, have been discovered on plants infected with PMs
353 since 1852. Currently, *Ampelomyces* mycoparasites have been identified in more than 64 species
354 of PM fungi found on more than 256 species of host plants from more than 28 countries (Clare
355 1964; Falk, Gadoury, Pearson, et al. 1995; Kiss 1997; Ranković 1997; Czerniawska 2001; Liang
356 et al. 2007; Angeli, Pellegrini, Pertot, 2009; Kim et al. 2009; Park et al. 2010; Kiss et al. 2011;
357 Gautam and Avasthi 2016; Younes et al. 2016; Parratt et al. 2017; Banupriya et al. 2019;
358 Németh, Mizuno, et al. 2021). These can coinhabit with other pycnidial fungi of the *Didymella*
359 and *Phoma* genera (Sullivan and White 2000) and can be found on plants infected by more than
360 one PM species (Parratt et al. 2017). In 1870, Anton de Bary described the *Ampelomyces*-plant
361 pathogenic mycohost interaction in detail where *Ampelomyces* pycnidia, asexual fruiting bodies,
362 develop intracellularly in the hyphae, conidiophores (Fig. 1a), and chasmothecia (sexual
363 structures) of PM fungi (Fig. 1b) (de Bary 1870; Hashioka and Nakai 1980; Angeli, Pellegrini,
364 Pertot 2009; Németh, Mizuno, et al. 2021).

365 In moist conditions with the highest relative humidity (RH) values over 80% (Verhaar et
366 al. 1999; Romero et al. 2007; Németh, Mizuno, et al. 2021) and temperatures ranging from

367 15°C–25°C (Mhaskar and Rao 1974; Czerniawska 2001; Angeli, Maurhofer, et al. 2012), and in
368 the presence of PMs, *Ampelomyces* conidia rapidly germinate by forming germ tubes. The effect
369 of germinal stimulation by the presence of their mycohosts conidia has been observed on several
370 occasions (Gu and Ko 1997; Angeli, Maurhofer, et al. 2012). The germ tubes of *Ampelomyces*
371 were also observed to growth directly towards the host hyphae which, later, penetrate the host
372 cell wall by mechanical (Sundheim and Krekling 1982) and enzymatic actions (Rotem et al.
373 1999; Angeli, Puopolo, et al. 2012). Appressorium-like structures were identified at the
374 penetration site (Sundheim and Krekling 1982) and cell wall-degrading enzymes were also
375 identified in several *Ampelomyces* strains (Rotem et al. 1999; Angeli, Puopolo, et al. 2012).
376 Further, *A. quisqualis* Ces. can produce, *in vitro*, extracellular enzymes such as β -glucosidase,
377 acid phosphatase, and ribonuclease, suggesting cell wall synthesis, mycelial energy metabolism,
378 and protein synthesis, respectively, are affected during the initial stage of mycoparasitism
379 (Philipp 1995).

380 Furthermore, we hypothesize that, during host recognition, *A. quisqualis* strain AQ10
381 could release elicitors of plant immune responses as Siozios et al. (2015) demonstrated that a
382 virulence-related gene encoding a presumed protein of the SnodProt family was up-regulated
383 during mycohost recognition. Secreted SnodProt1-like proteins can have different functions in
384 fungi, in which some are involved in the virulence and activation of plant defenses (Zhang et al.
385 2017). Plant immunity refers to mechanisms of defense used in plants to respond to abiotic or
386 biotic stresses, such as the recognition of secreted molecules from pathogens or non-pathogenic
387 organisms (Saijo and Loo 2020). In the case of *Ampelomyces* mycoparasites, the biological
388 function of this putative SnodProt protein remains to be elucidated

389 Conversely, during conidial germination, and after mycohost recognition, most of the up-
390 regulated genes encode putative cell wall- and plasma membrane-degrading proteins whose
391 functions are likely associated with mycoparasitism (Siozios et al. 2015). Examples of these
392 proteins are a probable secreted dipeptidyl-peptidase 5 (PP5) and a 26S protease-like protein
393 regulatory subunit 4, respectively (Siozios et al. 2015). PP5 was originally discovered in the
394 opportunistic human pathogenic fungus *Aspergillus fumigatus* and degrades cell-wall-associated
395 proteins where dipeptides are released from the N-terminus end of polypeptides (Jaton-Ogay et
396 al. 1992; Beauvais et al. 1997). Whereas the 26S proteasome-like protein regulatory subunit 4
397 forms part of the eukaryotic proteasome complex (Tanaka 2009) and its inhibition eliminates the
398 pathogenicity of the rice blast fungus *Magnaporthe oryzae* (Oh et al. 2012). In *Ampelomyces*, the
399 mechanisms of action of the PP5 and the 26S proteasome in mycoparasitism are unknown.

400 During the mycoparasitic stage, *Ampelomyces* hyphae invade intracellularly the host
401 mycelia, where their pycnidia develop inside the mycohost conidia, hyphae, and conidiophores.
402 It was recently determined that a mature pycnidium, developed in a conidiophore, released ca.
403 200–1500 conidia (Németh, Mizuno, et al. 2021).

404 After 5 to 10 days of hyperparasitic infection, host conidia-bearing structures and hyphae
405 are destroyed as a result of *Ampelomyces* pycnidia development, causing a reduction of PM
406 mycelia. Abiotic factors, such as rain or strong winds, contribute to the spread of hyperparasite
407 conidia and hyphal fragments within mycohost conidia to the soil and nearby diseased leaves
408 (Jarvis and Slingsby 1977; Speer 1978; Sundheim 1982). It has been suggested that
409 *Ampelomyces* develop saprophytic *Phoma*-like pycnidia on leaf litter, which survive up to the
410 next spring (Yarwood 1932). In laboratory tests, *Ampelomyces* can produce saprophytic pycnidia
411 in PM-infected senescent leaf tissues and, in some instances, the hyperparasites can survive by

412 overwintering in these pycnidia. Whereas an *Ampelomyces* teleomorph structure playing a role in
413 overwintering has been proposed to develop saprophytically in the leaf tissues of *Helianthus*
414 *tuberosus* (Emmons 1930), but this has not been confirmed until today.

415 A recent study using green fluorescent protein *Ampelomyces* transformant conidia
416 revealed that hyperparasites can survive for up to 21 days in PM-free soils and leaves, and PM-
417 infected leaves on soils, although, with limited hyphal growth and not sporulation, suggesting the
418 ecological niche of *Ampelomyces* is located in the phyllosphere where these mycoparasites
419 invade PM-structures and form intracellular pycnidia (Németh et al. 2019).

420

421 ***Overwintering of Ampelomyces mycoparasites***

422 *Ampelomyces* mycoparasites can overwinter in their mycohost chasmothecia, and subsequently,
423 start their life cycle in the following season. In apple trees, for example, the hyperparasites
424 attacking APM survive by overwintering as pycnidia in their PM chasmothecia on barks and
425 scales of apple buds and as resting hyphae in the dried mycelia of APM covering the apple
426 shoots (Szentiványi and Kiss 2003). This survival strategy has been also observed in
427 *Ampelomyces* whose conidia can be found in immature chasmothecia from grape PM (Falk,
428 Gadoury, Cortesi, et al. 1995), and in those from several other PM genera, i.e., *Blumeria*,
429 *Golovinomyces*, *Podosphaera*, and *Phyllactinia*, in the Coastal regions of Syria (Younes et al.
430 2016). In the Trentino-Alto Adige region of northern Italy, conidia were also found in
431 chasmothecia and mycelia of *E. necator* while pycnidia were only detected in the PM mycelia,
432 but in immature or semi mature chasmothecia (Angeli, Pellegrini, and Pertot 2009).
433 Nevertheless, *Ampelomyces* conidia have been also reported to be released from mature

434 chasmothecia, but immature, with fully developed appendages from *Erysiphe flexuosa* and
435 *Erysiphe vanbruntiana* in urban places of Northeastern Poland (Sucharzewska et al. 2012).

436

437 ***Microcyclic conidiogenesis in Ampelomyces***

438 *Ampelomyces* pycnidium also develops inside a PM microcyclic (MC) conidiophore that directly
439 originates from a conidium, with or without minimum formation of hypha, and this can affect the
440 natural directional growth of mycohost MC conidial germ tubes (Kiss et al. 2010). Notably,
441 powdery mildew MC conidia are not destroyed by mycoparasitism but seem to function as a
442 vector to allow spreading to nearby uninfected mycohost colonies. No further studies have been
443 conducted on this topic, and the molecular mechanisms underlying mycoparasitism within MC
444 spores remain to be determined.

445

446 ***Ampelomyces and disease epidemiology***

447 The study of the population dynamics of plant pathogens is of general interest for predicting
448 epidemic outbreaks and developing agronomical plans based on BCAs and the minimal use of
449 agrochemicals to prevent plant diseases. In the current climate change situation, it is also of
450 economic importance to understand the mechanisms involved in top-down regulation of plant
451 pathogen populations, i.e., hyperparasitism, and the role of climatic conditions and geographical
452 locations as drivers of population structure. Few studies have been conducted to unveil the role
453 of *Ampelomyces* hyperparasites in controlling PM population distribution (Tollenaere et al. 2014;
454 Parratt et al. 2017; Parratt and Laine 2018). Mycoparasites can act as top-down regulators in the
455 dynamics of parasite-host interactions as they are very efficient in reducing the mycelial growth
456 and overwintering inoculum of their PM hosts and, consequently, may notably affect the fungal

457 host population (Parratt and Laine 2016). At large scale, environmental factors, or geographical
458 barriers are more effective in determining hyperparasite population distribution than
459 hyperparasite-mycobhost genotype interactions (Tollenaere et al. 2014).

460 Within a cryptic pathogen complex, *Erysiphe* spp., on the pedunculate oak *Quercus*
461 *robur*, it was found that there is no a relationship between temperature or humidity and
462 *Ampelomyces* incidence at continental or national scales. However, in France, it was found that
463 climate can be associated with *Ampelomyces* population distribution, and probably, this occurred
464 as the *Ampelomyces* incidence was related to its host presence, i.e., *Erysiphe alphitoides*, which
465 are most abundant in northeastern France, in localities with cold winters (Faticov et al. 2022).
466 Further investigation is required to identify biotic and abiotic factors that drive the distribution of
467 the plant pathogens, Erysiphales, and their natural enemies, *Ampelomyces* mycoparasites, at
468 different spatial scales; and these studies are crucial to guide future control measures of plant
469 protection.

470

471 ***Biocontrol of powdery mildews by Ampelomyces***

472 The lack of host specificity makes the hyperparasitic *Ampelomyces* suitable agents to control
473 different PM species. Moreover, these hyperparasites are very efficient in reducing PM disease
474 severity up to 98% of the control value (Elad et al. 1998), and in reducing the overwintering
475 inoculum of PMs (Shishkoff and McGrath 2002)). To reduce the overwintering chasmothecia of
476 *E. necator*, spraying either a highly virulent *Ampelomyces* strain, RS1-a, extracted from *P.*
477 *pannosa*, or the commercial AQ10 strain in vineyards during autumn significantly delays and
478 reduces the early season development of PM in the following year (Legler et al. 2016). Even

479 though *Ampelomyces* do not stop the spread of powdery infections during the late stages of
480 epidemics (Falk, Gadoury, Cortesi, et al. 1995; Falk, Gadoury, Pearson, et al. 1995)

481 The application of *Ampelomyces* reduces the host sporulation rate (Angeli, Puopolo, et al.
482 2012), destroys immature chasmothecia by 50% or 60% (Falk, Gadoury, Cortesi, et al. 1995),
483 and improves plant health by preventing chlorophyll and stroma loss and protecting thylakoids
484 damage. For example, chlorophyll contents in cucumber leaves infected with *P. fuliginea* were
485 lost in ~50%, but insignificantly reduced in *A. quisqualis*-treated leaves (Abo-Foul et al. 1996).
486 Altogether, these findings support the notion that these hyperparasites play an important role in
487 reducing disease severity, which makes them potential BCAs.

488 Several *Ampelomyces* isolates have been tested to evaluate their biocontrol potential
489 action on PMs which has resulted in the commercialization of five strains (Table 1). The first
490 biocontrol agent based on *Ampelomyces* conidia was registered in 1988 under the name AQ10[®]
491 (Sztejnberg et al. 1989; Sztejnberg 1993). It consisted of a pure strain, *A. quisqualis* AQ10 or M-
492 10 strain (CNCM accession number: I-807), originally extracted in Israel from *Oidium* sp.
493 (Sztejnberg et al. 1989; Sztejnberg 1993) on *Catha edulis* which, in field trials, was proved to
494 reduce disease severity of PMs on cucumber, carrots, and melon; and it was compatible with the
495 fungicide pyrazophos (Sztejnberg et al. 1989). Further, it has been shown to be unharmed, at
496 concentrations indicated by the manufacturer, on the biology and behaviour of *Bombus terrestris*,
497 a member of the family Apidae (Mommaerts et al. 2009). In some instances, the efficacy of
498 AQ10[®] was shown to be consistently satisfactory, for example, against *P. pannosa* on Rosa with
499 an average efficacy of 70% (Pasini et al. 1997). However, other investigations showed that this
500 commercial biofungicide alone cannot successfully control PMs on other plants, i.e., *E. necator*

501 on grapes (Legler et al. 2016), *P. fusca* on cucurbit (McGrath and Shishkoff 1999), and *P.*
502 *xanthii* on zucchini (Gullino et al. 2020).

503 The underlying mechanisms causing these variations are not understood, although, part of
504 the problem can be due to formulation issues and/or environmental conditions such as low RH.
505 Differences in growth rate among *Ampelomyces* isolates can be observed in culture at different
506 temperatures where the highest values of growth rate are obtained between 15°C–25°C
507 (Czerniawska 2001; Liang et al. 2004; Angeli, Maurhofer, et al. 2012). As environmental factors
508 contribute to the initiation of *Ampelomyces* infections, it is not expected that virulent strains will
509 have the same effect in greenhouse and field conditions. It is likely that in greenhouses,
510 *Ampelomyces*-based BCAs will be much more efficient as temperature and RH can be controlled,
511 but in the field, their combined use with fungicides will be required.

512

513 ***Formulations of Ampelomyces-based biocontrol agents***

514 New formulations to maintain the life of *Ampelomyces*-based biofungicides have been sought.
515 For example, when AQ10[®] was combined with polymers Nu Film 17 and Nu Film P, which used
516 to protect biofungicides against degradation caused by heat and UV, the effectiveness of AQ10[®]
517 against oak PM, caused by *E. alphitoides*, was enhanced from 48% to 73.60%-94.59% (Rajković
518 et al. 2010). As a high RH is needed to enhance biocontrol potential of *Ampelomyces* isolates,
519 several strategies have been tested, i.e., to reduce the high demand of RH for conidial
520 germination, it can be used an emulsion of liquid parafilm at 1% and at 80% of RH together with
521 a suspension of *A. quisqualis* conidia (Philipp and Hellstern 1986). To improve the performance
522 of AQ10[®], wetting Add-Q was used to maintain humidity of the strain M-10 contained in
523 AQ10[®], but this additive also decreased PM in the absence of the biofungicide (Shishkoff and

524 McGrath 2002). Similarly, the application of ADDIT adjuvant, which is an emulsifiable
525 vegetable oil, alone reduced PM disease, caused by *P. fusca*, severity of greenhouse-grown
526 melon plants (Romero et al. 2007). Whereas the commercial AQ10[®] significantly reduced PM
527 disease severity only when used combined with ADDIT adjuvant, which is an emulsifiable
528 vegetable oil.

529

530 The same *A. quisqualis* AQ10 strain has been commercialized into a new dry-formulated product
531 consisting of spores and mycelial fragments, Bio-Dewcon 2% wettable powder (WP), by T.
532 Stanes & Co Ltd in India (Lewis et al. 2016). This new formulated bio fungicide has been tested
533 in fruit and leaves of cucumber against *P. fuliginea* where the PM disease incidence decreased
534 after three applications of *Ampelomyces* foliar spraying (Sivakumar et al. 2020). The least per
535 cent disease index of PM disease was 10.92 after 35 days and 14.32 after 45 days of the last
536 spray, and crop yield improved over control by 30.56% when used Bio-Dewcon at 5 kg. ha⁻¹
537 (Sivakumar et al. 2020).

538 As *Ampelomyces* strains efficacy vary (Angeli, Puopolo, et al. 2012), an IDM program
539 can be implemented as suggested by Romero et al. (2007) which involves minimum use of
540 agrochemicals together with new BCAs containing coadjuvants. The latter is possible as
541 hyperparasites resist certain pesticides directed against some PMs where crop yields are restored
542 to those values obtained when using fungicide alone, i.e., Triforine (Sundheim 1982). Moreover,
543 a virulence synergistic effect has been observed in *Ampelomyces* when combined with the
544 fungicide myclobutanil (Gilardi et al. 2008).

545 In a recent study, an effective strain, CPA-9, against PM on cucurbits was used to
546 produce conidia in an optimised liquid medium of potato dextrose broth modified with 2.5%

547 (w/v) of glycerol and incubated at 25°C for 11 days in the dark and without agitation. The
548 resulting conidia were viable as reduced *P. xanthii* disease incidence in cucumber plants by up to
549 83% (Carbó, Torres, Usall, et al. 2020).

550 Other formulations have been tested to enhance the resilience of *Ampelomyces* - based
551 BCA against variations of temperature and RH. A new formulated CPA-9 BCA was developed
552 where conidia were dehydrated by using a fluidised-bed spray-drying system. Whereas to
553 enhance adherence of conidia to the surface of leaves, biodegradable coatings were included in
554 the solid formulation (Carbó, Teixidó, Usall, et al. 2021). It was found that the biodegradable
555 coatings-based solid formulation of the *A. quisqualis* Ces. CPA-9 BCA was compatible with (1)
556 some fungicides against mildew diseases, i.e., sulphur, but not Kresoxim-methyl, myclobutanil,
557 and Trifloxystrobin; and (2) some insecticides, i.e., Abamectin, Azadirachtin, and Imidacloprid,
558 but not Chlorpyrifos, and Flufenoxuron. The compatibility observed between the formulated
559 CPA-9 and the different phytosanitary products was at concentrations recommended by the
560 manufacturers. These results are promising and indicate this BCA can be included into IDM. In
561 addition, the fluidized-bed spray-dried treated CPA-9 conidia were viable and successfully
562 mycoparasitised hyphae of *P. xanthii* on zucchini leaves. Conidial adherence between formulated
563 and non-formulated CPA-9 conidia on zucchini leaves was similar under the rainfall treatment as
564 biodegradable coatings were water soluble. Unlike the AQ10[®], survival of the new formulated
565 CPA-9 conidia was also consistent across variations of temperatures and RH, which are ideal for
566 *Ampelomyces* conidial germination (Carbó, Teixidó, Usall, et al. 2021). These results indicate
567 that CPA-9 is a promising BCA, although further testing is required to confirm its effectivity in
568 field conditions. Similarly, the combined use of new formulations based on a derivative of chitin,
569 chitosan, and *Ampelomyces* was found to successfully reduce *E. necator* on grapes and enhanced

570 the weight of the fruit compared to the control (untreated PM grapes) (Thosar et al. 2020). This
571 is advantageous when using *Ampelomyces*-based BCAs because it will help to decrease chemical
572 usage and reduce the chemical burden on the environment. The mechanisms underlying fungal
573 chemical resistance are initiated by genetic mutations that make fungi less susceptible to
574 fungicides (Goldman et al. 1993). This has been effectively studied in *Trichoderma* spp.
575 (Goldman et al. 1993), but not in *Ampelomyces*, and it will be important to elucidate the
576 mechanisms operating within hyperparasites for biocontrol development purposes.

577

578 **Conclusions**

579 The identification of *Ampelomyces* mycoparasites was achieved as early as 1852 by Cesati.
580 These hyperparasites attack a wide variety of PM fungi on different plants, can destroy the
581 mycelia of their hosts, and are tolerant to several fungicides. However, their efficacies are
582 variable as their virulence strength depends on environmental factors and genetic interactions
583 with their hosts. In addition, these hyperparasites may serve as a novel source of natural products
584 as suggested by the information provided by new genome sequences. However, the identification
585 of *Ampelomyces* species is challenging. Several nucleotide sequences of the ITS region are
586 included in databases where they are annotated as belonging to the genus *Ampelomyces*.
587 However, based on sequence analysis of their ITS2 and S2s, they do not belong to this genus.
588 The S2s also reflect the phylogeny of *Ampelomyces* and are a valuable molecular tool to
589 elucidate evolutionary mechanisms. The presence of pseudogenes can explain the origin of some
590 *Ampelomyces* groups, and the phenotypic variations detected at strain level. Finally, these
591 hyperparasites can be classified into lineages that cannot be differentiated by the morphological
592 features of their asexual structures, indicating that species delimitation relies on the use of multi-

593 locus phylogenetic analysis. Extensive sampling of isolates per PM species and plants from
594 several geographical areas is required to answer questions involving association of lineages with
595 physiological and biochemical characters, and their underlying mechanisms of evolution.
596 Finally, improving the identification of *Ampelomyces* will contribute to the development of
597 better eco-friendly approaches for management of powdery mildew diseases.

598

599 **Author Contributions**

600 Writing-original draft preparation, R.P.; review and editing, R.P., S.K. and R.D.; supervision,
601 S.K and R.D. All authors have read and agreed to the published version of the manuscript.

602

603 **Funding**

604 This work was supported by the School of Sciences and the Graduate Research School of the
605 University of Southern Queensland, Australia.

606

607 **Acknowledgements**

608 We thank Dr. Douglas Eacersall from University of Southern Queensland and the reviewers for
609 their valuable suggestions.

610

611 **Conflicts of Interest**

612 The authors declare no conflict of interest.

613

614 **References**

615 Abo-Foul S, Raskin VI, Szejnberg A, Marder JB. 1996. Disruption of chlorophyll organization and
616 function in powdery mildew-diseased cucumber leaves and its control by the hyperparasite
617 *Ampelomyces quisqualis*. *Phytopathology*. 86:195–199.

618 AgriLife™. 2021. PowderyCare® *Ampelomyces quisqualis* biofungicide approved for use in organic
619 agriculture. [accessed 2021 May 18]. <https://www.agrilife.in/>.

620 Agrobrest Grup. 2021. OVNIER: Biological & Botanical. [accessed 2021 Dec 15].
621 <https://agrobrestgrup.com/bitki-koruma-urunleri/ovnier>.

622 Angeli D, Maurhofer M, Gessler C, Pertot I. 2012. Existence of different physiological forms within
623 genetically diverse strains of *Ampelomyces quisqualis*. *Phytoparasitica*. 40:37–51.

624 Angeli D, Pellegrini E, Maurhofer M, Pertot I, Micheli S, Ress D, Gessler C. 2009. Molecular
625 characterization of *Ampelomyces* spp. isolates from different hosts and geographic origins and
626 evaluation of their potential to control powdery mildew of cucumber. *IOBC/WPRS Bull.* 43:40–
627 44.

628 Angeli D, Pellegrini E, Pertot I. 2009. Occurrence of *Erysiphe necator* chasmothecia and their natural
629 parasitism by *Ampelomyces quisqualis*. *Phytopathology*. 99:704–710. doi:10.1094/PHYTO-99-6-
630 0704.

631 Angeli D, Puopolo G, Maurhofer M, Gessler C, Pertot I. 2012. Is the mycoparasitic activity of
632 *Ampelomyces quisqualis* biocontrol strains related to phylogeny and hydrolytic enzyme
633 production? *Biol Control*. 63:348–358. doi:10.1016/j.biocontrol.2012.08.010.

634 Aveskamp MM, de Gruyter J, Woudenberg JHC, Verkley GJM, Crous PW. 2010. Highlights of the
635 Didymellaceae: a polyphasic approach to characterise *Phoma* and related pleosporalean genera.
636 *Stud Mycol.* 65:1–60. doi:10.3114/sim.2010.65.01.

637 Banupriya M, Ushamalini C, Nakkeeran S, Raguchander T. 2019. Morphological characterization of
638 *Ampelomyces* spp., a hyperparasite of grapevine [*Vitis vinifera* (L.)] powdery mildew. *Int J Curr*
639 *Microbiol App Sci.* 8:1725–1731. doi:10.20546/ijemas.2019.806.206.

640 Beauvais A, Monod M, Debeauvais J-P, Diaquin M, Kobayashi H, Latgé J-P. 1997. Biochemical and
641 antigenic characterization of a new dipeptidyl-peptidase isolated from *Aspergillus fumigatus*. J
642 Biol Chem. 272:6238–6244. doi:10.1074/jbc.272.10.6238.

643 Berg G. 2009. Plant–microbe interactions promoting plant growth and health: perspectives for controlled
644 use of microorganisms in agriculture. Appl Microbiol Biotechnol. 84:11–18. doi:10.1007/s00253-
645 009-2092-7.

646 Carbó A, Teixidó N, Usall J, Solsona C, Torres R. 2021. Formulated *Ampelomyces quisqualis* CPA-9
647 applied on zucchini leaves: influence of abiotic factors and powdery mildew mycoparasitization.
648 Eur J Plant Pathol. 161:37–48. doi:10.1007/s10658-021-02302-y.

649 Carbó A, Torres R, Usall J, Ballesta J, Teixidó N. 2020. Biocontrol potential of *Ampelomyces quisqualis*
650 strain CPA-9 against powdery mildew: conidia production in liquid medium and efficacy on
651 zucchini leaves. Sci Hortic. 267:109337. doi:10.1016/j.scienta.2020.109337.

652 Cesati V. 1852. *Ampelomyces quisqualis* Ces. Bot Zeitung. 10:301–302.

653 Cheetham SW, Faulkner GJ, Dinger ME. 2020. Overcoming challenges and dogmas to understand the
654 functions of pseudogenes. Nat Rev Genet. 21:191–201. doi:10.1038/s41576-019-0196-1.

655 Chemknock. 2021. Q-fect. [accessed 2021 Jun 23].
656 <https://chemknock.com/view.do?no=194&pgMode=view&dvsn=pdt&idx=25100>.

657 Chen Q, Jiang JR, Zhang GZ, Cai L, Crous PW. 2015. Resolving the *Phoma* enigma. Stud Mycol.
658 82:137–217. doi:10.1016/j.simyco.2015.10.003.

659 Chen X, Wan L, Wang W, Xi WJ, Yang AG, Wang T. 2020. Re-recognition of pseudogenes: from
660 molecular to clinical applications. Theranostics. 10:1479–1499. doi:10.7150/thno.40659.

661 Clare BG. 1964. *Ampelomyces quisqualis* (*Cicinnobolus cesatii*) on Queensland Erysiphaceae (University
662 of Queensland, Dept. of Botany). St. Lucia, Qld, Australia: University of Queensland Press.

663 Côté CA, Peculis BA. 2001. Role of the ITS2-proximal stem and evidence for indirect recognition of
664 processing sites in pre-rRNA processing in yeast. Nucleic Acids Res. 29:2106–2116. doi:
665 10.1093/nar/29.10.2106.

666 Czerniawska B. 2001. Studies on the biology and occurrence of *Ampelomyces quisqualis* in the Drawski
667 Landscape Park (NW Poland). *Acta Mycol.* 36:191–201.

668 Dik AJ, Verhaar MA, Be'langer RR. (1998). Comparison of three biological control agents against
669 cucumber powdery mildew (*Sphaerotheca fuliginea*) in semi-commercial-scale glasshouse trials.
670 *Eur J Plant Pathol.* 104:413–423. doi: 10.1023/A:1008025416672.

671 de Bary A. 1870. *Eurotium, Erysiphe, Cicinnobolus*, nebst bemerkungen über die geschlechtsorgane der
672 Ascomyceten. In: de Bary A, Woronin M, editors. Beiträge zur morphologie und physiologie der
673 pilze. Frankfurt, Germany: Verlag von C. Winter; p. 1–95.

674 de Gruyter J, Aveskamp MM, Woudenberg JH, Verkley GJ, Groenewald JZ, Crous PW. 2009. Molecular
675 phylogeny of *Phoma* and allied anamorph genera: towards a reclassification of the *Phoma*
676 complex. *Mycol Res.* 113:508–519. doi:10.1016/j.mycres.2009.01.002.

677 Ehrenberg CG. 1853. Weintrauben krankheit. *Bot Zeitung.* 11:15–16.

678 Elad Y, Kirshner B, Yehuda N, Sztejnberg A. 1998. Management of powdery mildew and gray mold of
679 cucumber by *Trichoderma harzianum* T39 and *Ampelomyces quisqualis* AQ10. *BioControl.*
680 43:241–251. doi:10.1023/A:1009919417481.

681 Emmons CW. 1930. *Cicinnobolus cesatii*, a study in host-parasite relationships. *Bull Torrey Bot Club.*
682 57:421–439.

683 European Food Safety Authority (EFSA), Arena M, Auteri D, Barmaz S, Bellisai G, Brancato A, Brocca
684 D, Bura L, Byers H, Chiusolo A, et al. 2017. Peer review of the pesticide risk assessment of the
685 active substance *Ampelomyces quisqualis* strain AQ10. *EFSA J.* 15:e05078.
686 doi:10.2903/j.efsa.2017.5078.

687 Falk SP, Gadoury DM, Cortesi P, Pearson RC, Seem RC. 1995. Parasitism of *Uncinula necator*
688 cleistothecia by the mycoparasite *Ampelomyces quisqualis*. *Phytopathology.* 85:794–800.
689 doi:10.1094/Phyto-85-794.

690 Falk SP, Gadoury DM, Pearson RC, Seem RC. 1995. Partial control of grape powdery mildew by the
691 mycoparasite *Ampelomyces quisqualis*. *Plant Dis.* 79:483–490. doi:10.1094/PD-79-0483.

692 Faticov M, Desprez-Loustau M-L, Kiss L, Massot M, d'Arcier JF, Mutz J, Németh MZ, Roslin T, Tack
693 AJM. 2022. Niche differentiation within a cryptic pathogen complex: climatic drivers and
694 hyperparasitism at multiple spatial scales. *Ecography*. 2022:e06062. doi:10.1111/ecog.06062.

695 Gautam AK, Avasthi S. 2016. *Ampelomyces quisqualis* - a remarkable mycoparasite on *Xanthium*
696 *strumarium* powdery mildew from Himachal Pradesh India. *Phytopathol Pest Manag*. 3:64–70.

697 Gilardi G, Manker DC, Garibaldi A, Gullino ML. 2008. Efficacy of the biocontrol agents *Bacillus subtilis*
698 and *Ampelomyces quisqualis* applied in combination with fungicides against powdery mildew of
699 zucchini. *J Plant Dis Prot*. 115:208–213. doi:10.1007/BF03356265.

700 Glawe DA. 2008. The powdery mildews: a review of the world's most familiar (yet poorly known) plant
701 pathogens. *Annu Rev. Phytopathol*. 46:27–51. doi:10.1146/annurev.phyto.46.081407.104740.

702 Goldman GH, Temmerman W, Jacobs D, Contreras R, Van Montagu M, Herrera-Estrella A. 1993. A
703 nucleotide substitution in one of the β -tubulin genes of *Trichoderma viride* confers resistance to
704 the antimetabolic drug methyl benzimidazole-2-yl-carbamate. *Mol Gen Genet*. 240:73–80.
705 doi:10.1007/BF00276886.

706 Gong L, Luo H, Shi W, Yang M. 2019. Intra-individual variation and transcribed pseudogenes in the
707 ribosomal ITS1-5.8S-ITS2 rDNA of *Paraplagusia japonica* (Pleuronectiformes: Cynoglossidae).
708 *Biochem Biophys Res Commun*. 513:726–731. doi:697 10.1016/j.bbrc.2019.04.064.

709 Gorfer M, Blumhoff M, Klaubauf S, Urban A, Inselsbacher E, Bandian D, Mitter B, Sessitsch A, Wanek
710 W, Strauss J. 2011. Community profiling and gene expression of fungal assimilatory nitrate
711 reductases in agricultural soil. *ISME J*. 5:1771–1783. doi:10.1038/ismej.2011.53.

712 Groen JN, Capraro D, Morris KV. 2014. The emerging role of pseudogene expressed non-coding RNAs
713 in cellular functions. *Int J Biochem Cell Biol*. 54:350–355. doi:10.1016/j.biocel.2014.05.008.

714 Gu YH, Ko WH. 1997. Water agarose medium for studying factors affecting germination of conidia of
715 *Ampelomyces quisqualis*. *Mycol Res*. 101:422–424.

716 Gullino ML, Tabone G, Gilardi G, Garibaldi A. (2020). Effects of elevated atmospheric CO₂ and
717 temperature on the management of powdery mildew of zucchini. *J. Phytopathol*. 168:405–415.

718 Hage H, Rosso MN, Tarrago L. 2021. Distribution of methionine sulfoxide reductases in fungi and
719 conservation of the free-methionine-R-sulfoxide reductase in multicellular eukaryotes. *Free Radic*
720 *Biol Med.* 169:187–215. doi:10.1016/j.freeradbiomed.2021.04.013.

721 Haridas S, Albert R, Binder M, Bloem J, LaButti K, Salamov A, Andreopoulos B, Baker SE, Barry K,
722 Bills G, et al. 2020. 101 *Dothideomycetes* genomes: a test case for predicting lifestyles and
723 emergence of pathogens. *Stud Mycol.* 96:141–153. doi:10.1016/j.simyco.2020.01.003.

724 Harpke D, Peterson A. 2008. Extensive 5.8S nrDNA polymorphism in *Mammillaria* (Cactaceae) with
725 special reference to the identification of pseudogenic internal transcribed spacer regions. *J Plant*
726 *Res.* 121:261–270.

727 Hashioka Y, Nakai Y. 1980. Ultrastructure of pycnidial development and mycoparasitism of
728 *Ampelomyces quisqualis* parasitic on *Erysiphales*. *Trans Mycol Soc Jpn.* 21:329–338.

729 Huth L, Ash GJ, Idnurm A, Kiss L, Vaghefi N. 2021. The "bipartite" structure of the first genome of
730 *Ampelomyces quisqualis*, a common hyperparasite and biocontrol agent of powdery mildews,
731 may point to its evolutionary origin from plant pathogenic fungi. *Genome Biol Evol.* 7:evab182.
732 doi:10.1093/gbe/evab182.

733 Jarvis WR, Slingsby K. 1977. The control of powdery mildew of greenhouse cucumber by water spray
734 and *Ampelomyces quisqualis*. *Plant Dis. Rep.* 61:728–730.

735 Jatou-Ogay K, Suter M, Crameri R, Falchetto R, Fatih A, Monod M. 1992. Nucleotide sequence of a
736 genomic and a cDNA clone encoding an extracellular alkaline protease of *Aspergillus fumigatus*.
737 *FEMS Microbiol Lett.* 92:163–168. doi:10.1111/j.1574-462 6968.1992.tb05253.x.

738 Joseph N, Krauskopf E, Vera MI, Michot B. 1999. Ribosomal internal transcribed spacer 2 (ITS2)
739 exhibits a common core of secondary structure in vertebrates and yeast. *Nucleic Acids Res.*
740 27:4533–4540. doi:10.1093/nar/27.23.4533.

741 Kim JY, Lee WH, Kim HM. 2009. Physical characteristics and antagonistic effect of *Ampelomyces*. *Res*
742 *Plant Dis.* 15:209–216. doi:10.5423/RPD.2009.15.3.209.

743 Kiss L. 1997. Genetic diversity in *Ampelomyces* isolates, hyperparasites of powdery mildew fungi,
744 inferred from RFLP analysis of the rDNA ITS region. *Mycol Res.* 101:1073–1080.
745 doi:10.1017/s0953756297003705.

746 Kiss L. 1998. Natural occurrence of *Ampelomyces* mycoparasites in mycelia of powdery mildew fungi.
747 *New Phytol.* 140:709–714. doi:10.1046/j.1469-8137.1998.00316.x.

748 Kiss L. 2003. A review of fungal antagonists of powdery mildews and their potential as biocontrol agents.
749 *Pest Manage Sci.* 59:475–483.

750 Kiss L. 2008. Intracellular mycoparasites in action: interactions between powdery mildew fungi and
751 *Ampelomyces*. In: Avery SV, Stratford M, Van West P, editors. *Stress in yeasts and filamentous*
752 *fungi*. London: Academic Press, Elsevier; p. 37–52. doi:10.1016/S0275-0287(08)80045-8.

753 Kiss L, Nakasone KK. 1998. Ribosomal DNA internal transcribed spacer sequences do not support the
754 species status of *Ampelomyces quisqualis*, a hyperparasite of powdery mildew fungi. *Curr Genet.*
755 33:362–367. doi:10.1007/s002940050348.

756 Kiss L, Pintye A, Kovács GM, Jankovics T, Fontaine MC, Harvey N, Xu X, Nicot PC, Bardin M, Shykoff
757 JA, et al. 2011. Temporal isolation explains host-related genetic differentiation in a group of
758 widespread mycoparasitic fungi. *Mol Ecol.* 20:1492–1507. doi:10.1111/j.1365-
759 294X.2011.05007.x.

760 Kiss L, Pintye A, Zséli G, Jankovics T, Szentiványi O, Hafez YM, Cook RTA. 2010. Microcyclic
761 conidiogenesis in powdery mildews and its association with intracellular parasitism by
762 *Ampelomyces*. *Eur J Plant Pathol.* 126:445–451. doi:10.1007/s10658-009-9558-4.

763 Kiss L, Vagna L. (1995). New approaches in the study of the genus *Ampelomyces*, hyperparasites of
764 powdery mildew fungi. In *Environmental Biotic Factors in Integrated Plant Disease Control* (ed.
765 M. Manka), pp. 301–304. Polish Phytopathological Society: Poznań, Poland.

766 Lee SY, Lee SB, Kim CH. 2004. Biological control of powdery mildew by Q-fect WP (*Ampelomyces*
767 *quisqualis*) in various crops. *IOBC/wprs Bull.* 27:329–331.

768 Legler SE, Pintye A, Caffi T, Gulyas S, Bohar G, Rossi V, Kiss L. 2016. Sporulation rate in culture and
769 mycoparasitic activity, but not mycohost specificity, are the key factors for selecting
770 *Ampelomyces* strains for biocontrol of grapevine of powdery mildew (*Erysiphe necator*). Eur J
771 Plant Pathol. 144:723–736. doi:10.1007/s10658-015-0834-1.

772 Lewis KA, Tzilivakis J, Warner D, Green A. 2016. An international database for pesticide risk
773 assessments and management. Human and Ecological Risk Assessment: An international Journal.
774 22:1050–1064. doi:10.1080/10807039.2015.1133242.

775 Liang C, Honghai Z, Baodu L, Yingchen Z, Guozhong L. 2004. Biological characteristics of
776 *Ampelomyces quisqualis* hyperparasite on tickseed powdery mildew. J Yunnan Agric Univ.
777 19:648–652.

778 Liang C, Yang J, Kovacs GM, Szentiványi O, Li B, Xu XM, Kiss L. 2007. Genetic diversity of
779 *Ampelomyces* mycoparasite isolated from different powdery mildew species in China inferred
780 from analyses of rDNA ITS sequences. Fungal Divers. 24:225–240.

781 Liyanage KK, Khan S, Brooks S, Mortimer PE, Karunaratna SC, Xu J, Hyde KD. 2018.
782 Morphomolecular characterization of two *Ampelomyces* spp. (Pleosporales) strains mycoparasites
783 of powdery mildew of *Hevea brasiliensis*. Front Microbiol. 9:12. doi:10.3389/fmicb.2018.00012.

784 Lücking R, Aime MC, Robbertse B, Miller AN, Ariyawansa HA, Aoki T, Cardinali G, Crous PW,
785 Druzhinina IS, Geiser DM, Hawksworth DL, Hyde KD, Irinyi L, Jeewon R, Johnston PR, Kirk
786 PM, Malosso E, May TW, Meyer W, Öpik M, Robert V, Stadler M, Thines M, Vu D, Yurkov
787 AM, Zhang N, Schoch CL. 2020. Unambiguous identification of fungi: where do we stand and
788 how accurate and precise is fungal DNA barcoding? IMA Fungus. 11:14. doi: 10.1186/s43008-
789 020-00033-z.

790 McGrath MT, Shishkoff N. (1999). Evaluation of biocompatible products for managing cucurbit powdery
791 mildew. Crop Protect. 18:471–478. doi: 10.1016/S0261-2194(99)00048-4.

792 Manjunatha L, Singh S, Ravikumara BM, Narasa Reddy G, Senthilkumar M. 2020. *Ampelomyces*. In:
793 Amaresan N, Senthil Kumar M, Annapurna K, Kumar K, Sankaranarayanan A, editors.
794 Beneficial microbes in agro-ecology. Amsterdam, Netherlands: Academic Press; p. 833–860.
795 Mhaskar DN, Rao VG. 1974. The mycoparasite *Ampelomyces quisqualis* Ces. in artificial culture. II.
796 Effect of environmental factors. *Phytopathol Mediterr.* 13:147–154.
797 Mommaerts V, Sterk G, Hoffmann L, Smagghe G. 2009. A laboratory evaluation to determine the
798 compatibility of microbiological control agents with the pollinator *Bombus terrestris*. *Pest Manag*
799 *Sci.* 65:949–955. doi: 10.1002/ps.1778.
800 Németh MZ, Li G, Seress D, Pintye A, Molnár O, Kovács GM, Kiss L, Gorfer M. 2021. What is the role
801 of the nitrate reductase (*euknr*) gene in fungi that live in nitrate-free environments? A targeted
802 gene knock-out study in *Ampelomyces* mycoparasites. *Fungal Biol.* 125:905–913.
803 doi:10.1016/j.funbio.2021.06.004.
804 Németh MZ, Mizuno Y, Kobayashi H, Seress D, Shishido N, Kimura Y, Takamatsu S, Suzuki T,
805 Takikawa Y, Kakutani K, et al. 2021. *Ampelomyces* strains isolated from diverse powdery
806 mildew hosts in Japan: their phylogeny and mycoparasitic activity, including timing and
807 quantifying mycoparasitism of *Pseudoidium neolycopersici* on tomato. *PLoS One.* 16:e0251444.
808 doi:10.1371/journal.pone.0251444.
809 Németh MZ, Pintye A, Horváth ÁN, Vági P, Kovács GM, Gorfer M, Kiss L. 2019. Green fluorescent
810 protein transformation sheds more light on a widespread mycoparasitic interaction.
811 *Phytopathology.* 109:1404–1416. doi:10.1094/PHYTO-01-19-0013-R.
812 Nguyen TTT, Lee HB. 2016. First report of *Ampelomyces quisqualis* from Sycamore and Crape myrtle
813 and its potential as a mycoparasite of powdery mildew. *Kor J Mycol.* 44:64–67.
814 doi:10.4489/KJM.2016.44.1.64.
815 Nonomura T, Matsuda Y, Takikawa Y, Kakutani K, Toyoda H. 2014. Successional changes in powdery
816 mildew pathogens prevailing in common and wild tomato plants rotation-cultivated in a
817 greenhouse. *Ann Rept Kansai PI Prot.* 56:17–20. doi:10.4165/kapps.56.17.

818 Oh Y, Franck WL, Han SO, Shows A, Gokce E, Muddiman DC, Dean RA. 2012. Polyubiquitin is
819 required for growth, development and pathogenicity in the rice blast fungus *Magnaporthe oryzae*.
820 PLoS One. 7:e42868. doi:10.1371/journal.pone.0042868.

821 Park MJ, Choi YJ, Hong SB, Shin HD. 2010. Genetic variability and mycohost association of
822 *Ampelomyces quisqualis* isolates inferred from phylogenetic analyses of ITS rDNA and *actin*
823 gene sequences. Fungal Biol. 114:235–247. doi:10.1016/j.funbio.2010.01.003.

824 Parratt SR, Barrès B, Penczykowski RM, Laine A-L. 2017. Local adaptation at higher trophic levels:
825 contrasting hyperparasite-pathogen infection dynamics in the field and laboratory. Mol Ecol.
826 26:1964–1979. doi:10.1111/mec.13928.

827 Parratt SR, Laine A-L. 2016. The role of hyperparasitism in microbial pathogen ecology and evolution.
828 ISME J. 10:1815–1822.

829 Parratt SR, Laine A-L. 2018. Pathogen dynamics under both bottom-up host resistance and top-down
830 hyperparasite attack. J Appl Ecol. 55:2976–2985. doi:10.1111/1365-2664.13185.

831 Pasini C, D’Aquila F, Curir P, Gullino ML. (1997). Effectiveness of antifungal compounds against rose
832 powdery mildew (*Sphaerotheca pannosa* var *rosae*) in glasshouses. Crop Protect. 16:251–256.
833 doi:10.1016/S0261-2194(96)00095-6. Paulitz TC, Bélanger RR. 2001. Biological control in
834 greenhouse systems. Annu Rev Phytopathol. 39:103–133.

835 Philipp WD. 1995. Extracellular enzymes and nutritional physiology of *Ampelomyces quisqualis* Ces.,
836 hyperparasite of powdery mildew, *in vitro*. J. Phytopathol. 114:274–283. doi:10.1111/j.1439-
837 0434.1985.tb00853.x.

838 Philipp WD, Hellstern A. 1986. Biological control of powdery mildew by *Ampelomyces quisqualis* under
839 reduced air humidity. Z Pflanzenk Pflanzen. 93:384–391.

840 Phookamsak R, Liu JK, McKenzie EHC, Manamgoda DS, Ariyawansa H, Thambugala KM, Dai D-Q,
841 Camporesi E, Chukeatirote E, Wijayawardene NN, et al. 2014. Revision of Phaeosphaeriaceae.
842 Fungal Divers. 68:159–238. doi:10.1007/s13225-014-0308-3.

843 Pink RC, Carter DR. 2013. Pseudogenes as regulators of biological function. *Essays Biochem.* 54:103–
844 112. doi:10.1042/bse0540103.

845 Pintye A, Bereczky Z, Kovács GM, Nagy LG, Xu X, Legler SE, Váczy Z, Váczy KZ, Caffi T, Rossi V, et
846 al. 2012. No indication of strict host associations in a widespread mycoparasite: grapevine
847 powdery mildew (*Erysiphe necator*) is attacked by phylogenetically distant *Ampelomyces* strains
848 in the field. *Phytopathology.* 102:707–716. doi:10.1094/PHYTO-10-11-0270.

849 Pintye A, Ropars J, Harvey N, Shin HD, Leyronas C, Nicot PC, Giraud T, Kiss L. 2015. Host phenology
850 and geography as drivers of differentiation in generalist fungal mycoparasites. *PLoS One.*
851 10:e0120703. doi:10.1371/journal.pone.0120703.

852 Prahel RE, Khan S, Deo RC. 2021. The role of internal transcribed spacer 2 secondary structures in
853 classifying mycoparasitic *Ampelomyces*. *PLoS One.* 16:e0253772.
854 doi:10.1371/journal.pone.0253772.

855 Rajković S, Tabaković-Tošić M, Marković M, Milovanović J, Mitić D. 2010. Application of AQ-10
856 biofungicide on *quercus robur* l. seedlings. *Fresenius Environ Bull.* 19:2987–2992.

857 Ranković B. 1997. Hyperparasites of the genus *Ampelomyces* on powdery mildew fungi in Serbia.
858 *Mycopathologia.* 139:157–164. doi: 10.1023/A:1006811924205.

859 Riess H. 1852. Über *Byssocystis textilis*. *Hedwigia.* 1:23.

860 Romero D, De Vicente A, Zerriouh H, Cazorla FM, Fernández-Ortuño D, Torés JA, Pérez-García A. 2007.
861 Evaluation of biological control agents for managing cucurbit powdery mildew on greenhouse-
862 grown melon. *Plant Pathol.* 56:976–986. doi:10.1111/j.1365-3059.2007.01684.x.

863 Rotem Y, Yarden O, Szejnberg A. 1999. The mycoparasite *Ampelomyces quisqualis* expresses *exgA*
864 encoding an exo-beta-1,3-Glucanase in culture and during mycoparasitism. *Phytopathology.*
865 89:631–638. doi:10.1094/PHYTO.1999.89.8.631.

866 Rudakov OL. 1979. Fungi of the genus *Ampelomyces* Ces. Ex Schlecht Mikol Fitopatol. 13:104–110.

867 Saijo Y, Loo EP. 2020. Plant immunity in signal integration between biotic and abiotic stress responses.
868 *New Phytol.* 225:87–104. doi:10.1111/nph.15989.

869 Shishkoff N, McGrath MT. 2002. AQ10 biofungicide combined with chemical fungicides or AddQ spray
870 adjuvant for control of *Cucurbit* powdery mildew in detached leaf culture. *Plant Dis.* 86:915–918.
871 doi:10.1094/PDIS.2002.86.8.915.

872 Siozios S, Tosi L, Ferrarini A, Ferrari A, Tononi P, Bellin D, Maurhofer M, Gessler C, Delledonne M,
873 Pertot I. 2015. Transcriptional reprogramming of the mycoparasitic fungus *Ampelomyces*
874 *quisqualis* during the powdery mildew host-induced germination. *Phytopathology.* 105:199–209.
875 doi:10.1094/PHYTO-01-14-0013-R.

876 Sivakumar T, Balabaskar P, Renganathan P, Sanjeevkumar K. 2020. To evaluate the bio-efficacy and
877 phytotoxicity of powder formulation of Biodewcon (*Ampelomyces quisqualis* 2.00% Wp) against
878 powdery mildew (*Sphaerotheca fuliginea*) in cucumber crop. *Plant Arch.* 20:3811–3815.

879 Speer EO. 1978. Beitrag zur Morphologie von *Ampelomyces quisqualis* Ces. *Sydowia.* 31:242–246.

880 Stalder L. (1955). Beobachtungen über das Verhalten von *Podosphaera leucotricha* (Ellis et Everh.)
881 Salm. in Apfelknospen. *Phytopathologische Zeitschrift* 23:341–344.

882 Sucharzewska E, Dynowska M, Kubiak D, Ejdyś E, Biedunkiewicz A. 2012. *Ampelomyces* hyperparasites
883 – occurrence and effect on the development of ascomata of Erysiphales species under conditions
884 of anthropopressure. *Acta Soc Bot Pol.* 81:147–152. doi:10.5586/asbp.2012.023.

885 Sullivan RF, White JF Jr. 2000. *Phoma glomerata* as a mycoparasite of powdery mildew. *Appl Environ*
886 *Microbiol.* 66:425–427. doi:10.1128/aem.66.1.425-427.2000.

887 Sundheim L. 1982. Control of cucumber powdery mildew by the hyperparasite *Ampelomyces quisqualis*
888 and fungicides. *Plant Pathol.* 31:209–214. doi:10.1111/j.1365-3059.1982.tb01270.x.

889 Sundheim L, Krekling T. 1982. Host-parasite relationships of the hyperparasite *Ampelomyces quisqualis*
890 and its powdery mildew host *Sphaerotheca fuliginea*. I. Scanning electron microscopy. *J*
891 *Phytopathol.* 104:202–210. doi:10.1111/j.1439-0434.1982.tb00527.x.

892 Szentiványi O, Kiss L. 2003. Overwintering of *Ampelomyces* mycoparasites on apple trees and other
893 plants infected with powdery mildews. *Plant Pathol.* 52:737–746. doi:10.1111/j.1365-
894 3059.2003.00937.x.

895 Szentiványi O, Kiss L, Russell JC, Kovács GM, Varga K, Jankovics T, Lesemann S, Xu XM, Jeffries P.
896 2005. *Ampelomyces* mycoparasites from apple powdery mildew identified as a distinct group
897 based on single-stranded conformation polymorphism analysis of the rDNA ITS region. *Mycol*
898 *Res.* 109:429–438.

899 Sztejnberg A. 1993. *Ampelomyces quisqualis* AQ10, CNCM I-807, for biological control of powdery
900 mildew. Israel: Yissum Research Development Company of the Hebrew University of Jerusalem.
901 [accessed 2022 Jun. 22]. <https://patents.google.com/patent/US5190754A/en>.

902 Sztejnberg A, Galper S, Mazar S, Lisker N. 1989. *Ampelomyces quisqualis* for biological and
903 integrated control of powdery mildew in Israel. *J. Phytopathol.* 124:285–295. doi:10.1111/j.1439-
904 0434.1989.tb04925.x.

905 Tanaka K. 2009. The proteasome: overview of structure and functions. *Proc Jpn Acad Ser B Phys Biol*
906 *Sci.* 85:12–36. doi:10.2183/pjab.85.12.

907 Thosar RU, Sawant I, Chavan VM, Sawant SD, Saha S, Suthakar AV. 2020. Generation of a bio-intensive
908 strategy using chitosan formulations and *Ampelomyces quisqualis* for the management of
909 powdery mildew of grapes. [accessed 2022 Feb. 21].
910 <http://krishi.icar.gov.in/jspui/handle/123456789/50941>.

911 Tollenaere C, Pernechele B, Mäkinen HS, Parratt SR, Németh MZ, Kovács GM, Kiss L, Tack AJ, Laine
912 A-L. 2014. A hyperparasite affects the population dynamics of a wild plant pathogen. *Mol Ecol.*
913 23:5877–5887. doi:10.1111/mec.12908.

914 Tye BW, Commins N, Ryazanova LV, Wühr M, Springer M, Pincus D, Churchman LS. 2019.
915 Proteotoxicity from aberrant ribosome biogenesis compromises cell fitness. *Elife.* 8:e43002.
916 doi:10.7554/eLife.43002.

917 Verhaar MA, Keressies A, Hijwegen T. 1999. Effect of relative humidity on mycoparasitism of rose
918 powdery mildew with and without treatments with mycoparasites. *Zeitschrift für*
919 *Pflanzenkrankheiten und Pflanzenschutz* 106:158–65.

920 Wijayawardene NN, Camporesi E, Song Y, Dai DQ, Bhat DJ, Mckenzie EHC, Chukeatirote E, Mel'nik
921 VA, Wang Y, Hyde KD. (2013). Multigene analyses reveal taxonomic placement of
922 *Scolicosporium minkeviciusii* in Phaeosphaeriaceae (Pleosporales). *Cryptogam Mycol.* 34:357–
923 366. doi:10.7872/crym.v34.iss2.2013.357

924 Yarwood CE. 1932. *Ampelomyces quisqualis* on clover mildew. *Phytopathology.* 22:31.

925 Younes G, Ahmad M, Ali N. 2016. Mycoparasitism of *Ampelomyces quisqualis* Ces. ex Schlecht on
926 powdery mildew fungi in Syria. *JJAS.* 12:223–237.

927 Zhang Y, Gao Y, Liang Y, Dong Y, Yang X, Yuan J, Qiu D. 2017. The *Verticillium dahliae* SnodProt1-
928 like protein VdCP1 contributes to virulence and triggers the plant immune system. *Front Plant*
929 *Sci.* 8:1880. doi:10.3389/fpls.2017.01880.

930 Zhang Y, Schoch CL, Fournier J, Crous PW, de Gruyter J, Woudenberg JH, Hirayama K, Tanaka K,
931 Pointing SB, Spatafora JW, et al. 2009. Multi-locus phylogeny of Pleosporales: a taxonomic,
932 ecological and evolutionary re-evaluation. *Stud Mycol.* 64:85–102. doi:10.3114/sim.2009.64.04.

933

934

935 **Fig. 1** *Ampelomyces* mycoparasites of powdery mildews. Mycelia of powdery mildew fungi are
936 observed as white powdery spots covering the surface of a leaf and *Ampelomyces* pycnidia develop
937 in the host mycelia. (a) Asexual life cycle of powdery mildew fungi. It starts by germination of a
938 PM conidium, formation of a germ tube, which will develop into a cuticular peg and an appendage.
939 Once inside the plant host cytoplasm, haustorium is intracellularly formed where the uptake of
940 nutrients takes place. *Ampelomyces* conidium germinates and invades host hypha. During the
941 mycoparasitic stage, *Ampelomyces* pycnidium develops inside the mycohost conidiophore. From
942 a mature pycnidium, *Ampelomyces* conidia are massively released which will cause destruction of
943 the host conidiophore. (b) Sexual life cycle of powdery mildew fungi. The sexual cycle starts with
944 the transference of antheridial nucleus to the ascogonium through means of the PM reproductive
945 sexual structures (the female ascogonium and the male antheridium). This cycle ends with the
946 formation of chasmothecium and release of asci containing ascospores. Massive release of
947 *Ampelomyces* conidia causes destruction of host chasmothecium and, thus, stops the mycohost
948 reproductive sexual stage. Abbreviations: Ascogonium (As); Antheridium (An); Chasmothecium
949 (Ch); Conidiophore (Cp); Haustorium (Ht); Hypha (Hy); Pycnidium (Py); Powdery mildew (PM).
950

951

Chapter 5

Characterization of the ITS 1 and 2 belonging to Ampelomyces

Article III: The ITS 1 and 2 are under functional constraints of their secondary structures

Summary:

In the previous chapter four main different ITS2 S2s models were elucidated in the *Ampelomyces* population [Prahl et al. 2021]. However, the characterization of its structural characteristics was not conducted.

Several studies showed that ITS2 sequences are under functional constrain of their S2s [Paredes-Esquivel and Townson 2014]. A recent investigation showed that ITS2 sequences are under evolutionary constraint of their S2s through differences in nucleotide contents and transitional and transversional bias ratio between stems and bulges or loops forming the S2 derived from a recent lineage of the plant *Corydalis* [Zhang et al. 2020]. This chapter aims to evaluate if ITS 1 and 2 sequences are subjected to molecular evolutionary constraints of their S2s and provide new insights into the evolution and phylogeny of *Ampelomyces* mycoparasites. Furthermore, the results of the present study will help to establish a framework for identification of ITS nucleotide sequences derived from eDNA.

Please see below Paper 3. Paper 3 is in final preparation for its submission soon.

1 **Secondary structure analyses of the nuclear rRNA Internal Transcribed**
2 **Spacers of mycoparasites *Ampelomyces***

3

4 Rosa E. Prah¹, Shahjahan Khan², and Ravinesh C. Deo³

5

6 ¹*School of Sciences, University of Southern Queensland, Toowoomba, Queensland 4350,*
7 *Australia*

8 ²*School of Sciences, University of Southern Queensland, Centre for Health Research and*
9 *Centre for Applied Climate Sciences, Toowoomba, Queensland 4350, Australia*

10 ³*School of Sciences, University of Southern Queensland, Springfield Lakes, Queensland*
11 *4300, Australia*

12

13 Correspondence to: Rosa Prah. Email: u1114537@uemail.usq.edu.au

14 ORCID: <https://orcid.org/0000-0003-1243-9881>

15

16

17

18

19

20 Manuscript for consideration as a Research article in Journal

21

22 **Abstract**

23 The nuclear ribosomal DNA internal transcribed spacer, nrDNA ITS, region is the preferred
24 molecular barcode for fungal taxonomy and phylogeny. It is constituted by the internal
25 transcribed spacer regions 1 (ITS1) and 2 (ITS2) that are separated by the 5.8S gene. The ITS
26 is a suitable molecular marker as: 1) it can be easily amplified by using conserved primers, 2)
27 it is a cost-effective method, and 3) it is assumed that these sequences are not-functional and,
28 thus, neutrally evolving molecular markers. *Ampelomyces* are among the first fungi used as
29 biocontrol agents against powdery mildew diseases of economical important crops. Despite
30 many studies based on their ITS region, their taxonomy and phylogeny remain unresolved. We
31 investigated if the ITS 1 and 2 sequences are under evolutionary constraint of their secondary
32 structures by using 26 *Ampelomyces* ITS sequences freely available in the GenBank database.
33 Our results showed ITS 1 and 2 sequences are under selective constraint of their structures,
34 which are required to maintain the orchestrated mechanisms of pre-ribosomal processing. This
35 finding suggests that these molecular markers are not neutrally evolving. Moreover, the lowest
36 energy state and the number of possible secondary structures are significantly different between
37 *Ampelomyces* ITS1 and random sequences generated with equal sequence length and cytosine
38 and guanine (C/G) contents. Whereas ITS2 adenine (A) contents and (C/G) nucleotide contents
39 were higher in stems than loops of their secondary structures and suggesting their importance
40 for tertiary molecular interactions and structure stability, respectively. Finally, the predicted
41 ITS1 structures by minimum free energies methods give different models and, thus, we
42 recommend an additional analysis based on a multi-locus phylogenetic analysis; nonetheless,
43 ITS1 secondary structures were valuable as an alternative strategy to differentiate ITS
44 sequences derived from environmental DNA samples and deposited in public databases under
45 the generic name of *Ampelomyces*.

46

47 **Keywords:** *Ampelomyces*, *Ampelomyces humuli*, environmental DNA, phylogeny, ribosomal
48 ITS1, secondary structures.

49

50 **Introduction**

51 Ribosomes are essentially complex structures responsible for protein biosynthesis (Zhang et
52 al. 2020). Components of the ribosomal RNA (rRNA) are partially encoded by repeated rDNA
53 operons that consisted of the small subunit (18S), the large subunit (5.8S and 28S) ribosomal
54 RNA genes separated by external and internal transcribed spacers (Perry 1976). For the
55 synthesis of ribosomes, the whole operon is transcribed as a pre-rRNA molecule by the RNA
56 polymerase I (Grummt 2003; Scull and Schneider 2019); and followed by excision of their
57 spacers by successive post-transcriptional processes that are depending on their own secondary
58 structures (S2s) (Cote et al. 2002; Coleman 2015). Mutations in these conserved structures can
59 lead to decreased production of ribosomal subunits as well as slow cellular growth rates in
60 culture (Côté and Peculis 2001; Hang et al. 2014). The rDNA ITS region consists of two
61 internal transcribed spacers, 1 and 2, separated by the 5.8S gene (Lafontaine and Tollervey
62 2001). The ITS is the preferred molecular identifier for fungi (Schoch et al. 2012) as (1) it is
63 easy to amplify by using conserved primers, and (2) it is assumed that the ITS1 and ITS2 evolve
64 neutrally by concerted evolution (Elder and Turner 1995; Naidoo et al. 2013; De Luca et al.
65 2021) where mutations are homogenized along the ribosomal gene clusters by unequal
66 crossing-over and other turnover mechanisms (Szostak and Wu 1980). This assumption has
67 been considered when reconstructing the phylogeny of organisms via DNA models of
68 evolution. However, several findings indicate that the ITS sequences are under evolutionary
69 functional constrain of their S2s (Edger et al. 2014; Paredes-Esquivel and Townson 2014;
70 Zhang et al. 2020).

71 Fungi belonging to the genus *Ampelomyces* are mycoparasites of the Erysiphales (Manjunatha
72 et al. 2020), which are fungal phytopathogens causing powdery mildew (PM) diseases on
73 economically important crops (Glawe 2008). Phylogenetic analyses based on the ITS region
74 and actin 1 (*act1*) gene fragment have revealed that *Ampelomyces* mycoparasites consisted of

75 at least five genetically distinct clades that can be distinguished into sub-cladal types (Németh
76 et al. 2021). Each lineage is (1) thought to consist of distinct species group (2) some groups
77 represents differences in colony morphology of *Ampelomyces* strains (Angeli et al. 2012), and
78 (3) forms distinct ITS2 S2s ‘types’ (Prah et al. 2021). Despite evidence showing S2s are
79 required for pre-ribosomal processing (Pillon et al. 2019), phylogenetic analyses based on the
80 ITS 1 and 2 sequences together with their S2s have been less evaluated than the traditional ITS
81 sequences. Hence, we investigated if the *Ampelomyces* ITS 1 and 2 sequences are under
82 functional constraint of their S2s and evaluated the utility of ITS1 S2s in phylogenetic analysis
83 of *Ampelomyces*. Despite the variability of the ITS region between species confers with enough
84 resolution barcode gap, genetic distances among some *Ampelomyces* lineages can reach up to
85 15% (Kiss and Nakasone 1998); and potentially causing biases when working with closely
86 related unknown taxa. To resolve this caveat, other barcodes have been suggested to use in this
87 type of analysis (Kiss 2012; Schoch et al. 2012). Based on these premises, there are around 817
88 ITS sequences named *Ampelomyces*, and available in the GenBank database (30 Jun 2021) that
89 can be used to extract and predict ITS1 S2s. Currently, a single ITS1 model from anaerobic
90 fungi was proposed (Koetschan et al. 2014). It consists of an open loop with three helices,
91 although more helices can be present (Coleman 2015). However, further studies are required
92 to establish a conserved core of ITS1 S2s for other fungi, which is difficult as length ITS1
93 variations can occur in different taxonomical groups (Koetschan et al. 2014). In this paper, we
94 will contribute to this area by predicting the ITS1 S2s of 26 ITS *Ampelomyces* sequences
95 representing the four major lineages of this genus. The results of this research will be a future
96 reference for further works to advance in our knowledge of the biology, ecology, and
97 phylogeny of these important mycoparasitic fungi.

98

99

100 **Materials and methods**

101 To investigate if the ITS1 sequences are under functional constraint of their S2s, we
102 implemented the methods described in (Edger et al. 2014). All possible ITS1 S2s of 26
103 *Ampelomyces* ITS sequences, which represent the four main lineages of this genus, and 300
104 nucleotide sequences randomly generated were modelled via the UNAFold web server (Zuker
105 2003). Suppl. Table 1 contains the NCBI GenBank accession numbers of each sequence. The
106 300 nucleotide sequences were randomly generated with equal sequence length and C/G
107 contents to the 26 *Ampelomyces* ITS1 sequences by using the online tool at
108 <https://www.molbiotools.com/randomsequencegenerator.php>. A Kruskal-Wallis test was
109 conducted to establish statistical significance value between both the total number of possible
110 S2s and lowest energy state from *Ampelomyces* ITS sequences and from the sequences
111 randomly generated. The test was conducted via the online tool available at
112 <https://www.socscistatistics.com/tests/kruskal/default.aspx> (Statistics 2018). The total number
113 of hairpins and paired bases were calculated manually. In this study, we considered a hairpin
114 structure, either with single or branches structures, as a continuous loop build by the
115 approximation of paired bases nucleotides between two distance positions. At least four
116 nucleotide bonds are required to form a hairpin. Whereas stems are those structures no forming
117 immediately loops.

118 **Sequence acquisition**

119 We retrieved from the NCBI GenBank database 26 complete *Ampelomyces* ITS nucleotide
120 sequences (Suppl. Table 1). These sequences were used in an early work based on ITS2 S2s
121 (Prah et al. 2021) and utilized in this research to compare the efficiency of the ITS1 sequences
122 and their S2s in phylogenetic analyses of *Ampelomyces*. We confirmed that these ITS
123 sequences belonged to the *Ampelomyces* mycoparasites by manually checking their original

124 references. The ‘true’ *Ampelomyces* nucleotide sequences are those whose morphology of
 125 pycnidia and growth rate in culture are like those from type specimen of *Ampelomyces* (Kiss
 126 and Nakasone 1998; Sullivan and White 2000; Németh et al. 2021). In addition, five other ITS
 127 sequences were retrieved which belonged to fungal isolates extracted from human nasal mucus
 128 with GenBank identifiers (GI) AF455518 and AF455498 (Buzina et al. 2003), including from
 129 environmental DNA (eDNA) samples: (1) creosote-treated crosstie wastes with GI: GQ241274
 130 (Dominguez-Monino 2014), (2) Rhizospheric soil with GI: HQ649997 (Maciá-Vicente et al.
 131 2012), and (3) from the sea turtle *Caretta* with GI: KJ789852 (Domiciano et al. 2014), Suppl.
 132 Table 2.

133 On the other hand, four and one ITS sequences derived from *Didymella glomerata* and *Phoma*
 134 *herbarum*, respectively, were used as outgroup taxa, Suppl. Table 3. The *D. glomerata* strains
 135 are derived from *Erysiphe penicillata*, GI: AF126819, (Sullivan and White 2000), soil, GI:
 136 MH864401, (Vu et al. 2019), *Juniperus* sp. FJ427015, (Aveskamp et al. 2009), and *Poa*
 137 *pratensis*, GI: KT387236, (Yang et al. 2016). Whereas the *P. herbarum* strain was extracted
 138 from *Malus sylvestris*, GI: JF810528, (Woudenberg et al. 2012).

139 Partial 18S and 28S nucleotide sequences were eliminated before the analyses.

140 **ITS1 structure prediction**

141 To evaluate the utility of ITS1 S2s in studying the evolutionary relationship of *Ampelomyces*
 142 and if these can be used to differentiate them from those ITS sequences deposited on the generic
 143 name of *Ampelomyces*, the ITS1 sequences from each *Ampelomyces* sp. *sensu stricto*, from
 144 those of powdery mildew-free environments, and from the outgroup taxa were predicted by
 145 using the online tool Mfold version 3.6 (Zuker 2003) at UNAFold web server
 146 (<http://www.unafold.org/mfold/applications/rna-folding-form-v2.php>). Default parameters
 147 were used; and the folding energy parameters were used according to Mathews *et al.* (Mathews

148 et al. 1999); and the minimum free energy (ΔG at 37°C) was estimated for stability comparison
149 (SantaLucia 1998). The structures were further analysed to calculate manually the number of
150 paired bases and hairpins.

151 **DNA repeats prediction in ITS1 sequences from *Ampelomyces* isolates and** 152 **those from putative *Ampelomyces***

153 Complete ITS1 sequences were aligned by using the web tool MAFFT v 7.481 based on the L-
154 INS-I approach with default values (Katoh et al. 2005; Katoh and Toh 2008). The resulting
155 alignment was used as input in the software the molecular evolutionary genetics analysis
156 (MEGA)-X v10.1.8 to determine the best DNA model of evolution (Kumar et al. 2018). The
157 ITS sequences were extracted from each PM genus (*Arthrocladiella*, *Erysiphe*, *Golovinomyces*,
158 *Podosphaera*, *Phyllactinia*, *Oidium* and its subgenus *Pseudoidium*) using MEGA-X software.
159 The ITS1 sequences from fungi derived from PM- free environments and deposited in the
160 GenBank under the generic name of *Ampelomyces* as well as the outgroup taxa were grouped
161 together to form a whole outgroup taxon consisting of 10 sequences in total. Each ITS1
162 sequence was uploaded into the online web tool ‘Repeats Finder for DNA/Protein Sequences’
163 to search for putative DNA tandem repeats. This online tool is available from the NovoPro web
164 site at www.novoprolabs.com/tools/repeats-sequences.

165 **Multiple ITS1 sequence-structure alignment and phylogenetic tree**

166 To determine *Ampelomyces* lineages based on their ITS1 S2s, a simultaneous multiple
167 sequence alignment of ITS1 S2s was firstly estimated. We used the online tool LocARNA
168 v4.8.3 at <http://rna.informatik.uni-freiburg.de> for multiple alignment of RNA molecules (Will
169 et al. 2012). The input data comprised 26 ITS1 sequences and structures, which were obtained
170 from the following sources: (1) 17 *Ampelomyces* spp., Suppl Table 1, (2) one putative
171 *Ampelomyces* extracted from *Caretta* (KJ789852), Suppl. Table 2, and (3) one outgroup

172 member from *D. glomerata* (GI: MH864401), Suppl. Table 3. The selected parameters
173 consisted of a global alignment in LocARNA-P (probabilistic) mode (Will et al. 2012) where
174 the complete input ITS1 sequences were aligned. For the alignment scoring, the default values
175 were used. Thus, the values for structure weight, insertion-deletion (indel) opening score and
176 indel score were 200, -800 and -50, respectively. The match score for the alignment of two
177 identical sequences was 50, while the mismatch score for the alignment of two different
178 sequences was 0. The RIBOSUM matrix was used to score sequence match/mismatch. The
179 parameters of RNA folding energy were used with a temperature of 37°C. The energy
180 parameter settings were described by the Turner model 2004 (Turner and Mathews 20010).
181 The resulting multiple ITS1 sequence-structure alignment was analysed by using the MEGA-
182 X software in order to calculate a maximum likelihood (ML) tree based on the Tamura three-
183 parameter DNA model of evolution (Tamura 1992). This analysis was conducted with a gamma
184 distribution for the evolutionary rate among sites. The branches of the inferred unrooted tree
185 were assayed using the bootstrap analysis with 1 000 replicates. The phylogram of 26
186 *Ampelomyces* sequence structure pairs was visualized using FigTree v1.4.4 software (Rambaut
187 2014).

188 Phylogenetic trees based on ITS and ITS1 sequences were built to compare the distribution of
189 *Ampelomyces* clades and not related fungi with those obtained using ITS1 S2s, but the input
190 data comprised 26 ITS1 sequences and structures, which were obtained from the following
191 sources: (1) 26 *Ampelomyces* spp., (2) three putative *Ampelomyces* extracted from human nasal
192 mucus (GI: AF455518), creosote-treated crosstie wastes (GI:GQ241274), *Caretta* (KJ789852),
193 and (3) one outgroup member from *D. glomerata* (GI: MH864401), (Suppl. Tables 1–3,
194 respectively). The dataset was utilized to conduct a multiple sequence alignment (MSA) via
195 the MAFFT web server at <https://mafft.cbrc.jp/alignment/server/> (Kato and Toh 2008) under
196 the previous conditions. Next, phylogenetic analysis was performed with MEGA-X software

197 using the maximum likelihood method and the Tamura model (T92) (Tamura 1992) with a
198 proportion of invariable sites. The branches of the inferred unrooted tree were assayed using
199 bootstrap analysis with 1 000 replicates. The phylogram was visualized using FigTree v1.4.4
200 software (Rambaut 2014).

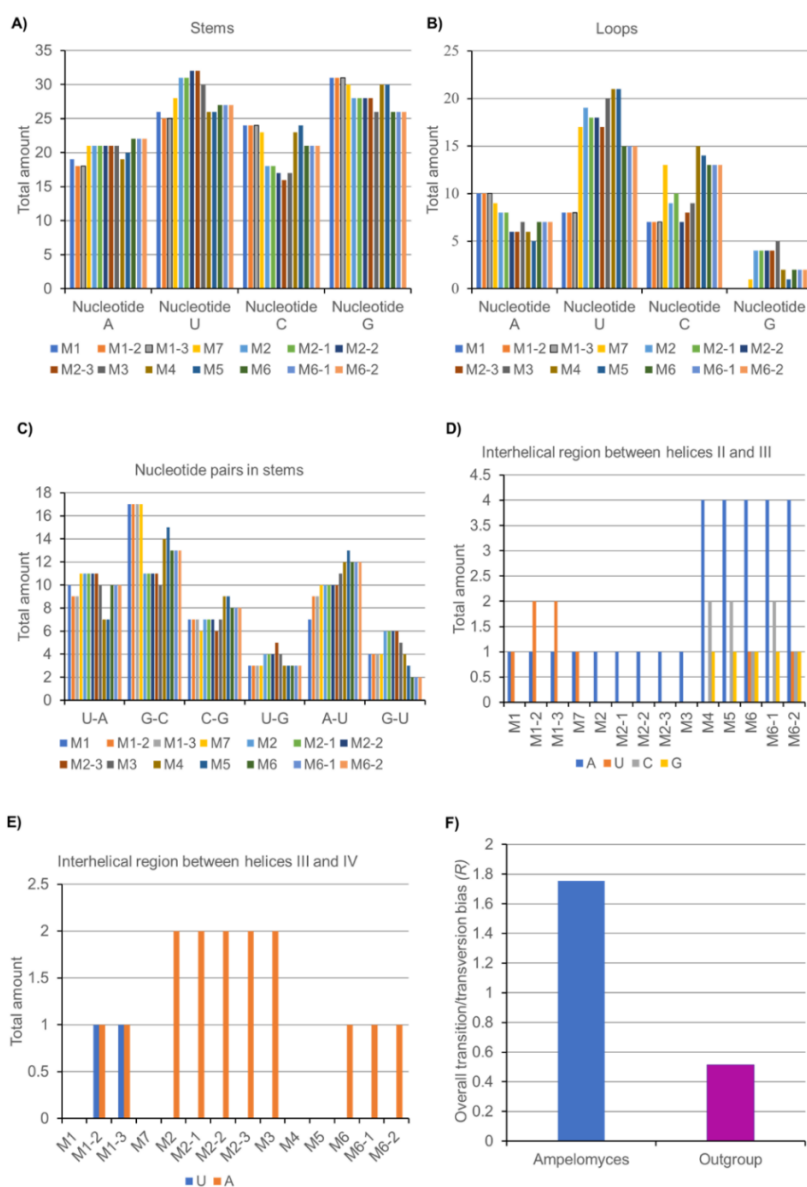
201 **Results**

202 For the *Ampelomyces* group, the average ITS1 sequence length is in average 188 bp where
203 54.82% of its nucleotides form paired bases in the predicted S2s. The means for all possible
204 ITS1 S2s together with their total number of loops are 25.5 and 5.6, respectively. In addition,
205 the lowest energy state for the ITS1 S2s has a mean of -20.0. To test if ITS1 sequences obtained
206 with the lowest energy state are an indicative that the sequences are under constraint of their
207 S2s, 300 sequences with sequence length and C/G nucleotide contents like the *Ampelomyces*
208 ITS1 sequences were randomly generated, and then, used as input in UNAFold/MFold to
209 predict the possible number of S2s. From the random sequences, the mean of total number of
210 possible S2s was 92.0 while the mean value for the lowest free energy was -13.9. We also
211 determined if the values of minimum free energies and the number of probable S2s between
212 ITS1 sequences and those randomly generated were significantly different by using a Kruskal-
213 Wallis test. The lowest energy stage and number of S2s predicted between both groups were
214 significantly different at $p < .05$ with p -values $< .00001$ and $.01583$, respectively. The total
215 number of possible structures, and their respective lowest energy state values can be seen in
216 Suppl. 1. Sheet 2.

217 For the analysis of ITS2 S2s, we used the directly predicted ITS2 S2 via the ITS2-Database
218 (ITS2-DB) from Prah et al. (2021) of which represent four main lineages of the genus
219 *Ampelomyces* and calculated the nucleotide statistics of adenine (A), cytosine (C), and Guanine
220 (G) nucleotide contents between loops (unpaired regions) and stems (paired regions) of the
221 seven unique major models with its variations predicted by *Ampelomyces* in this early work.

222 All these models have in common the motif U-U in Helix II. Further, motifs UGG, UGGU and
223 UU, and UGGU were noticed in Helices III although not at the tip as other reported organisms
224 (Schultz et al. 2005; Poczai et al. 2015). The polyadenine motif located on the single-stranded
225 ring between helices II and III, and found in yeast and vertebrates (Schultz et al. 2005), were
226 only detected in ITS2 S2s M4, M5, and M6 of *Ampelomyces* strains isolated from *Podosphaera*
227 *leucotricha*, *Podosphaera ferruginea* and *Erysiphe necator*, respectively. It was also
228 determined that in average 66.7% of nucleotides of all ITS2 S2s models formed base pairs in
229 stems. In addition, A, C, and G nucleotide contents were higher in stems than in loops, Figs.
230 **1A-B**, respectively, across all *Ampelomyces* ITS2 S2s models.

231



232

233 **Fig. 1**

234 Nucleotide contents for each component of *Ampelomyces* ITS2 S2s. Each model (M1-M6) and
 235 its variations (M1-3; M2-3 and M6-2) are represented by one ITS2 sequence. Figures (A) and
 236 (B) represent total amount of nucleotides (A, U, C and G) found in stems and loops of the four
 237 helices of each ITS2 S2s, respectively. Figure (C) represents the total amount of nucleotide
 238 base pairs found in stems of the four helices of each ITS2 S2s. Figures 1D and 1E show the
 239 unpaired nucleotide contents on the single-stranded region between helices II and III, and III
 240 and IV, respectively. Figure 1F depicts the transition/transversion bias ratio (R) between
 241 *Ampelomyces* and outgroup (*Didymella*) ITS2 sequences.

242

243

244 Compared to other pair base nucleotides, the G-C were higher in stems (Fig. 1C) than in loops
245 from all ITS2 S2s. In concordance to previous published works (Zhang et al. 2017), the G-C
246 content in stems is higher than in loops as these confer to the helices with strong stability.
247 Surprisingly, the adenine nucleotide content was higher in stems than loops for ITS2 sequences
248 belonging to *Ampelomyces* extracted from the seven powdery mildew genera. Higher values of
249 A are expected to be found in loops and single-strand rings than in stems because this
250 nucleotide can participate in long-range interactions with tertiary structures (Gutell et al. 2000).
251 However, in our pilot study the A contents were higher in stems than loops. The functional
252 implications of this difference need to be determined.

253 On the other hand, we observed that A and U contents on single-stranded rings between helices
254 II and III (Fig. 1D) and III and IV (Fig. 1E) were different for main models M1-M6. We also
255 noticed that variations in model 1 detected in *Ampelomyces* isolates from *A. mougeotii* and
256 sampled in different local areas of Hungary (Kiss et al. 2011) were found not only in helices
257 but also on the single-stranded rings regions. Interesting, the transition and transversion bias
258 (Ts/Tv) ratio among *Ampelomyces* lineages were notably different from those fungi belonging
259 to the genus *Didymella* (Fig. 1F). This is an important feature that can be used to distinguish
260 those *Didymella* or *Phoma*- like fungi from the 'true' *Ampelomyces*. The number of transition
261 mutations in stems were higher than in loops across all *Ampelomyces* ITS2 S2s. These are
262 compensatory base changes that occur to maintain the integrity of the helices.

263 **Sequence Variation of the ITS1**

264 We searched for putative short DNA repeats in the aligned sequences, we found, surprisingly,
265 a common motif of (UAUAGUA) of seven nucleotides across all ITS1 of *Ampelomyces*
266 representing their characteristic lineages, Table 1. Further, the strain (HM124978) ex.
267 *Arthrocladiella mougeotii* contains two times the motif, nucleotide positions 3 and 42. We
268 also found that those *Ampelomyces* extracted from *P. leucotricha* contained a hexanucleotide

269 (GTCTGT) repeat at positions 30 and 38, which was separated by two nucleotides (n3). We
270 also found a 9-nucleotide (TTGCTACTG) repeat at positions 8 and 45, which was separated
271 by 29 nucleotides in all isolates from Europe and in the lineage containing apple powdery
272 (APM)-*Ampelomyces* and from *P. ferruginea* (GI: DQ490763). In contrast, in the
273 *Ampelomyces* strain (DQ490766) extracted from *Erysiphe polygoni* (sampled in China) only
274 8-nucleotide (AACCCCTTG) repeat was found at the aligned positions 83 and 148. Interesting,
275 this strain was found in clade 1 together with other isolates sampled in Europe (Pintye et al.
276 2012; Németh et al. 2021). In addition, *Ampelomyces* sequences (GI: DQ490763) derived from
277 PMs of three genera *Arthrocladiella*, *Golovinomyces*, and *Podosphaera* and all sampled in
278 China (Liang et al. 2007) have a unique and distinctive DNA tandem repeats of three
279 nucleotides in positions 12, 15, and 18. In accordance to these results, the sequence length
280 variation observed in ITS1 *Ampelomyces* is mainly due to indels rather than DNA sequence
281 repeats.

282

283

284

285

286

287

288

289

290

291

292

293 **Table 1**294 DNA sequence repeats on *Ampelomyces* ITS1 sequences

<i>Ampelomyces</i> extracted from	Sequence n ^a sequence (b)	Sequence length (bp)
<i>A. mougeotii</i> _ HM124942 (Hungary)	TTGCTACTG (12, 49) UAUAGUA (3-9, and 42-48) UGC n3 UGC (13, 19)	190
<i>A. mougeotii</i> _ HM124900 (Hungary) <i>A. mougeotii</i> _ HM12495 (Hungary) <i>Erysiphe euonymi</i> _ HM124986 (France) <i>E. polygona</i> _ HM125002 (Hungary) <i>Golovinomyces cichoracearum</i> _ HM124981 (France) <i>G. cichoracearum</i> _ AY663823 (UK) <i>Neoerysiphe galeopsidis</i> _ HM124978 (France) <i>Oidium</i> sp. _ AF035783 <i>Podosphaera pannosa</i> _ HM125010 (Hungary) <i>Phyllactinia fraxini</i> DQ490764 (Germany)	TTGCTACTG (12, 49); for HM125002 (10, 47) UAUAGUA (42); and for HM125002 (40) UGC n3 UGC (13, 19); for HM125002 (11, 17)	190 190 190
<i>E. polygona</i> _ DQ490766 (China)	AACCCTTG (83, 148) TGCTA (14, 20) UAUAGUA (42) UGC n3 UGC (13, 19) UGCUGC (50-55)	190
<i>P. ferruginea</i> _ DQ490763 (China) <i>P. leucotricha</i> _ AY663815 (Hungary)	TTGCTACTG (8, 45) GTCTGT (30, 38) UAUAGUA (42) TGC n3 TGC (13, 19)	191 189
<i>E. necator</i> _ HM125015-17 (USA)	CTACTGA (16, 53) GCCTGT (30, 38) UAUAGUA (42) UGC (13)	186 185 186
<i>E. necator</i> _ HM125018 (USA)	CTACTGA (16, 53) TATTA (33, 48) UAUAGUA (42) UGC (13)	186
<i>A. mougeotii</i> on <i>L. chinense</i> _ DQ490746 (China) <i>G. cichoracearum</i> _ DQ490751 (China) <i>Podosphaera fusca</i> _ DQ490745 (China) <i>P. fusca</i> _ DQ490747 (China) <i>P. fusca</i> _ DQ490754 (China) <i>Podosphaera xanthii</i> _ DQ490750 (China) <i>P. xanthii</i> _ DQ490752 (China) <i>P. xanthii</i> _ DQ490759 (China)	UAUAGUA (41) UGCUGCUGC (12-20)	189

295

296 ^a number of nucleotides (n); ^b Sequence repeat positions on the ITS1.

297

298 The maximum coverage of DNA repeats on the ITS1 sequence for the *Ampelomyces* population299 is up to 20% while for the outgroup taxa is up to 25%. Like in the case of *Ampelomyces*, the300 ITS1 sequences from putative *Ampelomyces* extracted from human mucus (GI: AF455518 and

301 AF455498) have identical motifs but different to those strains extracted from creosote treated

302 crosstie (GQ241274), *Caretta* (KJ789852) and soil (HQ649997) as contain 9-nucleotide
 303 (AAAACCTTAA) repeats at positions 92 and 130, respectively, (Table 2). Two other ITS1
 304 sequences from human nasal mucus contained two distinctive DNA repeats (TAGA) at
 305 positions 4 and 12, which were separated by 4 nucleotides (n4), and a 5-nucleotide repeat
 306 (TACCT) at positions 27 and 51, which were separated by 20 nucleotides (Table 2). These
 307 repeats were not found in other ITS1 sequences from the whole outgroup taxa (Table 3). Apart
 308 from that, the sequence obtained from creosote-treated crosstie waste contained the sequence
 309 (TCTT) at positions 30 and 41, which were separated by 7 nucleotides. This sequence was also
 310 found in the samples from *D. glomerata* (Table 3). *D. glomerata* also contained DNA repeats
 311 (CTTAC) previously detected in the sample of *P. herbarum* (JF810528), and a unique DNA
 312 repeat (CTTTGC) at positions 17 and 100.

313

314 **Table 2**315 DNA repeats in ITS1 sequences extracted from putative *Ampelomyces*

Species name	GI	Sequence	Position on the sequence	DNA repeat Length	Coverage of DNA repeats on ITS1
<i>A. humuli</i>	AF455518	UAGA	4, 12	4	142 bp (12.67%)
	AF455498	UACCU	27, 51	5	
<i>Ampelomyces</i> sp.	GQ241274	CUUUGC	16, 101	6	141 bp (21.27%)
	KJ789852	CUUAC	31, 53	5	
		UCUU	30, 41	4	
<i>Ampelomyces</i> sp.	HQ649997	AAAACUAAA	92, 130	9	144 bp (25%)
		GCGGG	14, 69	5	
		UUGC	12, 21	4	

316

317

318 All of the ITS1 sequences from *D. glomerata* contained the TCTT n7 TCTT repeats at positions
 319 30 and 41 and the TTTAA motif at nucleotide positions 44 and 91. In contrast, the ITS1 from
 320 *P. herbarum* (GI: JF810528) contained two DNA repeats, CTTTGC and CTTAC (Table 3).

321

322 **Table 3**

323 DNA repeats in ITS1 sequences extracted from outgroup taxa

Outgroup taxa	GI	Sequence	Position on the sequence	DNA repeat Length	Coverage of DNA repeats on ITS1
<i>D. glomerata</i>	AF126819	UUUAA	44, 91	5	139 bp (12.95%)
	FJ427015	UCUU	30, 41	4	
	KT387236				
	MH864401				
<i>P. herbarum</i>	JF810528	CUUUGC	17, 100	6	139 bp (15.82%)
		CUUAC	32, 53	5	

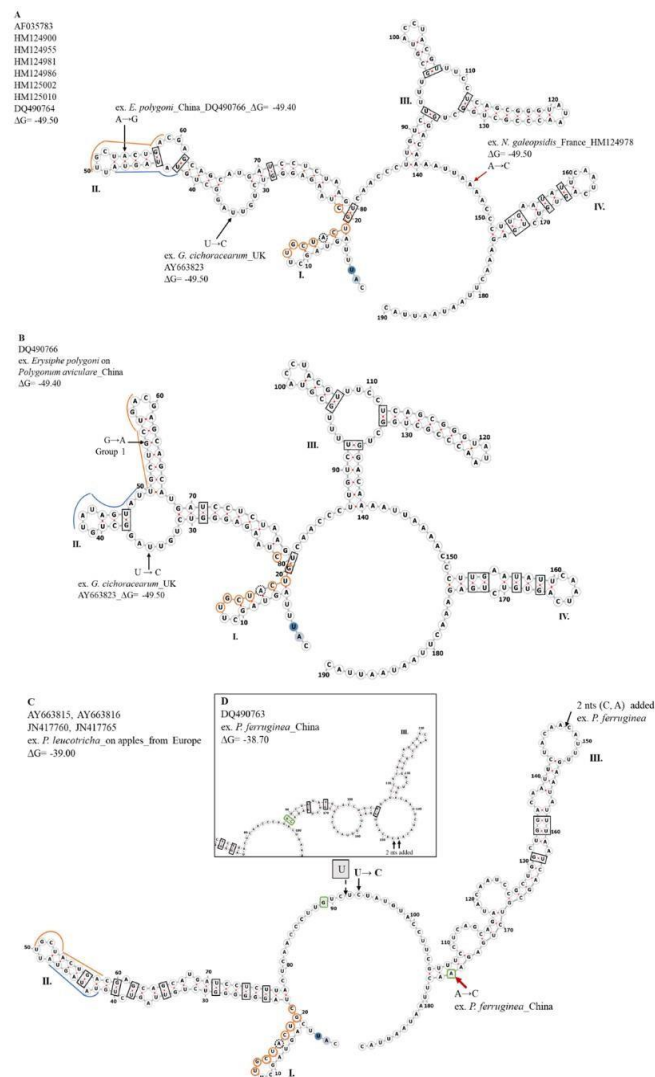
324

325 Nevertheless, we analyzed additional ITS1 sequences from *Ampelomyces* extracted from *A.*
326 *mougeotii*, *E. necator*, *Phyllactinia* sp. and *P. leucotricha*. In all cases, we did not identify the
327 same DNA repeats that were found on the putative *Ampelomyces* ITS1 sequences as well as
328 the outgroup taxa (data not shown).

329 **Characteristics of the ITS1 secondary structures**

330 The predicted ITS 1 secondary structures of *Ampelomyces* have typical three helices followed
331 by a single-stranded ring rich in A and U nucleotides (Figs. 1 and 2). However, those ITS1 S2s
332 from *Ampelomyces* strains extracted from several European locations contain four helices
333 where single-stranded rings between helices II and III, and III and IV are rich in A and C (Fig.
334 1A). Interesting, one strain isolated from China (DQ490766) has ITS1 S2 like those from
335 Europe, but helix II had a major modification where the second internal loop is bifurcated (Fig.
336 1B). The short single-stranded ring between helices I and II contains a G for those strains
337 extracted from *P. leucotricha* (Fig. 2C). While *Ampelomyces* strains from China contains only
338 one A nucleotide (Fig. 3A-C). The short single-stranded ring between helices I and II contains
339 a C for those strains extracted from *E. necator* (Figs. 3D-F). The rest of the strains isolated
340 from Europe and one from China (DQ490764) contain a motif ATCG. The long single-stranded
341 ring after helix III is rich in A and U but those strains isolated from *E. necator* (HM125015 and
342 HM125016).

343



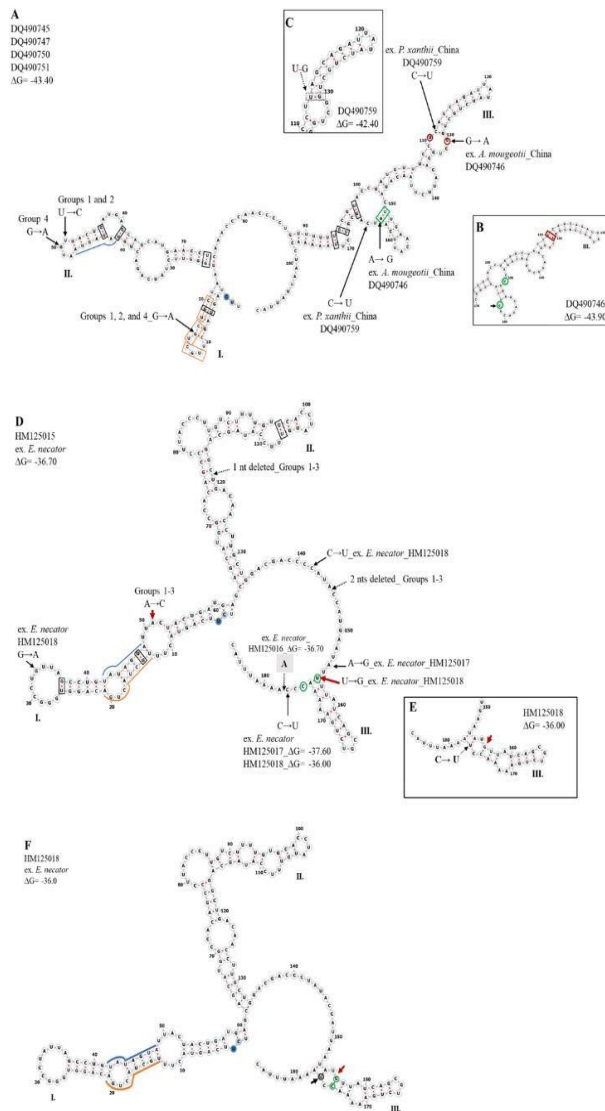
344

345

346 **Fig. 2**

347 ITS1 S2s of *Ampelomyces* isolates from *E. necator*. *Ampelomyces* ITS1 secondary structures predicted
 348 via the UNAFold/MFold method. In accordance to the phylogeny based on the ITS1 S2s, ITS1
 349 secondary structures of *Ampelomyces* strains from (A) clade 1, including the strain extracted from *E.*
 350 *polygoni* and sampled in China (B), where major variations were observed in Helix II (B). Clade 2
 351 constituted by *Ampelomyces* extracted from *P. leucotricha* (C). The strain extracted from *P. ferruginea*
 352 grouped in clade 2 together with apple powdery mildew (APM) *Ampelomyces* where major variations
 353 in its S2 were noticed on Helix III (D). Conserved motifs are indicated in blue and orange lines.

354



355
 356
 357
 358
 359
 360
 361
 362
 363
 364
 365
 366

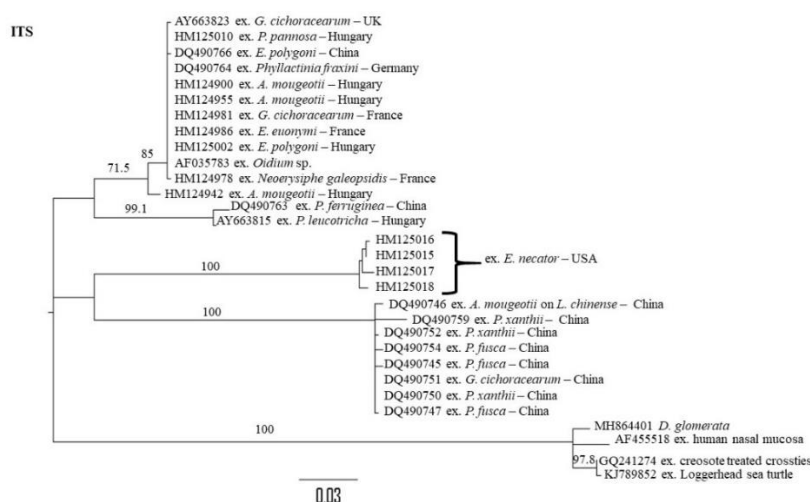
Fig. 3

ITS1 secondary structures for *Ampelomyces* extracted from *E. necator* and those strains isolated only in China. These S2s were predicted via the UNAFold/MFold method. Based on the ITS1 S2s phylogenetic analysis, these figures depict the ITS1 secondary structures of strains only sampled in China, clade 3 (A-C), and those extracted from *E. necator* and only sampled in the USA (D-F). Conserved motifs are indicated in blue and orange lines. Major variations were noticed on helices III for strains DQ490746 (B), DQ490759 (C), and HM125018 (E and F).

367 Phylogenetic analysis

368 We evaluated the utility of ITS1 sequences and their S2s to resolve *Ampelomyces* lineages by
 369 comparing the phylogeny of *Ampelomyces* based on ITS sequences, ITS1 sequences and ITS1
 370 and S2s. The best model of DNA substitution for the 26 *Ampelomyces* and four outgroup ITS
 371 sequences was the Tamura 3-parameter (T92) with a proportion of invariable sites (+G). This
 372 model was selected with the lowest score of a Bayesian information criterion, 4630.665, and
 373 maximum likelihood ($\ln L$) value of -2027.36 with gamma distribution of (+G) of 0.47. The
 374 tree with the highest log likelihood of -2025.69 (4 categories [+G, 0.4389% sites) is shown
 375 below (Fig. 4).

376



377

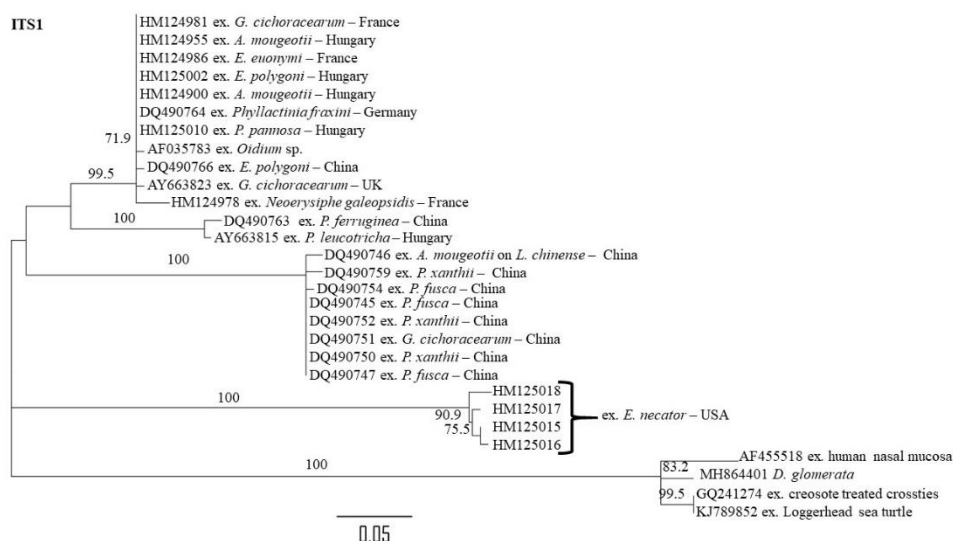
378 Fig. 4

379 Maximum Likelihood phylogram based on 26 *Ampelomyces* ITS sequences. The phylogram
 380 with the highest log likelihood (-2025.69) was based on the ITS and inferred via the maximum
 381 likelihood (ML) method and the Tamura three-parameter (T92) model. An evolutionary rate
 382 among sites was modelled with a discrete gamma distribution [4 categories (+G) parameter =
 383 0.48]. The ML bootstrap values are indicated over the branches and are expressed as
 384 percentages. The scale bar represents the nucleotide substitutions per site. The tree was edited
 385 with FigTree v1.4.4 software. Abbreviations: extracted (ex.). GenBank accession numbers are
 386 indicated first and followed by the species of PM hosts.

387

388 Conversely, when based the phylogenetic analysis on ITS1 sequences, the best model of DNA
 389 substitution that describes the evolution of the isolates was the Tamura 3-parameter (T92) with
 390 a proportion of invariable sites (+I). This model was selected with the lowest score of a
 391 Bayesian information criterion, 2382.743, and maximum likelihood (lnL) value of -933.117
 392 and a proportion of invariable sites (+I) of 0.34. Like the phylogram based on ITS sequences,
 393 the ITS1 sequences resolved better some branches within a clade, i.e., between two strains
 394 HM125015 and HM125016 and the one from HM125017, which were extracted from *E.*
 395 *necator* (Fig. 5).

396



397

398 Fig. 5

399 Maximum likelihood tree based on 26 *Ampelomyces* ITS1 sequences. The tree with the highest
 400 log likelihood of -933.05 and a proportion of invariable sites (+I, 34.18% sites) is shown above.
 401 The ML bootstrap values are indicated over the branches and are expressed as percentages. The
 402 scale bar represents the nucleotide substitutions per site.

403

404 As expected the ML analysis based on ITS1 sequences grouped *Ampelomyces* in four distinct
 405 clades that corresponded to the previous clades representing six ITS2 S2 models from an early

406 study. Conversely, when the combined use of ITS1 sequences and S2s revealed *Ampelomyces*
 407 can also be grouped in four distinct but subclades within monophyletic groups (strains from
 408 apple, HM125015–18, and grapevine, AY663815, AY663816 and DQ490763) powdery
 409 mildews) were greater separated with bootstrap support ≥ 80 percent (Fig. 6).



410

411 **Fig. 6**

412 Maximum likelihood phylogram based on ITS1 S2s improve the bootstrap values for
 413 *Ampelomyces* strains within subclades. The phylogram with the highest log likelihood (-
 414 862.37) was based on the ITS2 S2s and inferred via the maximum likelihood (ML) method and
 415 the Tamura three-parameter model. An evolutionary rate among sites was modelled with a
 416 proportion of invariable sites ([+I] 29.64% sites). The ML bootstrap values are indicated over
 417 the branches and are expressed as percentages. The scale bar represents the nucleotide
 418 substitutions per site. GenBank accession numbers are only indicated.

419

420 We investigated the utility of ITS1 S2s in resolve the phylogeny of *Ampelomyces*. The
421 Secondary structures of 26 ITS1 *Ampelomyces* strains ‘types’, representing four out of the five
422 well-known clades in *Ampelomyces*, were modelled via the UNAFold and minimum free
423 energies. The number of predicted loops among lineages was variable. Clade 1 S2s contains
424 between five and nine loops, clade 2 S2s has three or five loops, clade 3 between three and six
425 loops, and clade 4 between four and eight loops. These ITS1 sequences have a sequence length
426 of 191 nucleotides while those from putative *Ampelomyces* ranged between 141 and 142 and
427 the outgroup was 139. The % GC content range was between 40.74 and 45.16 while those for
428 putative *Ampelomyces* varied from 43.16 to 47.89. For the outgroup, the value was of 45.32.
429 For clade 1 the range was between 42.02 and 42.63. For clade 2 and formed by isolates from
430 *P. ferruginea* and *P. leucotricha*, the values were 41.80 and 42.41, respectively. For clade 3
431 constituted by strains from *E. necator*, the range was between 44.09 and 45.16 while for clade
432 4 the range was from (ex. *P. xanthii* DQ490759) 15 to 40.74. Despite the ITS1 S2s of
433 *Ampelomyces* are diverse, each clade can be grouped based on similar S2s. However, the ITS1
434 S2s for a given ITS sequence showed more variability than those from ITS2 S2s. To illustrate,
435 *Ampelomyces* isolates from *E. necator* have similar ITS1 S2s topologies but have major
436 variations in helices I and III while the strain extracted from *P. ferruginea* (DQ490763) was
437 different to those derived from *P. leucotricha* where major variations were noticed in helices
438 II and III and in the single-stranded region between helices II and III. This leads to differentiate
439 the strains from the rest within the clade with high posterior probabilities.

440 **Discussion**

441 The ribosomal RNA gene clusters consist of repeated subunits, involving seven components as
442 follows: the 5’ external transcribed spacer, the 18S rDNA exon, the ITS1, the 5.8S rDNA exon,
443 the ITS2, the 28S rDNA exon, and the 3’ external transcribed spacer (Lafontaine and Tollervey
444 2001). For phylogenetic purposes, the ITS 1 and 2 spacers are considered non-functional and

445 evolve neutrally by concerted evolution (Brown et al. 1972). It was proposed that evolution of
446 ribosomal genes depends on one another (Nei and Rooney 2005) and mutations are
447 homogenized along the cistrons by unequal crossing over and gene conversion (Naidoo et al.
448 2013). However, recent evidence indicates this is not the case for sequences of the ITS region
449 as these are under the evolutionary constraint of their S2s (Edger et al. 2014; Zhang et al. 2020).
450 Differences in adenine (A) and cytosine/guanine (C/G) nucleotide contents were noticed
451 between features of the common core eukaryotic ITS2 S2 from a new lineage of the plant
452 *Corydalis*, stems (base pairs) and loops (unpaired nucleotides). The A nucleotide contents were
453 higher in unpaired region than paired areas as in these positions A can form different structural
454 motifs (Gutell et al. 2000) involve in long-range interactions with other molecules or provide
455 with structural stability (Sweeney et al. 2015). This finding suggests ITS2 sequences are under
456 functional constraint of their S2 (Zhang et al. 2020). Further, 60% of the nucleotides forming
457 part of the ITS2 sequence are found in stems that suggests their importance in maintaining the
458 correct structure of the ITS2 sequences, which are required for the orchestrated mechanisms of
459 pre-ribosomal processing (Eickbush and Eickbush 2007; Zhang et al. 2020). Moreover,
460 compensatory base changes occur in nucleotides of stems to maintain the S2. Similarly, for ITS
461 sequences of *Ampelomyces* isolates, (1) C/G contents were higher in stems than in loops which
462 is expected as C/G base pairs provide strong stability to the S2. Whereas two other common
463 conserved nucleotides, the poly adenine nucleotides located on the single stranded- ring
464 between helices II and III and the U-G nucleotides found starting helix II in direction 5' to 3'
465 -end (Prah et al. 2021) were noticed in models 4, 5, and 6 from *Ampelomyces* isolates derived
466 from, *E. necator*, *P. ferruginea*, and *P. leucotricha*, respectively. In these positions, the A
467 contents were higher than other *Ampelomyces* groups. This finding suggests secondary
468 structure stability is maintained differently between these three *Ampelomyces* groups and those
469 from the rest of the *Ampelomyces* populations.

470 We found that the *Ampelomyces* ITS1 S2s share similar structures to those reported in yeasts,
471 plants and other non-vertebrates (Coleman 2015). As suggested by Coleman (2015), similar
472 ITS 1 S2s in yeast, plants and other non-vertebrates may imply that the two endonucleolytic-
473 cleavage sites occur similarly between helices I and II, which is rich in A and C, and in the
474 large unpaired region after helix III, which is also rich in A and C. This finding indicates that
475 in *Ampelomyces* the removal of ITS 1 may also occur by cleavage in these two sites and
476 independently of sequence length and nucleotide contents as these regions contained different
477 sequence length and nucleotide contents from yeasts. In addition, the ITS1 S2s from putative
478 *Ampelomyces* were very distinct to those of the ‘true’ *Ampelomyces* spp., which suggests the
479 removal of ITS 1 in these fungal groups may occur at different sites and can be used to identify
480 the ‘true’ *Ampelomyces* from those *Phoma*-like fungi.

481 The genetic variability of *Ampelomyces* isolates has been demonstrated in several works. This
482 variation can be up to 15% and causing problems to differentiate among some *Ampelomyces*
483 groups and closely and unknown fungi. Nevertheless, when predicting the ITS1 S2s, the
484 genetic distances were better resolved between strains derived from apple powdery mildew or
485 from grapevine powdery mildew. These results suggest ITS1 and S2s can differentiate
486 *Ampelomyces* mycoparasites within subclades. As the ITS1 S2s were characteristic for both
487 clades we suggest these strains can be re-named as *Ampelomyces* variants with defined S2s
488 whose mechanisms of ribosomal processing are likely to be different. In a recent work, it was
489 demonstrated that two *Ampelomyces* ITS2 sequences (HM125018 and DQ490750) may be of
490 pseudogenic origin as revealed by variations observed in the hybridization model of the
491 proximal stem 5.8S and ITS2 (Prah et al. 2021). However, we did not observed deviations of
492 the typical model of the ITS1 spacer and 5.8S gene for these two sequences. Further, we did
493 not find the conserved motifs found in yeast ITS1 on *Ampelomyces* ITS1 and suggesting the
494 pathway for ITS1 cleavage can be different from those of yeast. Furthermore, conserved motifs

495 on *Ampelomyces* ITS1 were not detected either in ITS1 sequences from eDNA samples or *D.*
496 *glomerata*. Herein, *Ampelomyces* is closer related to *D. glomerata*, and the mechanisms of
497 ribosomal biogenesis can be different. In addition, these differences can be also used as another
498 feature to distinguish ITS sequences misidentified as *Ampelomyces*. Further research is still
499 required to validate these predicted S2s; and it may be worth to consider include S2s analyses
500 when studying species of the genus *Ampelomyces*. According to these results, RNA models of
501 evolution may be more applicable for investigating the evolutive relationship among
502 *Ampelomyces* lineages. Furthermore, the potential use of these ITS1 and 2 sequences and S2s
503 can be extended to differentiate between ITS2 sequences of the ‘true’ *Ampelomyces* and from
504 those of eDNA fungal samples.

505 **Conclusions**

506 We demonstrated that nucleotide sequences derived from eDNA and deposited under the name
507 of *Ampelomyces* are not related to this genus by differences found in the DNA repeats of the
508 ITS1 and its secondary structures. On the other hand, the phylogenetic analyses based on the
509 ITS1 S2s provided a better barcode gap than by using the ITS region alone. This suggested us
510 that by including secondary structures the phylogenetic resolution power of this molecular
511 barcode improved. We propose to include in future analyses the S2s to resolve better the
512 barcode gap within- and inter-species.

513

514 **Acknowledgements**

515 This research work was supported by the Department of Education from Australia and the
516 Postgraduate School at the University of Southern Queensland as a Research Training Stipend
517 scholarship granted to Rosa E. Prah1. Funding was granted to Rosa E. Prah1 from the Graduate
518 school of the University of Southern Queensland to develop this research work.

519 **Declaration of competing interest**

520 The authors declare that they have no conflict of interest.

521 **Supplementary data**

522 Supplementary data is available in excel format

523 **References**

524

525 Allen, J. E., & Whelan, S. (2014). Assessing the state of substitution models describing
 526 noncoding RNA evolution. *Genome Biology and Evolution*, 6, 65–75.
 527 Doi:10.1093/gbe/evt206.

528

529 Angeli, D., Maurhofer, M., Gessler, C., & Pertot, I. (2012). Existence of different physiological
 530 forms within genetically diverse strains of *Ampelomyces quisqualis*. *Phytoparasitica*, 40,
 531 37–51. Doi:10.1007/s12600-011-0197-x.

532

533 Ankenbrand, M. J., Keller, A., Wolf, M., Schultz, J., & Förster, F. (2015). ITS2 database V:
 534 twice as much. *Molecular Biology and Evolution*, 32, 3030–3032.
 535 Doi:10.1093/molbev/msv174.

536

537 Aveskamp, M. M., Verkley, G. J. M., Gruyter, J. d., Murace, M. A., Perelló, A., Woudenberg,
 538 J. H. C., Groenewald, J. Z., & Crous, P. W. (2009). DNA phylogeny reveals polyphyly of
 539 *Phoma* section Peyronellaea and multiple taxonomic novelties. *Mycologia*, 101, 363–382.
 540 Doi:10.3852/08-199.

541

542 Brown, D. D., Wensink, P. C., & Jordan, E. (1972). A comparison of the ribosomal DNA's of
 543 *Xenopus laevis* and *Xenopus mulleri*: the evolution of tandem genes. *Journal of Molecular*
 544 *Biology*, 63, 57–73. Doi:10.1016/0022-2836(72)90521-9.

545

546 Buzina, W., Braun, H., Freudenschuss, K., Lackner, A., Habermann, W., & Stammberger, H.
 547 (2003). Fungal biodiversity - as found in nasal mucus. *Medical Mycology*, 41, 149–161.
 548 Doi:10.1080/mmy.41.2.149.161.

549

550 Byun, Y., & Han, K. (2006). PseudoViewer: web application and web service for visualizing
 551 RNA pseudoknots and secondary structures. *Nucleic Acids Research*, 34, W416–W422.
 552 Doi:10.1093/nar/gkl210.

553

554 Coleman, A. W. (2015). Nuclear rRNA transcript processing versus internal transcribed spacer
 555 secondary structure. *Trends in Genetics*, 31, 157–163. Doi:10.1016/j.tig.2015.01.002.

556

557 Cote, C. A., Greer, C. L., & Peculis, B. A. (2002). Dynamic conformational model for the role
 558 of ITS2 in pre-rRNA processing in yeast. *RNA*, 8, 786–797. Doi:10.1017/s1355838202023063.

559

- 560 Côté, C. A., & Peculis, B. A. (2001). Role of the ITS2-proximal stem and evidence for indirect
 561 recognition of processing sites in pre-rRNA processing in yeast. *Nucleic Acids Research*, *29*,
 562 2106–2116. Doi:10.1093/nar/29.10.2106.
- 563
- 564 De Luca, D., Kooistra, W. H. C. F., Sarno, D., Biffali, E., & Piredda, R. (2021). Empirical
 565 evidence for concerted evolution in the 18S rDNA region of the planktonic diatom genus
 566 *Chaetoceros*. *Scientific Reports*, *11*, 807. Doi:10.1038/s41598-020-80829-6.
- 567
- 568 Domiciano, I. G., Domit, C., Trigo, C. C., de Alcântara, B. K., Headley, S. A., & Bracarense,
 569 A. P. (2014). Phaeohyphomycoses in a free-ranging loggerhead turtle (*Caretta caretta*) from
 570 Southern Brazil. *Mycopathologia*, *178*, 123–128. Doi:10.1007/s11046-014-9769-x.
- 571
- 572 Dominguez-Monino, I. (2014). *Evaluacion y control de comunidades microbianas en cuevas*
 573 *turisticas* [Thesis, CSIC - Instituto de Recursos Naturales y Agrobiología de Sevilla (IRNAS)
 574 Universidad de Sevilla]. GenBank. Universidad de Sevilla.
 575 <http://fondosdigitales.us.es/tesis/autores/2758/>.
- 576
- 577 Edger, P. P., Tang, M., Bird, K. A., Mayfield, D. R., Conant, G., Mummenhoff, K., Koch, M.
 578 A., & Pires, J. C. (2014). Secondary structure analyses of the nuclear rRNA internal transcribed
 579 spacers and assessment of its phylogenetic utility across the *Brassicaceae* (mustards). *PLoS*
 580 *One*, *9*, e101341. Doi:10.1371/journal.pone.0101341.
- 581
- 582 Eickbush, T. H., & Eickbush, D. G. (2007). Finely orchestrated movements: evolution of the
 583 ribosomal RNA genes. *Genetics*, *175*, 477–485. Doi:10.1534/genetics.107.071399
- 584
- 585 Elder, J. F. J., & Turner, B. J. (1995). Concerted evolution of repetitive DNA sequences in
 586 eukaryotes. *The Quarterly Review of Biology*, *70*, 297–320. Doi:10.1086/419073
- 587
- 588 Glawe, D. A. (2008). The powdery mildews: a review of the world's most familiar (yet poorly
 589 known) plant pathogens. *Annual Review of Phytopathology*, *46*, 27–51.
 590 Doi:10.1146/annurev.phyto.46.081407.104740
- 591
- 592 Gottschling, M., & Plötner, J. (2004). Secondary structure models of the nuclear internal
 593 transcribed spacer regions and 5.8S rRNA in Calciodinelloideae (Peridiniaceae) and other
 594 dinoflagellates. *Nucleic Acids Research*, *32*, 307–315. Doi:10.1093/nar/gkh168.
- 595
- 596 Grummt, I. (2003). Life on a planet of its own: regulation of RNA polymerase I transcription
 597 in the nucleolus. *Genes & Development*, *17*, 1691–1702. Doi:10.1101/gad.1098503R.
- 598
- 599 Gutell, R. R., Cannone, J. J., Shang, Z., Du, Y., & Serra, M. J. (2000). A story: unpaired
 600 adenosine bases in ribosomal RNAs. *Journal of Molecular Biology*, *304*, 335–354.
 601 Doi:10.1006/jmbi.2000.4172.
- 602
- 603 Hang, R., Liu, C., Ahmad, A., Zhang, Y., Lu, F., & Cao, X. (2014). *Arabidopsis* protein
 604 arginine methyltransferase 3 is required for ribosome biogenesis by affecting precursor
 605 ribosomal RNA processing. *Proceedings of the National Academy of Sciences of the United*
 606 *States of America*, *111*, 16190–16195. Doi:10.1073/pnas.1412697111.
- 607

- 608 Joseph, N., Krauskopf, E., Vera, M. I., & Michot, B. (1999). Ribosomal internal transcribed
609 spacer 2 (ITS2) exhibits a common core of secondary structure in vertebrates and yeast. *Nucleic*
610 *Acids Research*, *27*, 4533–4540. Doi:10.1093/nar/27.23.4533.
- 611
612 Katoh, K., Kuma, K., Toh, H., & Miyata, T. (2005). MAFFT version 5: improvement in
613 accuracy of multiple sequence alignment. *Nucleic Acids Research*, *33*, 511–518.
614 Doi:10.1093/nar/gki198.
- 615
616 Katoh, K., & Toh, H. (2008). Improved accuracy of multiple ncRNA alignment by
617 incorporating structural information into a MAFFT-based framework. *BMC Bioinformatics*, *9*,
618 212. Doi:10.1186/1471-2105-9-212.
- 619
620 Kiss, L. (2012). Limits of nuclear ribosomal DNA internal transcribed spacer (ITS) sequences
621 as species barcodes for Fungi. *Proceedings of the National Academy of Sciences of the United*
622 *States of America*, *109*, E1811. Doi:10.1073/pnas.1207143109.
- 623
624 Kiss, L., & Nakasone, K. K. (1998). Ribosomal DNA internal transcribed spacer sequences do
625 not support the species status of *Ampelomyces quisqualis*, a hyperparasite of powdery mildew
626 fungi. *Current Genetics*, *33*, 362–367. Doi:10.1007/s002940050348.
- 627
628 Kiss, L., Pintye, A., Kovács, G., Jankovics, T., Fontaine, M., Harvey, N., Xu, X., Nicot, P.,
629 Bardin, M., Shykoff, J., & Giraud, T. (2011). Temporal isolation explains host-related genetic
630 differentiation in a group of widespread mycoparasitic fungi. *Mol Ecol*, *20*, 1492–1507.
631 Doi:10.1111/j.1365-294X.2011.05007.x.
- 632
633 Koetschan, C., Kittelmann, S., Lu, J., Al-Halbouni, D., Jarvis, G. N., Müller, T., Wolf, M., &
634 Janssen, P. H. (2014). Internal transcribed spacer 1 secondary structure analysis reveals a
635 common core throughout the anaerobic fungi (Neocallimastigomycota). *PLoS One*, *9*, e91928.
636 Doi:10.1371/journal.pone.0091928.
- 637
638 Kumar, S., Stecher, G., Li, M., Knyaz, C., & Tamura, K. (2018). MEGA X: molecular
639 evolutionary genetics analysis across computing platforms. *Molecular Biology and Evolution*,
640 *35*, 1547–1549. Doi:10.1093/molbev/msy096.
- 641
642 Lafontaine, D., & Tollervey, D. (2001). The function and synthesis of ribosomes. *Nature*
643 *Reviews Molecular Cell Biology*, *2*, 514–520. Doi:10.1038/35080045.
- 644
645 Laley, A. I., & Nazar, R. N. (1999). Structural equivalence in the transcribed spacers of pre-
646 rRNA transcripts in *Schizosaccharomyces pombe*. *Nucleic Acids Research*, *27*, 3071–3078.
647 Doi:10.1093/nar/27.15.3071.
- 648
649 Maciá-Vicente, J. G., Ferraro, V., Burruano, S., & Lopez-Llorca, L. V. (2012). Fungal
650 assemblages associated with roots of halophytic and non-halophytic plant species vary
651 differentially along a salinity gradient. *Microbial Ecology*, *64*, 668–679. Doi:10.1007/s00248-
652 012-0066-2.
- 653
654 Manjunatha, L., Singh, S., Ravikumara, B. M., Narasa Reddy, G., & Senthilkumar, M. (2020).
655 *Ampelomyces*. In N. Amaresan, M. Senthil Kumar, K. Annapurna, K. Kumar, & A.
656 Sankaranarayanan (Eds.), *Beneficial microbes in agro-ecology* (Vol. 44, pp. 833–860).
657 Academic Press. Doi:10.1016/B978-0-12-823414-3.00044-7.

- 658
659 Mathews, D. H., Sabina, J., Zuker, M., & Turner, D. H. (1999). Expanded sequence
660 dependence of thermodynamic parameters improves prediction of RNA secondary structure.
661 *Journal of Molecular Biology*, 288, 911–940. Doi:10.1006/jmbi.1999.2700.
662
- 663 Naidoo, K., Steenkamp, E. T., Coetzee, M. P., Wingfield, M. J., & Wingfield, B. D. (2013).
664 Concerted evolution in the ribosomal RNA cistron. *PLoS One*, 8, e59355.
665 Doi:10.1371/journal.pone.0059355.
666
- 667 Nei, M., & Rooney, A. P. (2005). Concerted and birth-and-death evolution of multigene
668 families. *Annual Review of Genetics*, 39, 121–152.
669 Doi:10.1146/annurev.genet.39.073003.112240.
670
- 671 Németh, M., Mizuno, Y., Kobayashi, H., Seress, D., Shishido, N., Kimura, Y., Takamatsu, S.,
672 Suzuki, T., Takikawa, Y., Kakutani, K., Matsuda, Y., Kiss, L., & Nonomura, T. (2021).
673 *Ampelomyces* strains isolated from diverse powdery mildew hosts in Japan: their phylogeny
674 and mycoparasitic activity, including timing and quantifying mycoparasitism of *Pseudoidium*
675 *neolycopersici* on tomato. *PLoS One*, 16, e0251444. Doi:10.1371/journal.pone.0251444.
676
- 677 Paredes-Esquivel, C. C., & Townson, H. (2014). Functional constraints and evolutionary
678 dynamics of the repeats in the rDNA internal transcribed spacer 2 of members of the *Anopheles*
679 *barbirostris* group. *Parasites & Vectors*, 7, 106. Doi:10.1186/1756-3305-7-106.
680
- 681 Park, M. J., Choi, Y. J., Hong, S. B., & Shin, H. D. (2010). Genetic variability and mycohost
682 association of *Ampelomyces quisqualis* inferred from phylogenetic analyses of ITS rDNA and
683 *actin* gene sequences. *Fungal Biology*, 114, 235–247. Doi:10.1016/j.funbio.2010.01.003.
684
- 685 Perry, R. P. (1976). Processing of RNA. *Annual Review of Biochemistry*, 45, 605–629.
686 Doi:10.1146/annurev.bi.45.070176.003133.
687
- 688 Pillon, M. C., Lo, Y. H., & Stanley, R. E. (2019). IT'S 2 for the price of 1: multifaceted ITS2
689 processing machines in RNA and DNA maintenance. *DNA Repair (Amst)*, 81, 102653.
690 Doi:10.1016/j.dnarep.2019.102653.
691
- 692 Pintye, A., Bereczky, Z., Kovács, G. M., Nagy, L. G., Xu, X., Legler, S. E., Váczy, Z., Váczy,
693 K. Z., Caffi, T., Rossi, V., & Kiss, L. (2012). No indication of strict host associations in a
694 widespread mycoparasite: grapevine powdery mildew (*Erysiphe necator*) is attacked by
695 phylogenetically distant *Ampelomyces* strains in the field. *Phytopathology*, 102, 707–716.
696 Doi:10.1094/PHYTO-10-11-0270.
697
- 698 Poczai, P., Varga, I., & Hyvönen, J. (2015). Internal transcribed spacer (ITS) evolution in
699 populations of the hyperparasitic European mistletoe pathogen fungus, *Sphaeropsis visci*
700 (*Botryosphaeriaceae*): The utility of ITS2 secondary structures. *Gene*, 558, 54–64.
701
- 702 Prah1, R. E., Khan, S., & Deo, R. C. (2021). The role of internal transcribed spacer 2 secondary
703 structures in classifying mycoparasitic *Ampelomyces*. *PLoS One*, 16, e0253772.
704 Doi:10.1371/journal.pone.0253772.
705
- 706 Rambaut, A. (2014). *FigTree v1.4.2: tree figure drawing tool*. Retrieved from 09 November
707 2021 from <http://tree.bio.ed.ac.uk>.

- 708
 709 SantaLucia, J. J. (1998). A unified view of polymer, dumbbell, and oligonucleotide DNA
 710 nearest-neighbor thermodynamics. *Proceedings of the National Academy of Sciences of the*
 711 *United States of America*, 95, 1460–1465. Doi:10.1073/pnas.95.4.1460.
 712
- 713 Schoch, C. L., Seifert, K. A., Huhndorf, S., Robert, V., Spouge, J. L., Levesque, C. A., Chen,
 714 W., Consortium, F. B., & List, F. B. C. A. (2012). Nuclear ribosomal internal transcribed spacer
 715 (ITS) region as a universal DNA barcode marker for Fungi. *Proceedings of the National*
 716 *Academy of Sciences of the United States of America*, 109, 6241–6246.
 717 Doi:10.1073/pnas.1117018109.
 718
- 719 Schultz, J., Maisel, S., Gerlach, D., Müller, T., & Wolf, M. (2005). A common core of
 720 secondary structure of the internal transcribed spacer 2 (ITS2) throughout the Eukaryota. *RNA*,
 721 11, 361–364. Doi:10.1261/rna.7204505.
 722
- 723 Scull, C. E., & Schneider, D. A. (2019). Coordinated control of rRNA processing by RNA
 724 Polymerase I. *Trends in Genetics*, 35, 724–733. Doi:10.1016/j.tig.2019.07.002.
 725
- 726 Seibel, P. N., Müller, T., Dandekar, T., Schultz, J., & Wolf, M. (2006). 4SALE--a tool for
 727 synchronous RNA sequence and secondary structure alignment and editing. *BMC*
 728 *Bioinformatics*, 7, 498. Doi:10.1186/1471-2105-7-498.
 729
- 730 Statistics, S. S. (2018). *Kruskal-Wallis Test Calculator. Social Science Statistics*. Retrieved
 731 from November 08, 2021 from
 732 <https://www.socscistatistics.com/tests/chisquare2/default2.aspx>.
 733
- 734 Sullivan, R. F., & White, J. F. J. (2000). *Phoma glomerata* as a mycoparasite of powdery
 735 mildew. *Applied and Environmental Microbiology*, 66, 425–427. Doi:10.1128/aem.66.1.425-
 736 427.2000.
 737
- 738 Sundaresan, N., Sahu, A. K., Jagan, E. G., & Pandi, M. (2019). Evaluation of ITS2 molecular
 739 morphometrics effectiveness in species delimitation of Ascomycota - A pilot study. *Fungal*
 740 *Biology*, 123, 517–527. Doi:10.1016/j.funbio.2019.05.002.
 741
- 742 Sweeney, B. A., Roy, P., & Leontis, N. B. (2015). An introduction to recurrent nucleotide
 743 interactions in RNA. *Wiley Interdisciplinary Reviews: RNA*, 6, 17–45. Doi:10.1002/wrna.1258.
 744
- 745 Szostak, J. W., & Wu, R. (1980). Unequal crossing over in the ribosomal DNA of
 746 *Saccharomyces cerevisiae*. *Nature*, 284, 426–430. Doi:10.1038/284426a0.
 747
- 748 Tamura, K. (1992). Estimation of the number of nucleotide substitutions when there are strong
 749 transition-transversion and G + C-content biases. *Molecular Biology and Evolution*, 9,
 750 678–687. Doi:10.1093/oxfordjournals.molbev.a040752.
 751
- 752 Turner, D. H., & Mathews, D. H. (2010). NNDB: the nearest neighbor parameter database for
 753 predicting stability of nucleic acid secondary structure. *Nucleic Acids Research*, 38 (*Database*
 754 *issue*), D280–D282. Doi:10.1093/nar/gkp892.
 755
- 756 Uhart, M., Sirand-Pugnet, P., & Labarère, J. (2007). Evolution of mitochondrial SSU-rDNA
 757 variable domain sequences and rRNA secondary structures, and phylogeny of the Agrocycbe

- 758 aegerita multispecies complex. *Research in Microbiology*, 158, 203–212.
 759 Doi:10.1016/j.resmic.2006.12.009.
- 760
- 761 Vu, D., Groenewald, M., de Vries, M., Gehrman, T., Stielow, B., Eberhardt, U., Al-Hatmi,
 762 A., Groenewald, J. Z., Cardinali, G., Houbraken, J., Boekhout, T., Crous, P. W., Robert, V., &
 763 Verkley, G. J. M. (2019). Large-scale generation and analysis of filamentous fungal DNA
 764 barcodes boosts coverage for kingdom fungi and reveals thresholds for fungal species and
 765 higher taxon delimitation. *Studies in Mycology*, 92, 135–154.
 766 Doi:10.1016/j.simyco.2018.05.001.
- 767
- 768 Will, S., Joshi, T., Hofacker, I. L., Stadler, P. F., & Backofen, R. (2012). LocARNA-P: accurate
 769 boundary prediction and improved detection of structural RNAs. *RNA*, 18, 900–914.
 770 Doi:10.1261/rna.029041.111.
- 771
- 772 Wolf, M., Achtziger, M., Schultz, J., Dandekar, T., & Müller, T. (2005). Homology modeling
 773 revealed more than 20,000 rRNA internal transcribed spacer 2 (ITS2) secondary structures.
 774 *RNA*, 11, 1616–1623. Doi:10.1261/rna.2144205.
- 775
- 776 Wolf, M., Koetschan, C., & Müller, T. (2014). ITS2, 18S, 16S or any other RNA - simply
 777 aligning sequences and their individual secondary structures simultaneously by an automatic
 778 approach. *Gene*, 10, 145–149. Doi:10.1016/j.gene.2014.05.065.
- 779
- 780 Woudenberg, J. H., De Gruyter, J., Crous, P. W., & Zwiers, L. H. (2012). Analysis of the
 781 mating-type loci of co-occurring and phylogenetically related species of *Ascochyta* and *Phoma*.
 782 *Molecular Plant Pathology*, 13, 350–362. Doi:10.1111/j.1364-3703.2011.00751.x.
- 783
- 784 Yang, C.-D., Yao, Y.-L., Zhang, Z.-F., & Xue, L. (2016). First report of leaf blight of *Poa*
 785 *pratensis* caused by *Peyronellaea glomerata* in China. *Plant Disease*, 100, 862.
 786 Doi:10.1094/PDIS-08-15-0954-PDN.
- 787
- 788 Zhang, W., Tian, W., Gao, Z., Wang, G., & Zhao, H. (2020). Phylogenetic utility of rRNA
 789 ITS2 sequence-structure under functional constraint. *Int J Mol Sci*, 21, 6395.
 790 Doi:10.3390/ijms21176395.
- 791
- 792 Zhang, X., Xu, Z., Pei, H., Chen, Z., Tan, X., Hu, J., Yang, B., & Sun, J. (2017). Intraspecific
 793 variation and phylogenetic relationships are revealed by ITS1 secondary structure analysis and
 794 single-nucleotide polymorphism in *Ganoderma lucidum*. *PLoS One*, 12, e0169042.
 795 Doi:10.1371/journal.pone.0169042.
- 796
- 797 Zuker, M. (2003). Mfold web server for nucleic acid folding and hybridization prediction.
 798 *Nucleic Acids Research*, 31, 3406–3415. Doi:10.1093/nar/gkg595.
- 799

Chapter 6

Discussion, Summary of findings and conclusions

The results of this thesis have shown that phylogenetic analyses of *Ampelomyces* based on the simultaneous alignment of ITS 1 and 2 sequences and their respective S2s can notably enhance the barcode gap within- and inter- species. In the following section, brief discussions and conclusions regarding the main findings of this research are presented.

6. 1. Discussions

Ampelomyces spp. are species complex whose similar morphological characteristics of their asexual structures cannot be used as species recognition. Their sexual stage is also unknown. Therefore, their identification relies on the use of DNA barcodes. The ITS is widely used in fungal identification despite some disadvantages [Schoch et al. 2012]. In the case of *Ampelomyces*, previous ITS analyses showed that the hyperparasites are genetically diverse [Kiss 1997; Kiss and Nakasone 1998; Liang et al. 2007; Park et al. 2010], causing difficulties to delimitate within- and inter- species.

APM and other non-APM can coinhabit in the same habitat, but the first group overwinters in apple buds, causing epidemics in spring, while non-APM, i.e., *A. mougeotii* on *L. halimifolium*, cause infections later in the autumn season (Kiss 1998). In this situation, APM *Ampelomyces* and non APM *Ampelomyces* can also coinhabit in the same habitat, but *Ampelomyces* strains overwintering in, or nearby apple buds infected with APM have a unique genotype [Kiss et al. 2011]. Despite this differentiation, APM *Ampelomyces* can parasitise APM and non APMs with no significant differences in mycoparasitic activities [Kiss et al. 2011]. This is another example of host association when the phenology of some PM hosts (Szentiványi et al. 2005; Kiss et al. 2011) drove the genetic

differentiation of *Ampelomyces* into a different phylogenetic group. However, in this analysis, APM *Ampelomyces* strains grouped with other *Ampelomyces* isolates from PM on Rosaceous, including an *Ampelomyces* strain extracted from *P. ferruginea* and sampled in China [Liang et al. 2007], and thus, the differentiation of APM *Ampelomyces* caused by differences in their host phenology remained unclear.

The results of this thesis showed that this strain grouped in the same clade of APM *Ampelomyces* as these share similar ITS2 S2s (Prahl et al. 2021). *Ampelomyces* ITS2 S2s were predicted directly via the ITS2-DB, and the phylogenetic analysis based on the simultaneous alignment of S2s and ITS2 sequences notably improve the barcode gap among *Ampelomyces* lineages and inter-species (*Ampelomyces* and closely related fungi). Moreover, their S2s reflect the *Ampelomyces* phylogeny where four main S2s models represent four major lineages. The APM *Ampelomyces* and GPM *Ampelomyces* were represented by ITS2 S2s containing two motifs involved in pre-ribosomal processing and previously found in vertebrates and yeasts [Joseph et al. 1999]. This finding suggests pre-ribosomal processing is different across *Ampelomyces* lineages.

Apart from the APM *Ampelomyces*, the origins of *Ampelomyces* lineages are unknown. The results of this thesis, however, suggest some lineages can be originated by the random appearance of pseudogenes where a few can mislead the phylogenetic analysis by generating a new clade while others can have a determined function (Prahl et al. 2021). Pseudogenes are assumed to be unfunctional as these do not produce functional transcripts; nonetheless, recent evidence shows that this is not the case where some pseudogenes can actually be transcribed [Gong et al. 2019] and suggesting the concept of pseudogenes as unfunctional genes need to be revised [Cheetham et al. 2020]. As variations in the proximal stem model of the ITS2 is reliable evidence of the presence of pseudogenes [Harpke and Peterson 2008], the comparative analyses of the ITS2-proximal stem model in *Ampelomyces* ITS2 sequences reveal the presence of two putative pseudogenes [Prahl et al. 2021]. One of them was found in the ITS sequence of *Ampelomyces* extracted originally from *E. necator* (HM125018)

[Falk, Gadoury, Pearson, et al. 2012] whose mutation observed in the ITS2-proximal stem may drastically reduce the length of the stem of this conserved structure (Prahl et al. 2021) as Côté and Peculis (2001) demonstrated that the short length of the stem negatively affected the correct pre-ribosomal processing. Conversely, the second variation was noticed in a Chinese *Ampelomyces* strain derived originally from *P. xanthii* (DQ490750) [Liang et al. 2007]. In this case, the mutation does not alter the length of the stem, and it may not deter the ribosomal maturation. If the pseudogene produces a functional transcript, a new phenotype can evolve. In accordance to this, it is possible that new lineages in *Ampelomyces* were originated by randomly appearance of pseudogenes in which some can be functional and undergo natural selection while others are eliminated by the fate of genetic drift. In conclusion, the results of this thesis provide significant contributions in the current research gap of phylogenetic studies of *Ampelomyces* and resolve the problem of misidentification of ITS sequences from eDNA and PM- free environments deposited in the GenBank under the generic name of *Ampelomyces*.

In terms of the ITS1 S2s analyses, several models were predicted by each ITS sequence representing the four main *Ampelomyces* lineages based on the phylogeny using ITS2 S2s. Unlike the ITS2, a common core of ITS1 S2 has not been established yet for fungi belonging to the order Pleosporales. An early study established a representative ITS1 model for anaerobic fungi through a Hidden Markov Model-based ITS1 sequence annotation together with a helix-wise folding method [Koetschan et al. 2014]. In this thesis, the *Ampelomyces* ITS1 sequences were represented by different models, which were predicted by minimum free energies method via the only UNAFold/MFold online tool [Zuker 2003]. These models reflect the phylogeny of *Ampelomyces* and APM- and GPM *Ampelomyces* ITS1 sequences contained DNA sequence motifs not found in other *Ampelomyces* lineages. These conserved regions were also different from those found in putative *Ampelomyces* ITS sequences.

As the analyses of ITS1 and ITS2 sequences and S2s reflect the phylogeny of *Ampelomyces* where those strains extracted from APM and GPM, have distinctive S2s, further studies in *Ampelomyces* can rely on this strategy to

estimate fungal biodiversity. A comprehensive multi-locus sequence analysis together with analyses of sequences and S2s will short the path to resolve the phylogeny of *Ampelomyces*.

In terms of phylogenetic analysis, the ITS region is assumed to evolve neutrally as mutations in the nrDNA ITS gene clusters are homogenized by unequal crossing-over and other DNA turnover mechanisms [Szostak and Wu 1980] and, thus, the phylogenetic signal is similar within species but different between them. The ITS provides a barcode gap with enough resolution to delimitate some fungal species [Schoch et al. 2012] but not in *Ampelomyces* whose genetic distances can reach up to 15% among some lineages [Kiss and Nakasone 1998].

In this thesis was shown that *Ampelomyces* ITS 1 and ITS 2 sequences and S2s are better molecular approaches to enhance the phylogeny of *Ampelomyces*. Moreover, the results of this thesis showed that the hyperparasites ITS sequences are under evolutionary constraints of their S2s. For *Ampelomyces* ITS2 S2s, values of C/G nucleotide contents were higher in stems than in loops. In addition, the highest number of transitional mutations were obtained in stems. As reviewed in Zhang et al. (2020), the higher values of both C/G contents and transitional mutations and observed in stems provide strong stability to the S2 suggesting the importance of the conserved conformational stage of the S2 for pre-ribosomal mechanisms, which depend on the S2 itself [Côté et al. 2002; Baßler and Hurt 2019]. Likewise, the ITS1 S2s are also under functional constraints of their S2s. The number of possible *Ampelomyces* ITS1 S2s, which were assembled with minimum free energies values, were significantly lower than those S2s predicted by using randomly generated sequences. According to these results, phylogenetic analyses based on RNA models of evolution, which consider the evolutionary process of the stem (paired regions) as a whole unit and the transient base pairs (GC, CG, AU, UA, GU, and UG) occurring as compensatory base changes in stems to maintain the integrity of the S2 for the RNA splicing function, are more representational of the evolutive history of the ITS region. Altogether, ITS 1 and 2 S2s analyses together with RNA models of evolution will describe better the phylogeny of *Ampelomyces* than studies based on only ITS sequences.

This thesis produced three papers as follows:

In the first published article (Paper 1), the study has demonstrated that:

- ITS sequences from eDNA samples that were deposited in the GenBank database under the name of *Ampelomyces* did not belong to the genus *Ampelomyces* based on sequence lengths and nucleotide contents of ITS, ITS1, and ITS2. Further *Ampelomyces* spp. *sensu stricto* are different to those putative *Ampelomyces* based on differences of their ITS2 secondary structures.
- For the first time, the presence of pseudogene formation was demonstrated to occur randomly in the nrDNA ITS of two *Ampelomyces* strains.
- In *Ampelomyces*, it is likely that sister clades were formed by the random appearance of pseudogenes, which some can have a biological function and undergo natural selection.
- *Ampelomyces* lineages can be differentiated based on its ITS2 secondary structures.
- *Ampelomyces* strains derived from *P. leucotricha*, *P. ferruginea*, *P. pannosa* and *E. necator* share a conserved single-stranded ring rich in adenine nucleotides that was also found in other eukaryotes such as fungi, fish, and mammals.

In the second submitted article (Paper 2), this review paper was written for the following reasons:

- There is no currently review of *Ampelomyces* that highlight the latest research conducted in these mycoparasites in terms of their genome, and insights about their phylogeny, which were provided in this thesis.
- A comprehensive review of the phylogeny of *Ampelomyces* was written where major recent advances are discussed, including the origin of some *Ampelomyces* lineages by the random appearance of pseudogenes. It is also proposed to revise the taxonomy of *Ampelomyces* based on the

characterization of the ITS2 secondary structures conducted in this thesis. Finally, the problem of databases containing nucleotide sequences under the generic name of *Ampelomyces* was also discussed to spread awareness about this situation and improve, in the future, database quality.

In the third article under consideration (Paper 3), it was demonstrated that:

- C/G nucleotide contents are higher in stems than single regions in the ITS2 S2s of *Ampelomyces* spp. *sensu stricto*.
- The transition and transversion bias ratio in ITS2 sequences from the ‘true’ *Ampelomyces* is significantly higher than those from putative *Ampelomyces*, and suggesting the former is under constant evolutionary pressure of their secondary structures. This can be another characteristic to take into account when identifying nucleotide sequences derived from eDNA samples.
- Based on the previous results, RNA models of evolution may be more realistic than DNA models to study the evolutionary relationship of *Ampelomyces* mycoparasites.

A conserved motif of seven nucleotides (TATAGTA) was identified across all ITS1 *Ampelomyces* sequences. Unlike other *Ampelomyces* strains, those isolates from powdery mildews in China contain a tandem sequence motif of three nucleotides (TGC TGC TGC), but one *Ampelomyces* isolate and extracted from *E. Polygoni*. The ITS1 sequence of the latter strain has the triple nucleotides separated by 3 nucleotides (TGC123TGC).

- Sequence motifs between the ‘true’ *Ampelomyces* and those fungal misidentified can be differentiated by different sequence motifs found in their ITS1 sequences.
- ITS1 sequences and secondary structures resolved notably well the bootstrap values of subclades within monophyletic groups. Putative *Ampelomyces* can be differentiated from the ‘true’ *Ampelomyces* by the content of DNA or tandem repeats in the ITS1 sequences.

6.2. Conclusions

The utility of ITS1 and ITS2 sequences and S2s was demonstrated in this doctoral thesis to fill the research gap about the evolution of ITS sequences of *Ampelomyces* mycoparasites. It also showed ITS nucleotide sequences from eDNA are deposited under the name of *Ampelomyces* but did not belong to this genus. Comparative analysis of ITS sequences and their S2s are a suitable molecular approach to differentiate the ‘true’ ITS sequences from *Ampelomyces* spp. *sensu stricto* from those *Phoma*-like fungi. Based on the results of this thesis, it seems the appearance of paralogous sequences as reflected as sister clades could be due to the random appearance of pseudogenes in the ITS region with some functionality.

In accordance with the findings, we propose to use ITS2 S2s (Figure 3) together with information of nucleotide contents and sequence lengths of the complete ITS region and its constituents, ITS1 and ITS2, to differentiate the identification of these hyperparasites from those not related to the genus and misidentified as *Ampelomyces*. The ITS2-DB can be used to predict accurately these structures, and together with simultaneous alignment of sequences and structures can be conducted by using the LocARNA website tool [Will et al. 2012].

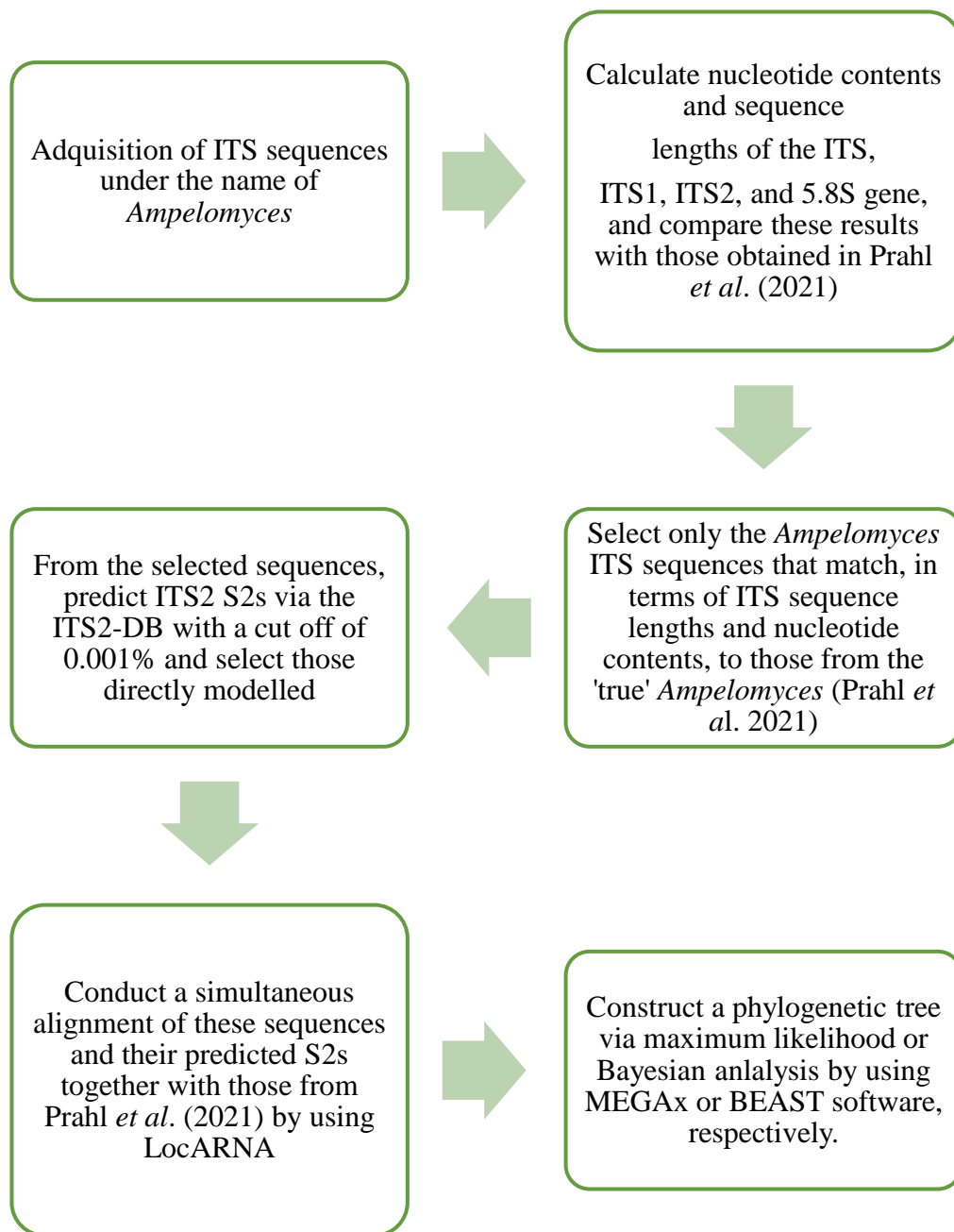


Figure 3

A practical workflow proposed to accurately select the ‘true’ *Ampelomyces* ITS sequences from public databases.

6.3. Future directions

One of the limitations in this doctorate research was that most of the ITS nucleotide sequences available in the GenBank database were either sampled once or contained a short sequence length, less than 150 nucleotides, of the 5' terminal of the 18S gene, which makes difficult to predict directly ITS2 S2s via the ITS2-DB. This is a significant problem for comparative analysis and prediction of the ITS2 secondary structures. In addition, the development of new software that incorporate the information of secondary structures into RNA models of evolution for phylogenetic analysis is lacking

References

- AgriLife™. 2021. PowderyCare® *Ampelomyces quisqualis* biofungicide approved for use in organic agriculture. [accessed 2021 May 18]. <https://www.agrilife.in/>.
- Angeli D, Maurhofer M, Gessler C, Pertot I. 2012. Existence of different physiological forms within genetically diverse strains of *Ampelomyces quisqualis*. *Phytoparasitica*. 40:37–51.
- Angeli D, Pellegrini E, Maurhofer M, Pertot I, Micheli S, Ress D, Gessler C. 2009. Molecular characterization of *Ampelomyces* spp. isolates from different hosts and geographic origins and evaluation of their potential to control powdery mildew of cucumber. *IOBC/WPRS Bull.* 43:40–44.
- Angeli D, Pellegrini E, Pertot I. 2009. Occurrence of *Erysiphe necator* chasmothecia and their natural parasitism by *Ampelomyces quisqualis*. *Phytopathology*. 99:704–710. DOI:10.1094/PHYTO-99-6-0704.
- Allmang C, Henry Y, Wood H, Morrissey JP, Petfalski E, Tollervey D. 1996. Recognition of cleavage site A2 in the yeast pre rRNA. *RNA*. 2:51–62.
- Ankenbrand M, Keller A, Wolf M, Schultz J, Förster F. 2015. ITS2 database V: twice as much. *Mol. Biol. Evol.* 32: 3030–3032. Doi:10.1093/molbev/msv174.
- Aveskamp MM, de Gruyter J, Woudenberg JHC, Verkley GJM, Crous PW. 2010. Highlights of the Didymellaceae: a polyphasic approach to characterise

- Phoma* and related pleosporalean genera. *Stud Mycol.* 65:1–60.
DOI:10.3114/sim.2010.65.01.
- Baßler J, Hurt E. 2019. Eukaryotic ribosome assembly. *Annu. Rev. Biochem.* 88:281–306. Doi:10.1146/annurev-biochem-013118-110817.
- Berg G. 2009. Plant–microbe interactions promoting plant growth and health: perspectives for controlled use of microorganisms in agriculture. *Appl Microbiol Biotechnol.* 84:11–18. DOI:10.1007/s00253-009-2092-7.
- Biedka S, Micic J, Wilson D, Brown H, Diorio-Toth L, Woolford JL Jr.. 2018. Hierarchical recruitment of ribosomal proteins and assembly factors remodels nucleolar pre-60S ribosomes. *J Cell Biol.* 217:2503–2518. DOI: 10.1083/jcb.201711037.
- Braun U and Cook R. (2012). Taxonomic manual of the *Erysiphales* (*Powdery Mildews*), *CBS Biodiversity Series*. CBS Biodiversity Series. Vol. 11. 2012, Utrecht, The Netherlands: CBSKNAW Fungal Biodiversity Centre. 1–707.
- Braun U, Bradshaw M, Zhao T-T, Cho, S-E Shin H-D. 2018. Taxonomy of the *Golovinomyces cynoglossi* complex (Erysiphales, Ascomycota) disentangled by phylogenetic analyses and reassessments of morphological traits. *Mycobiology.* 46:192–204. DOI: 10.1080/12298093.2018.1509512.
- Brauer V, Rezende CP, Pessoni AM, De Paula RG, Rangappa KS, Nayaka SC, Gupta VK, Almeida F. 2019. Antifungal agents in agriculture: friends and foes of public health. *Biomolecules.* 9:521. DOI: 10.3390/biom9100521.

- Burlacu E, Lackmann, F, Aguilar LC, et al. 2017. High-throughput RNA structure probing reveals critical folding events during early 60S ribosome assembly in yeast. *Nat Commun.* 8:1–14. DOI: 10.1038/s41467-017-00761-8.
- Carbó A, Teixidó N, Usall J, Solsona C, Torres R. 2021. Formulated *Ampelomyces quisqualis* CPA-9 applied on zucchini leaves: influence of abiotic factors and powdery mildew mycoparasitization. *Eur J Plant Pathol.* 161:37–48. DOI:10.1007/s10658-021-02302-y.
- Carbó A, Torres R, Usall J, Ballesta J, Teixidó N. 2020. Biocontrol potential of *Ampelomyces quisqualis* strain CPA-9 against powdery mildew: conidia production in liquid medium and efficacy on zucchini leaves. *Sci Hortic.* 267:109337. DOI:10.1016/j.scienta.2020.109337.
- Cheetham SW, Faulkner GJ, Dinger ME. 2020. Overcoming challenges and dogmas to understand the functions of pseudogenes. *Nat Rev Genet.* 21:191–201. DOI:10.1038/s41576-019-0196-1.
- Chemknock. 2021. Q-fect. [accessed 2021 Jun 23]. <https://chemknock.com/view.do?no=194&pgMode=view&dvsn=pdt&idx=25100>.
- Chen Q, Zobel J, Verspoor K. 2017. Duplicates, redundancies and inconsistencies in the primary nucleotide databases: a descriptive study. *Database.* baw163. DOI: 10.1093/database/baw163.
- Cherrad S, Charnay A, Hernandez C, Steva H, Belbahri L, Vacher S. 2018. Emergence of boscalid-resistant strains of *Erysiphe necator* in French vineyards. *Microbiol Res.* 216:79–84. DOI: 10.1016/j.micres.2018.08.007.

- Colcol J, Baudoin, A. 2016. Sensitivity of *Erysiphe necator* and *Plasmopara viticola* in Virginia to QoI fungicides, Boscalid, Quinoxifen, Thiophanate Methyl, and Mefenoxam. *Plant Dis.* 100:337–344. DOI: 10.1094/PDIS-01-15-0012-RE.
- Côté CA, Peculis BA. 2001. Role of the ITS2-proximal stem and evidence for indirect recognition of processing sites in pre-rRNA processing in yeast. *Nucleic Acids Res.* 29:2106–2116. DOI: 10.1093/nar/29.10.2106.
- Côté CA, Greer, CL, Peculis. BA. 2002. Dynamic conformational model for the role of ITS2 in pre-rRNA processing in yeast. *RNA.* 8:786–797. Doi: 10.1017/s1355838202023063.
- Czerniawska B. 2001. Studies on the biology and occurrence of *Ampelomyces quisqualis* in the Drawski Landscape Park (NW Poland). *Acta Mycol.* 36:191–201.
- Dean R, Van Kan JA, Pretorius ZA, Hammond-Kosack KE, Di Pietro A, Spanu PD, Rudd JJ, Dickman M, Kahmann R, Ellis J, Foster GD. 2012. The Top 10 fungal pathogens in molecular plant pathology. *Mol. Plant Pathol.* 13:414–430. DOI:10.1111/j.1364-3703.2011.00783.x.
- de Gruyter J, Aveskamp MM, Woudenberg JH, Verkley GJ, Groenewald JZ, Crous PW. 2009. Molecular phylogeny of *Phoma* and allied anamorph genera: towards a reclassification of the *Phoma* complex. *Mycol Res.* 113:508–519. DOI:10.1016/j.mycres.2009.01.002.
- De Luca D, Kooistra WHCF, Sarno D, Biffali E, Piredda R. 2021. Empirical evidence for concerted evolution in the 18S rDNA region of the planktonic

diatom genus *Chaetoceros*. Sci. Rep. 11:807. DOI:10.1038/s41598-020-80829-6.

Edger PP, Tang M, Bird KA, Mayfield DR, Conant G, Mummenhoff K, Koch MA, Pires JC. 2014. Secondary structure analyses of the nuclear rRNA internal transcribed spacers and assessment of its phylogenetic utility across the Brassicaceae (mustards). PLoS One. 9:e101341. DOI: 10.1371/journal.pone.0101341.

Elder JFJ, Turner BJ. 1995. Concerted evolution of repetitive DNA sequences in eukaryotes. Q. rev. Biol. 70:297–320.

Falk SP, Gadoury DM, Cortesi P, Pearson RC, Seem RC. 1995. Parasitism of *Uncinula necator* cleistothecia by the mycoparasite *Ampelomyces quisqualis*. Phytopathology. 85:794–800. DOI:10.1094/Phyto-85-794.

Falk SP, Gadoury DM, Pearson RC, Seem RC. 1995. Partial control of grape powdery mildew by the mycoparasite *Ampelomyces quisqualis*. Plant Dis. 79:483–490. DOI:10.1094/PD-79-0483.

Gadoury D, Seem RC, Pearson RC, Wilcox WF, Dunst RM. 2001. Effects of powdery mildew on vine growth, yield, and quality of concord grapes. Plant Dis. 85:137–140. DOI: 10.1094/PDIS.2001.85.2.137.

Garriga J, Ballesta, J, Vilaplana R. 2014. Composición para el control biológico del oídio en cultivos vegetales a base de una cepa de *Ampelomyces*. LAINCO, S.A. Patente ES 2 470 490 B2. ES 2 470 490 B2.

- Gent D, Grove GG, Nelson ME, Wolfenbarger SN, Woods JL. 2014. Crop damage caused by powdery mildew on hop and its relationship to late season management. *Plant Pathol.* 63:625–639. DOI: 10.1111/ppa.12123.
- Ghosh J, Bhattacharya S, Pal, A. 2017. Molecular phylogeny of 21 tropical bamboo species reconstructed by integrating non-coding internal transcribed spacer (ITS1 and 2) sequences and their consensus secondary structure. *Genetica*, 145:319–333. DOI: 10.1007/s10709-017-9967-9.
- Gilardi G, Manker DC, Garibaldi A, Gullino ML. 2008. Efficacy of the biocontrol agents *Bacillus subtilis* and *Ampelomyces quisqualis* applied in combination with fungicides against powdery mildew of zucchini. *J Plant Dis Prot.* 115:208–213. DOI:10.1007/BF03356265.
- Giudicelli G, Mäder G, Silva-Arias GA, Zamberlan PM, Bonatto SL, Freitas LB. 2017. Secondary structure of nrDNA Internal Transcribed Spacers as a useful tool to align highly divergent species in phylogenetic studies. *Genet Mol Biol.* 40:191–199. DOI: 10.1590/1678-4685-GMB-2016-0042.
- Glawe DA. 2008. The powdery mildews: a review of the world's most familiar (yet poorly known) plant pathogens. *Ann Rev Phytopathol.* 46:27–51. DOI:10.1146/annurev.phyto.46.081407.104740.
- Gong L, Luo H, Shi W, Yang M. 2019. Intra-individual variation and transcribed pseudogenes in the ribosomal ITS1-5.8S-ITS2 rDNA of *Paraplagusia japonica* (Pleuronectiformes: Cynoglossidae). *Biochem Biophys Res Commun.* 513:726–731. DOI:697 10.1016/j.bbrc.2019.04.064.

- Grummt I. 2003. Life on a planet of its own: regulation of RNA polymerase I transcription in the nucleolus. *Genes Dev.* 17:1691–702. DOI: 10.1101/gad.1098503R.
- Gutell R, Cannone JJ, Shang Z, Du Y, Serra MJ. 2000. A story: unpaired adenosine bases in ribosomal RNAs. *J Mol Biol.* 304:335–354. Doi:10.1006/jmbi.2000.4172.
- Harpke D, Peterson A. 2008. Extensive 5.8S nrDNA polymorphism in *Mammillaria* (Cactaceae) with special reference to the identification of pseudogenic internal transcribed spacer regions. *J Plant Res.* 121:261–270. Doi:10.1007/s10265-008-0156-x.
- Hashioka Y, Nakai Y. 1980. Ultrastructure of pycnidial development and mycoparasitism of *Ampelomyces quisqualis* parasitic on *Erysiphales*. *Trans Mycol Soc Jpn.* 21:329–338.
- Henras A, Soudet J, G erus M, Lebaron S, Caizergues-Ferrer M, Mougin A, Henry Y. 2008. The post-transcriptional steps of eukaryotic ribosome biogenesis. *Cell Mol Life Sci.* 65:2334–2359. Doi:10.1007/s00018-008-8027-0.
- Joseph N, Krauskopf E, Vera MI, Michot B. 1999. Ribosomal internal transcribed spacer 2 (ITS2) exhibits a common core of secondary structure in vertebrates and yeast. *Nucleic Acids Res.* 27:4533–4540. DOI:10.1093/nar/27.23.4533.
- Kappel K, Schr oder, U. 2020. Difficulties in DNA barcoding-based authentication of snapper products due to ambiguous nucleotide sequences in public databases. *Food Control.* 118:07348.

- Khan S, Baeshen MN, Ramadan HA, Baeshen NA. 2019. ITS2: an ideal DNA barcode for the arid medicinal plant *Rhazya stricta*. *Pharmaceut Med.* 33:53–61. Doi:10.1007/s40290-019-00266-3.
- Keller A, Schleicher T, Schultz J, Müller T, Dandekar T, Wolf M. 2009. 5.8S-28S rRNA interaction and HMM-based ITS2 annotation. *Gene.* 430:50–57. Doi: 10.1016/j.gene.2008.10.012.
- Kiss L. 1997. Genetic diversity in *Ampelomyces* isolates, hyperparasites of powdery mildew fungi, inferred from RFLP analysis of the rDNA ITS region. *Mycol Res.* 101:1073–1080. DOI:10.1017/s0953756297003705.
- Kiss L. 1998. Natural occurrence of *Ampelomyces* mycoparasites in mycelia of powdery mildew fungi. *New Phytol.* 140:709–714. DOI:10.1046/j.1469-8137.1998.00316.x.
- Kiss L. 2008. Intracellular mycoparasites in action: interactions between powdery mildew fungi and *Ampelomyces*. In: Avery SV, Stratford M, Van West P, editors. *Stress in yeasts and filamentous fungi*. London: Academic Press, Elsevier; p. 37–52. DOI:10.1016/S0275-0287(08)80045-8.
- Kiss L. 2012. Limits of nuclear ribosomal DNA internal transcribed spacer (ITS) sequences as species barcodes for Fungi. *PNAS.* 109:E1811.
- Kiss L, Nakasone KK. 1998. Ribosomal DNA internal transcribed spacer sequences do not support the species status of *Ampelomyces quisqualis*, a hyperparasite of powdery mildew fungi. *Curr Genet.* 33:362–367. DOI:10.1007/s002940050348.

- Kiss L, Pintye A, Kovács GM, Jankovics T, Fontaine MC, Harvey N, Xu X, Nicot PC, Bardin M, Shykoff JA, et al. 2011. Temporal isolation explains host-related genetic differentiation in a group of widespread mycoparasitic fungi. *Mol Ecol.* 20:1492–1507. DOI:10.1111/j.1365-294X.2011.05007.x.
- Kiss L, Vagna L. (1995). New approaches in the study of the genus *Ampelomyces*, hyperparasites of powdery mildew fungi. In *Environmental Biotic Factors in Integrated Plant Disease Control* (ed. M. Manka), pp. 301–304. Polish Phytopathological Society: Poznań, Poland.
- Kiss L, Vaghefi N, Bransgrove K, Dearnaley JDW, Takamatsu S, Tan YP, Marston C, Liu SY, Jin DN, Adorada DL, Bailey J, Cabrera de Álvarez MG, Daly A, Dirchwolf PM, Jones L, Nguyen TD, Edwards J, Ho W, Kelly L, Mintoff SJL, Morrison J, Németh MZ, Perkins S, Shivas RG, Smith R, Stuart K, Southwell R, Turaganivalu U, Váczy KZ, Blommestein AV, Wright D, Young A, Braun U. 2020. Australia: a continent without native powdery mildews? the first comprehensive catalog indicates recent introductions and multiple host range expansion events, and leads to the re-discovery of *Salmonomyces* as a new lineage of the Erysiphales. *Front Microbiol.* 11:1571. Doi:10.3389/fmicb.2020.01571.
- Koetschan C, Kittelmann S, Lu J, Al-Halbouni D, Jarvis GN, Müller T, Wolf M, Janssen PH. 2014. Internal transcribed spacer 1 secondary structure analysis reveals a common core throughout the anaerobic fungi (Neocallimastigomycota). *PLoS One.* 9:e91928. Doi:10.1371/journal.pone.0091928.

- Kumar S, Stecher G, Li M, Knyaz C, Tamura K. 2018. MEGA X: molecular evolutionary genetics analysis across computing platforms. *Mol Biol Evol.* 35:1547–1549. Doi:10.1093/molbev/msy096.
- Lafontaine D, Tollervey D. 2001. The function and synthesis of ribosomes. *Nature Rev. Mol. Cell Biol.* 2:514–520. Doi:10.1038/35080045.
- Lamanna A, Karbstein K. 2009. Nob1 binds the single-stranded cleavage site D at the 3'-end of 18S rRNA with its PIN domain. *Proc Natl Acad Sci U S A.* 106:14259–14264. Doi:10.1073/pnas.0905403106.
- Lathe W, Williams J, Mangan M, Karolchik, D. 2008. Genomic data resources: challenges and promises. *Nat Educ.* 1:2.
- Lee SY, Lee SB, Kim CH. 2004. Biological control of powdery mildew by Q-fect WP (*Ampelomyces quisqualis*) in various crops. *IOBC/wprs Bull.* 27:329–331.
- Legler SE, Pintye A, Caffi T, Gulyas S, Bohar G, Rossi V, Kiss L. 2016. Sporulation rate in culture and mycoparasitic activity, but not mycohost specificity, are the key factors for selecting *Ampelomyces* strains for biocontrol of grapevine of powdery mildew (*Erysiphe necator*). *Eur J Plant Pathol.* 144:723–736. DOI:10.1007/s10658-015-0834-1.
- Li M, Zhao H, Zhao F, Jiang L, Peng H, Zhang W, Simmons MP. 2019. Alternative analyses of compensatory base changes in an ITS2 phylogeny of *Corydalis* (Papaveraceae). *Ann. Bot.* 124:233–243. Doi: 10.1093/aob/mcz062.
- Liang C, Yang J, Kovacs GM, Szentiványi O, Li B, Xu XM, Kiss L. 2007. Genetic diversity of *Ampelomyces* mycoparasite isolated from different powdery

mildew species in China inferred from analyses of rDNA ITS sequences. *Fungal Divers.* 24:225–240.

Liang Q, Wei L, Xu B, Liu L, Calderón-Urrea A. 2020. First report of powdery mildew caused by *Podosphaera xanthii* on Hulless *Cucurbita pepo* of inner Mongolia and Xinjiang autonomous region in China. *Plant Dis.* Doi: 10.1094/PDIS-04-20-0703-PDN.

Liyanage KK, Khan S, Brooks S, Mortimer PE, Karunaratna SC, Xu J, Hyde KD. 2018. Morphomolecular characterization of two *Ampelomyces* spp. (Pleosporales) strains mycoparasites of powdery mildew of *Hevea brasiliensis*. *Front Microbiol.* 9:12. DOI:10.3389/fmicb.2018.00012.

Manjunatha L, Singh S, Ravikumara BM, Narasa Reddy G, Senthilkumar M. 2020. *Ampelomyces*. In: Amaresan N, Senthil Kumar M, Annapurna K, Kumar K, Sankaranarayanan A, editors. Beneficial microbes in agro-ecology. Amsterdam, Netherlands: Academic Press; p. 833–860.

Marmolejo J, Siahaan SAS, Takamatsu S, Braun U. 2018. Three new records of powdery mildews found in Mexico with one genus and one new species proposed. *Mycoscience.* 59:1–7. Doi:10.1016/j.myc.2017.06.010.

Matheron M, Porchas M. 2013. Efficacy of fungicides and rotational programs for management of powdery mildew on cantaloupe. *Plant Dis.* 97:196–200. Doi: 10.1094/PDIS-04-12-0370-RE.

Merget B, Koetschan C, Hackl T, Förster F, Dandekar T, Müller T, Schultz J, Wolf M. 2012. The ITS2 database. *J. Vis. Exp.* 61:806. Doi:10.1094/PDIS-04-12-0370-RE.

- Mezzalama M, Guarnaccia V, Martano G, Spadaro D. 2020. Presence of powdery mildew caused by *Erysiphe corylacearum* on hazelnut (*Corylus avellana*) in Italy. Plant Dis. Doi:10.1094/PDIS-10-20-2281-PDN.
- Mhaskar DN, Rao VG. 1974. The mycoparasite *Ampelomyces quisqualis* Ces. in artificial culture. II. Effect of environmental factors. Phytopathol Mediterr. 13:147–154.
- Milyutina I, Goryunov DV, Ignatov MS, et al. 2010. The phylogeny of *Schistidium* (Bryophyta, Grimmiaceae) based on the primary and secondary structure of nuclear rDNA internal transcribed spacers. Mol Biol. (Moscow). 44:883–897. Doi: 10.1134/S0026893310060051.
- Milyutina I, Ignatov M. 2015. Conserved motifs in the primary and secondary ITS1 structures in bryophytes. Mol. Biol. (Mosk). 49:394–404.
- Müller T, Philippi N, Dandekar T, Schultz J, Wolf M. 2007. Distinguishing species. RNA. 13:1469–1472. Doi: 10.1261/rna.617107.
- Naidoo K, Steenkamp ET, Coetzee MP, Wingfield MJ, Wingfield BD. 2013. Concerted evolution in the ribosomal RNA cistron. PLoS One. 8:e59355. Doi: 10.1371/journal.pone.0059355.
- Németh MZ, Mizuno Y, Kobayashi H, Seress D, Shishido N, Kimura Y, Takamatsu S, Suzuki T, Takikawa Y, Kakutani K, et al. 2021. *Ampelomyces* strains isolated from diverse powdery mildew hosts in Japan: their phylogeny and mycoparasitic activity, including timing and quantifying mycoparasitism of *Pseudoidium neolycopersici* on tomato. PLoS One. 16:e0251444. DOI:10.1371/journal.pone.0251444.

- Németh MZ, Pintye A, Horváth ÁN, Vági P, Kovács GM, Gorfer M, Kiss L. 2019. Green fluorescent protein transformation sheds more light on a widespread mycoparasitic interaction. *Phytopathology*. 109:1404–1416. DOI:10.1094/PHYTO-01-19-0013-R.
- Nguyen TTT, Lee HB. 2016. First report of *Ampelomyces quisqualis* from Sycamore and Crape myrtle and its potential as a mycoparasite of powdery mildew. *Kor J Mycol*. 44:64–67. DOI:10.4489/KJM.2016.44.1.64.
- Nicolopoulou-Stamati P, Maipas S, Kotampasi C, Stamatis P, Hens L. 2016. Chemical pesticides and human health: the urgent need for a new concept in agriculture. *Front Public Health*. 2016. 4:148. Doi:10.3389/fpubh.2016.00148.
- Nonomura T, Matsuda Y, Takikawa Y, Kakutani K, Toyoda H. 2014. Successional changes in powdery mildew pathogens prevailing in common and wild tomato plants rotation-cultivated in a greenhouse. *Ann Rept Kansai Pl Prot*. 56:17–20. DOI:10.4165/kapps.56.17.
- Opron K, Burton Z. 2018. Ribosome structure, function, and early evolution. *Int J Mol Sci*. 20:40. Doi:10.3390/ijms20010040.
- Paredes-Esquivel CC, Townson, H. 2014. Functional constraints and evolutionary dynamics of the repeats in the rDNA internal transcribed spacer 2 of members of the *Anopheles barbirostris* group. *Parasites & Vectors*. 7:106.
- Park MJ, Choi YJ, Hong SB, Shin HD. 2010. Genetic variability and mycohost association of *Ampelomyces quisqualis* isolates inferred from phylogenetic

- analyses of ITS rDNA and *actin* gene sequences. *Fungal Biol.* 114:235–247.
DOI:10.1016/j.funbio.2010.01.003.
- Perry RP. 1976. Processing of RNA. *Annu. Rev. Biochem.* 45:605–629. Doi:
10.1146/annurev.bi.45.070176.003133.
- Philipp W, Beuther E, Grossmann F. 1982. Untersuchungen über den einfluss von
fungiciden auf *Ampelomyces quisqualis* im hinblick auf eine integrierte
bekämpfung von gurkenmehltau unter glass. *Z. Pflkanzenkrankh.*
Pflanzenschutz. 89:575–581.
- Phookamsak R, Liu JK, McKenzie EHC, Manamgoda DS, Ariyawansa H,
Thambugala KM, Dai D-Q, Camporesi E, Chukeatirote E, Wijayawardene
NN, et al. 2014. Revision of Phaeosphaeriaceae. *Fungal Divers.* 68:159–
238. DOI:10.1007/s13225-014-0308-3.
- Pink RC, Carter DR. 2013. Pseudogenes as regulators of biological function. *Essays*
Biochem. 54:103–112. DOI:10.1042/bse0540103.
- Pirrello C, Mizzotti C, Tomazetti TC, Colombo M, Bettinelli P, Prodorutti D,
Peressotti E, Zulini L, Stefanini M, Angeli G, Masiero S, Welter LJ,
Hausmann L, Vezzulli S. (2019). Emergent Ascomycetes in viticulture: an
interdisciplinary overview. *Front Plant Sci.* 10:1394.
Doi:10.3389/fpls.2019.01394.
- Pintye A, Bereczky Z, Kovács GM, Nagy LG, Xu X, Legler SE, Váczy Z, Váczy
KZ, Caffi T, Rossi V, et al. 2012. No indication of strict host associations
in a widespread mycoparasite: grapevine powdery mildew (*Erysiphe*

necator) is attacked by phylogenetically distant *Ampelomyces* strains in the field. *Phytopathology*. 102:707–716. DOI:10.1094/PHYTO-10-11-0270.

Pintye A, Ropars J, Harvey N, Shin HD, Leyronas C, Nicot PC, Giraud T, Kiss L. 2015. Host phenology and geography as drivers of differentiation in generalist fungal mycoparasites. *PLoS One*. 10:e0120703. DOI:10.1371/journal.pone.0120703.

Poczai P, Varga I, Hyvönen J. 2015. Internal transcribed spacer (ITS) evolution in populations of the hyperparasitic European mistletoe pathogen fungus, *Sphaeropsis visci* (Botryosphaeriaceae): the utility of ITS2 secondary structures. *Gene*. 558:54–64. Doi:10.1016/j.gene.2014.12.042.

Polonio Á, Fernández-Ortuño D, de Vicente A, Pérez-García A. 2021. A haustorial-expressed lytic polysaccharide monooxygenase from the cucurbit powdery mildew pathogen *Podosphaera xanthii* contributes to the suppression of chitin-triggered immunity. *Mol Plant Pathol*. 22:580–601. Doi: 10.1111/mpp.13045.

Prahl RE, Khan S, Deo RC. 2021. The role of internal transcribed spacer 2 secondary structures in classifying mycoparasitic *Ampelomyces*. *PLoS One*. 16:e0253772. DOI:10.1371/journal.pone.0253772.

Prahl RE, Khan S, Deo RC. 2022. *Ampelomyces* mycoparasites of powdery mildews: a review. Under final review by *Canadian Journal of Plant Pathology*.

Riaz S, Menéndez, CM., Tenschler A, et al. 2020. Genetic mapping and survey of powdery mildew resistance in the wild Central Asian ancestor of cultivated

grapevines in Central Asia. *Hortic. Res.* 7:104. Doi:10.1038/s41438-020-0335-z.

Romero D, De Vicente A, Zerriouh H, Cazorla FM, Fernández-Ortuño D, Torés JA, Pérez-García A. 2007. Evaluation of biological control agents for managing cucurbit powdery mildew on greenhouse-grown melon. *Plant Pathol.* 56:976–986. DOI:10.1111/j.1365-3059.2007.01684.x.

Schäffer AA, McVeigh R, Robbertse B, Schoch CL, Johnston A, Underwood BA, Karsch-Mizrachi I, Nawrocki EP. 2021. Ribovore: ribosomal RNA sequence analysis for GenBank submissions and database curation. *BMC Bioinformatics.* 22:400. Doi:10.1186/s12859-021-04316-z.

Schill R, Förster, F., Dandekar, T, et al. 2010. Using compensatory base change analysis of internal transcribed spacer 2 secondary structures to identify three new species in *Paramacrobiotus* (Tardigrada). *Org Divers Evol.* 10:287–296. Doi: 0.1007/s13127-010-0025-z.

Schoch CL, Seifert KA, Huhndorf S, Schindel D. 2012. Nuclear ribosomal internal transcribed spacer (ITS) region as a universal DNA barcode marker for Fungi. *Proc. Natl. Acad. Sci. U.S.A.* 109:6241–6246. Doi:10.1073/pnas.1117018109.

Schultz J, Maisel S, Gerlach D, Müller T, Wolf M. 2005. A common core of secondary structure of the internal transcribed spacer 2 (ITS2) throughout the Eukaryota. *RNA.* 11:361–364. Doi:10.1261/rna.7204505.

- Seibel PN, Müller T, Dandekar T, Schultz J, Wolf M. 2006. 4SALE--a tool for synchronous RNA sequence and secondary structure alignment and editing. *BMC Bioinformatics*. 7:498. Doi: 10.1186/1471-2105-7-498.
- Shishkoff N, McGrath MT. 2002. AQ10 biofungicide combined with chemical fungicides or AddQ spray adjuvant for control of *Cucurbit* powdery mildew in detached leaf culture. *Plant Dis*. 86:915–918. DOI:10.1094/PDIS.2002.86.8.915.
- Selig C, Wolf M, Müller T, Dandekar T, Schultz J. 2008. The ITS2 Database II: homology modelling RNA structure for molecular systematics. *Nucleic Acids Res*. 36:D377–D380. Doi:10.1093/nar/gkm827.
- Singh R, Singh PK, Rutkoski J, Hodson DP, He X, Jørgensen LN, Hovmøller MS, Huerta-Espino J. 2016. Disease impact on wheat yield potential and prospects of genetic control. *Annu. Rev. Phytopathol*. 54:303–322. Doi:10.1146/annurev-phyto-080615-095835.
- Scull CE, Schneider DA. 2019. Coordinated control of rRNA processing by RNA Polymerase I. *Trends Genet*. 35:724–733. Doi:10.1016/j.tig.2019.07.002.
- Sims J, Sestini G, Elgert C, von Haeseler A, Schlögelhofer P. 2021. Sequencing of the *Arabidopsis* NOR2 reveals its distinct organization and tissue specific rRNA ribosomal variants. *Nat Commun*. 12:387. Doi:10.1038/s41467-020-20728-6.
- Stalder L. (1955). Beobachtungen über das Verhalten von *Podosphaera leucotricha* (Ellis et Everh.) Salm. in Apfelknospen. *Phytopathologische Zeitschrift* 23:341–344.

Stielow J, Lévesque CA, Seifert KA, Meyer W, Iriny L, Smits D, Renfurm R, Verkley GJ, Groenewald M, Chaduli D, Lomascolo A, Welti S, Lesage-Meessen L, Favel A, Al-Hatmi AM, Damm U, Yilmaz N, Houbraken J, Lombard L, Quaedvlieg W, Binder M, Vaas LA, Vu D, Yurkov A, Begerow D, Roehl O, Guerreiro M, Fonseca A, Samerpitak K, van Diepeningen AD, Dolatabadi S, Moreno LF, Casaregola S, Mallet S, Jacques N, Roscini L, Egidì E, Bizet C, Garcia-Hermoso D, Martín MP, Deng S, Groenewald JZ, Boekhout T, de Beer ZW, Barnes I, Duong TA, Wingfield MJ, de Hoog GS, Crous PW, Lewis CT, Hambleton S, Moussa TA, Al-Zahrani HS, Almaghrabi OA, Louis-Seize G, Assabgui R, McCormick W, Omer G, Dukik K, Cardinali G, Eberhardt U, de Vries M, Robert V 2015. One fungus, which genes? Development and assessment of universal primers for potential secondary fungal DNA barcodes. *Persoonia*. 35:242–263. Doi:10.3767/003158515X689135.

Sullivan RF, White JF Jr. 2000. *Phoma glomerata* as a mycoparasite of powdery mildew. *Appl Environ Microbiol*. 66:425–427. DOI:10.1128/aem.66.1.425-427.2000.

Sundaresan N, Sahu AK, Jagan EG, Pandi M. 2019. Evaluation of ITS2 molecular morphometrics effectiveness in species delimitation of Ascomycota - A pilot study. *Fungal Biol*. 123:517–527. Doi:10.1016/j.funbio.2019.05.002.

Sundheim L. 1982. Control of cucumber powdery mildew by the hyperparasite *Ampelomyces quisqualis* and fungicides. *Plant Pathol*. 31:209–214. DOI:10.1111/j.1365-3059.1982.tb01270.x.

- Sundheim L, Krekling T. 1982. Host-parasite relationships of the hyperparasite *Ampelomyces quisqualis* and its powdery mildew host *Sphaerotheca fuliginea*. I. Scanning electron microscopy. J Phytopathol. 104:202–210. DOI:10.1111/j.1439-0434.1982.tb00527.x.
- Szentiványi O, Kiss L. 2003. Overwintering of *Ampelomyces* mycoparasites on apple trees and other plants infected with powdery mildews. Plant Pathol. 52:737–746. DOI:10.1111/j.1365-3059.2003.00937.x.
- Szentiványi O, Kiss L, Russell JC, Kovács GM, Varga K, Jankovics T, Lesemann S, Xu XM, Jeffries P. 2005. *Ampelomyces* mycoparasites from apple powdery mildew identified as a distinct group based on single-stranded conformation polymorphism analysis of the rDNA ITS region. Mycol Res. 109:429–438. Doi:10.1017/s0953756204001820.
- Sztejnberg A, Galper S, Mazar S, Lisker N. 1989. *Ampelomyces quisqualis* for biological and integrated control of powdery mildew in Israel. J. Phytopathol. 124:285–295. DOI:10.1111/j.1439-0434.1989.tb04925.x.
- Szostak J, Wu, R. 1980. Unequal crossing over in the ribosomal DNA of *Saccharomyces cerevisiae*. Nature. 284:426–430.
- Takamatsu S. (2004). Phylogeny and evolution of the powdery mildew fungi (Erysiphales, Ascomycota) inferred from nuclear ribosomal DNA sequences. Mycoscience. 45:147–157. DOI:10.1007/S10267-003-0159-3.
- Takamatsu S, Ito Arakawa H, Shiroya Y, Kiss L, Heluta V. (2015a). First comprehensive phylogenetic analysis of the genus *Erysiphe* (Erysiphales,

- Erysiphaceae) I: The *Microsphaera* lineage. *Mycologia*. 107:475–489.
DOI: 10.3852/15-007.
- Takamatsu S, Ito Arakawa H, Shiroya Y, Kiss L, Heluta V. (2015b). First comprehensive phylogenetic analysis of the genus *Erysiphe* (Erysiphales, Erysiphaceae) II: the *Uncinula* lineage. *Mycologia*. 107:903–914.
DOI:10.3852/15-062.
- Takamatsu S, Matsuda S, Grigaliunaite B. 2013. Comprehensive phylogenetic analysis of the genus *Golovinomyces* (Ascomycota: Erysiphales) reveals close evolutionary relationships with its host plants. *Mycologia*. 105:1135–1152. Doi:10.3852/13-046.
- van Nues R, Rientjes JM, van der Sande CA, Zerp SF, Sluiter C, Venema J, Planta RJ, Raué HA. 1994. Separate structural elements within internal transcribed spacer 1 of *Saccharomyces cerevisiae* precursor ribosomal RNA direct the formation of 17S and 26S rRNA. *Nucleic Acids Res*. 22:912–919.
DOI:10.1093/nar/22.6.912.
- Vasavada N. 2016. Kruskal-Wallis rank sum (omnibus) test calculator - with follow-up post-hoc multiple comparison calculator by the methods of (1) Conover, (2) Dunn and (3) Nemenyi. Available at <https://astatsa.com/KruskalWallisTest/>.
- Venema J, Tollervey D. 1995. Processing of pre-ribosomal RNA in *Saccharomyces cerevisiae*. *Yeast*. 11:1629–1650.
- Vilnet A, Konstantinova N, Troitsky A. 2008. Phylogeny and systematic of the genus *Lophozia* s. str. (Dumort.) Dumort. (Hepaticae) and related taxa from

nuclear ITS1-2 and chloroplast *trnL-F* sequences. *Mol Phylogenet Evol.* 47:403–418. DOI: 10.1016/j.ympev.2007.12.013.

Vu D, G.M., de Vries M, Gehrman T, Stielow B, Eberhardt U, Al-Hatmi A, Groenewald JZ, Cardinali G, Houbraken J, Boekhout T, Crous PW, Robert V, Verkley GJM. 2019. Large-scale generation and analysis of filamentous fungal DNA barcodes boosts coverage for kingdom fungi and reveals thresholds for fungal species and higher taxon delimitation. *Stud. Mycol.* 91:135–154.

Wei-Li G, Chen BH, Guo YY, Yang HL, Mu JY, Wang YL, Li XZ, Zhou JG. 2019. Improved powdery mildew resistance of transgenic *Nicotiana benthamiana* overexpressing the *Cucurbita moschata CmSGT1* gene. *Front Plant Sci.* 10:955. DOI:10.3389/fpls.2019.00955.

Wijayawardene NN, Camporesi E, Song Y, Dai DQ, Bhat DJ, Mckenzie EHC, Chukeatirote E, Mel'nik VA, Wang Y, Hyde KD. (2013). Multigene analyses reveal taxonomic placement of *Scolicosporium minkeviciusii* in Phaeosphaeriaceae (Pleosporales). *Cryptogam Mycol.* 34:357–366. DOI:10.7872/crym.v34.iss2.2013.357.

Will S, Joshi T, Hofacker IL, Stadler PF, Backofen R. 2012. LocARNA-P: accurate boundary prediction and improved detection of structural RNAs. *RNA.* 18:900–914. DOI: 10.1261/rna.029041.111.

Wiseman M, Bates T, Garfinkel A, Ocamb CM, Gent DH. 2021. First report of powdery mildew caused by *Golovinomyces ambrosiae* on *Cannabis sativa* in Oregon. *Plant Dis.* 2021. DOI:10.1094/PDIS-11-20-2455-PDN.

- Wu B, Hussain M, Zhang W, Stadler M, Liu X, Xiang M. 2019. Current insights into fungal species diversity and perspective on naming the environmental DNA sequences of fungi. *Mycology*. 10:127–140. Doi: 10.1080/21501203.2019.1614106.
- Wolf M, Koetschan, C, Müller, T. 2014. ITS2, 18S, 16S or any other RNA - simply aligning sequences and their individual secondary structures simultaneously by an automatic approach. *Gene*. 10:145–149. DOI: 10.1016/j.gene.2014.05.065.
- Xue L, Li C, Zhao G. 2017. First report of powdery mildew caused by *Blumeria graminis* on *Avena sativa* in China. *Plant Dis*. 101:1954–1955. DOI:10.1094/PDIS-05-17-0678-PDN.
- Yarwood CE. 1932. *Ampelomyces quisqualis* on clover mildew. *Phytopathology*. 22:31.
- Zhang X, Xu Z, Pei H, Chen Z, Tan X, Hu J, Yang B, Sun J. 2017. Intraspecific variation and phylogenetic relationships are revealed by ITS1 secondary structure analysis and single-nucleotide polymorphism in *Ganoderma lucidum*. *PLoS One*. 12:e0169042. DOI:10.1371/journal.pone.0169042.
- Zhang Y, Schoch CL, Fournier J, Crous PW, de Gruyter J, Woudenberg JH, Hirayama K, Tanaka K, Pointing SB, Spatafora JW, et al. 2009. Multi-locus phylogeny of Pleosporales: a taxonomic, ecological and evolutionary re-evaluation. *Stud Mycol*. 64:85–102. DOI:10.3114/sim.2009.64.04.

Zhu M, Ji J, Duan X, Li Y. 2020. First report of *Golovinomyces cichoracearum* causing powdery mildew on *Zinnia elegans* in China. Plant Dis. DOI: 10.1094/PDIS-11-20-2333-PDN.

Zuker M. 2003. Mfold web server for nucleic acid folding and hybridization prediction. Nucleic Acids Res. 31:3406–3415. DOI:10.1093/nar/gkg595.